Human CPAP and CP110 in Centriole Elongation and Ciliogenesis

Dissertation
zur Erlangung des Doktorgrades der Naturwissenschaften
der Fakultät für Biologie der Ludwig-Maximilians Universität
München

Vorgelegt von
Thorsten I. Schmidt

München, 2010

Dissertation eingereicht am: 11.05.2010

Tag der mündlichen Prüfung: 25.10.2010

Erstgutachter: Prof. Dr. Erich A. Nigg
Zweitgutachter: Prof. Dr. Angelika Böttger

Hiermit erkläre ich, dass ich die vorliegende Dissertation selbständig und ohne unerlaubte Hilfe angefertigt habe. Sämtliche Experimente wurden von mir selbst durchgeführt, soweit nicht explizit auf Dritte verwiesen wird. Ich habe weder an anderer Stelle versucht, eine Dissertation oder Teile einer solchen einzureichen bzw. einer Prüfungskommission vorzulegen, noch eine Doktorprüfung zu absolvieren.

München, den 11.05.2010

TABLE OF CONTENTS

1. SUMMARY **1**

2. INTRODUCTION **2**

2.1 Function and Structure of the Centrosome **2**

2.1.1 The Centrosome as MTOC in Proliferating Cells 2

2.1.2 The Centriole as Template for Cilia and Flagella 3

2.1.3 Molecular Composition and Structure of the Centrosome 3

2.2 The Centrosome Cycle **5**

2.3 Centriole Biogenesis and Control of Centriole Length **7**

2.3.1 Centriole Biogenesis in *Caenorhabditis elegans* 7

2.3.2 Centriole Biogenesis in Human Cells 9

2.3.3 Control of Centriole Length during Procentriole Formation 11

2.4 Centrosome Abnormalities and Cancer **11**

2.5 Structure and Functions of Cilia **15**

2.6 Formation and Disassembly of Primary Cilia **19**

2.7 Cilia-related Human Diseases **20**

3. AIM OF THIS PROJECT **22**

4. RESULTS **23**

4.1 Generation of Anti-CP110 Antibodies and of a Cell Line to Induce CPAP Overexpression **24**

4.1.1 Production of Polyclonal Anti-CP110 Antibodies 24

4.1.2 Generation of Monoclonal Anti-CP110 Antibodies 26

4.1.3 Generation of an U2OS T-REx myc-CPAP Stable Cell Line 26

4.2 CP110 in Ciliogenesis **28**

4.2.1 CP110 and Cep97 are Absent from the Ciliated Basal Body 28

4.3 Centriole Elongation 29

4.3.1 Depletion of CP110 Causes the Elongation of Centrioles 29
4.3.2 CPAP is Required for Centriole Duplication in Cycling Cells 30
4.3.3 Overexpression of CPAP Leads to Centriole Elongation 31
4.3.4 Mapping of the CPAP Region Required for Centriole Elongation 33

4.4 Delineation of CPAP-mediated Procentriole Elongation 35

4.4.1 Analysis of Centriole Elongation with the myc-CPAP Inducible Cell Line 35
4.4.2 CPAP Overexpression Causes Enhanced Tubulin Accumulation at Centrioles . 37
4.4.3 Both Procentrioles and Mature Centrioles are Elongation-Competent 38

4.5 Comparison of Centriolar Elongations 40

4.5.1 Elongated Centrioles after CP110 Depletion and CPAP Overexpression are Highly Similar 40
4.5.2 Positioning of Distal and Subdistal Appendages on Elongated Centrioles 41

4.6 Centriolar Elongations are Fundamentally Different from Primary Cilia 43

4.7 Antagonistic Actions of CPAP and CP110 in Centriole Length Control 46

4.8 Screen for Further Proteins Involved in Centriole Length Control 47

5. DISCUSSION 49

5.1 Ciliogenesis is Dependent on a Multi-Step Regulatory Process which Includes the Removal of CP110/Cep97 from the Mature Basal Body 49

5.2 Centriolar Microtubules Elongate in the Absence of CP110 52

5.3 CPAP Controls Centriole Length during Procentriole Elongation 55

5.4 Centriole Length is Equilibrated by Antagonistic Actions of CPAP and CP110 58

5.5 Novel Proteins Controling Centriole Length 59

5.6 Are Ciliogenesis and the Control of Centriole Length Mechanistically Linked? 61

6. MATERIALS AND METHODS 62

7. ABBREVIATIONS 71

8. REFERENCES 72

9. APPENDIX 87

10. CURRICULUM VITAE 88

11. ACKNOWLEDGEMENTS 89

1. SUMMARY

Centrioles are the major components of centrosomes, which organize a wide range of microtubule (MT)-dependent processes in proliferating cells, and function as basal bodies for primary cilia formation in quiescent cells. Centrioles and basal bodies are structurally similar, barrel-shaped organelles composed of MTs and are associated with multiple proteins. In proliferating cells, two new centrioles, termed procentrioles, form at a near-orthogonal angle in close proximity to the proximal ends of the two pre-existing parental centrioles during S phase of the cell cycle (Kuriyama and Borisy 1981; Vorobjev and Chentsov Yu 1982; Chretien et al. 1997; comprehensively reviewed in Azimzadeh and Bornens 2007). These procentrioles then elongate until the beginning of the subsequent cell cycle (Azimzadeh and Bornens 2007). Considerable progress has been made towards understanding the initiation of centriole duplication, but the mechanisms that determine their lengths remain unknown.

In this work two questions have been addressed. Initially, we have found that CP110 and its interaction partner Cep97 are displaced from the mature basal body in ciliated cells and thus have identified a key step of ciliogenesis. The main focus of this work is on how centriole elongation is controlled during procentriole formation in human cells. We show that overexpression of the centriolar protein CPAP enhances the accumulation of centriolar tubulin, leading to centrioles of strikingly increased length. Consistent with other work (Spektor et al. 2007), we have found that elongated microtubular structures can be induced by depletion of CP110, a protein capping the distal end of centrioles in proliferating cells. Importantly, these centriolar structures differ from genuine primary cilia in quiescent cells. We thus propose that CPAP and CP110 play antagonistic roles in determining the extent of tubulin addition during centriole elongation, thereby controlling the length of newly formed centrioles. Based on these results, we have conducted further experiments to identify additional novel key regulatory proteins of centriole elongation.

2. INTRODUCTION

The centrosome has first been discovered by Édouard van Beneden in nematode eggs of *Ascaris megalocephala* and described by Theodor Boveri at the end of the 19th century (Van Beneden 1883; Boveri 1887). Despite the presence of centrosomes in the majority of cells in higher organisms, its composition, organization, mode of replication and its precise functions have remained elusive for many decades. In general, the centrosome has two important functions, on the one hand as the major Microtubule Organizing Centre (MTOC) during the cell cycle of proliferating cells, on the other hand as the scaffold comprising the basal bodies, needed for cilia formation in differentiated or quiescent cells. Over the past years, the pivotal cellular functions of centrosomes have increasingly gained scientific attention as they are implicated in the development of various human diseases.

2.1 Function and Structure of the Centrosome

2.1.1 The Centrosome as MTOC in Proliferating Cells

Centrosome function and structure are evolutionarily conserved from lower eukaryotes to mammals (Beisson and Wright 2003). As MTOC in proliferating cells the centrosome is required for the nucleation of MTs, predominantly facilitated by the associated γ-tubulin-containing multiprotein ring complexes (γ-TuRCs). During interphase, the centrosome is involved in the regulation of cell motility, cell shape, cell adhesion, cytoskeletal organization and organelle transport (reviewed in Doxsey 2001; Bornens 2002; Nigg 2004; Doxsey et al. 2005; Azimzadeh and Bornens 2007; Bornens 2008). In dividing cells the centrosome participates in the organization of the bipolar mitotic spindle and thereby in the faithful segregation of chromosomes into the two daughter cells. However, in the absence of centrosomes, spindles can form via a centrosome-independent pathway, as for example in higher plants and certain fungi (reviewed in Gadde and Heald 2004; Marshall 2009). In contrast to symmetric cell division, the spindle pole function of centrosomes has recently been shown to be essential for asymmetric cell division in the mouse embryonic neocortex (Wang et al. 2009).

2.1.2 The Centriole as Template for Cilia and Flagella

Ciliogenesis is a complex and highly coordinated process for which centrioles, in contrast to their mitotic functions, are strictly required (reviewed in Pedersen and Rosenbaum 2008). Initially, the centrosome is translocated from the periphery of the nucleus to the cell surface and the centrioles are then termed `basal bodies´. There, the mature basal body anchors the centrosome to the plasma membrane and functions as template for the outgrowth of the ciliary axoneme. Subsequently, the ciliary membrane is built and the components of the intra-ciliary transport processes are assembled. Despite recent advances in the basic understanding of ciliogenesis, several of the controlling pathways still remain elusive. Many different types of cilia/flagella with a wide range of specialized functions have evolved throughout the different kingdoms of life (reviewed in Marshall 2009; Nigg and Raff 2009; also see chapter 2.5).

2.1.3 Molecular Composition and Structure of the Centrosome

The centrosome is a non-membranous cell organelle of approximately 1 μm in diameter that is normally located in close proximity to the nucleus in cycling cells (Doxsey 2001). The centrosomal proteome is highly conserved between all organisms examined and consists of over one hundred proteins in humans (Andersen et al. 2003; Keller et al. 2005; Kilburn et al. 2007; Nogales-Cadenas et al. 2009).

In vertebrates, the single centrosome in G1 phase comprises a pair of centrioles surrounded by the pericentriolar material (PCM), an electron-dense matrix that contains proteins which mostly harbour protein-interaction motifs such as coiled-coil domains (Andersen et al. 2003). Many of these PCM proteins, in particular the components of the conserved γ-TuRCs, are involved in MT nucleation and anchoring (Moritz et al. 1995; Zheng et al. 1995; Moritz and Agard 2001) or in other cell cycle regulatory processes. G1 phase centrioles are loosely tethered together within the PCM at their proximal ends via interconnecting proteins, C-Nap1 and rootletin (Fry et al. 1998; Bahe et al. 2005), allowing a flexible orientation towards another. The two centrioles are highly symmetrical, barrel-shaped arrays of nine MT triplets, referred to as A-, B- and C-tubule, and reach a length of approximately 400 nm (Figure 1; Bornens 2002; Bettencourt-Dias and Glover 2007). In contrast to the A- and B- tubules, which extend across the complete proximal to distal length of a fully grown centriole, the C-tubule does not stretch to the distal end of the tube.

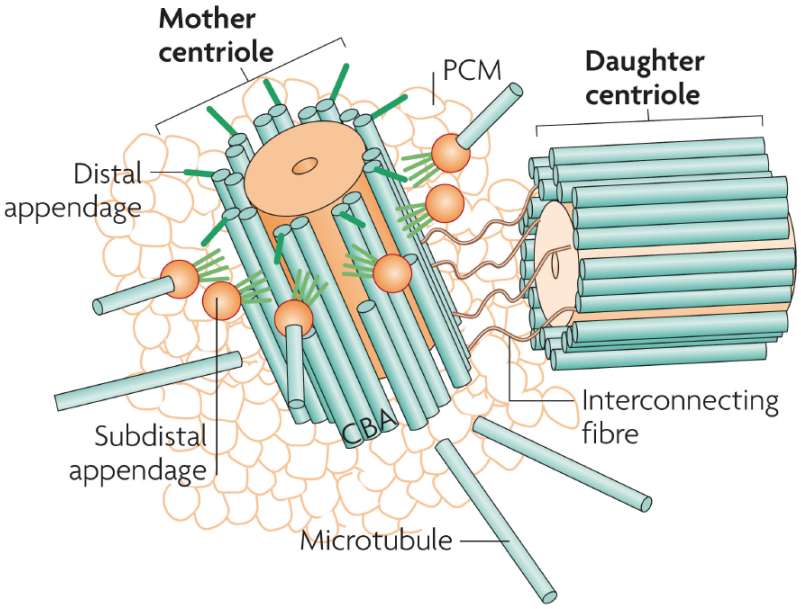

Figure 1: Centrosome and centriole structure. Schematic view of a G1 phase centrosome, illustrating the nine-fold triplet structure of the centriolar MTs. In each triplet, the most internal tubule is called the A-tubule, the following ones are the B- and C-tubule. At its distal end, the centriole is constituted of MT doublets. The two centrioles are surrounded by a cloud of PCM proteins and are interconnected by a proteinacous tether in G1 phase. The γ-tubulin complex-containing PCM is the major cellular MT nucleation site. Note that the mature "mother" centriole carries distal and subdistal appendage structures which the procentriole "daughter" lacks (adapted from Bettencourt-Dias and Glover 2007).

Despite their similar architecture, the two centrioles of one centrosome are structurally and functionally distinct throughout the cell cycle, because the older, parental centriole anchors most of the MTs to the centrosome and exclusively carries distal and subdistal appendages once it is matured (Figure 1; Piel et al. 2000; Azimzadeh and Bornens 2007). Those appendage structures are attached to each of the nine distal centriolar MT pairs and several proteins have been characterized as their components, such as ε-tubulin, Cep164, Cep170, ninein, and the ODF-2 splice variant hCenexin1 (Mogensen et al. 2000; Chang et al. 2003; Guarguaglini et al. 2005; Ishikawa et al. 2005; Graser et al. 2007; Soung et al. 2009).

2.2 The Centrosome Cycle

To ensure faithful execution of the centrosomal functions during the cell cycle and in the process of cilium formation in differentiating cells, centriole numbers need to be under precise control. Therefore, regulatory mechanisms ensure that centrioles are only duplicated once per cell cycle ('cell cycle control') and that, in addition, only one procentriole per parental centriole is assembled during S phase ('copy number control') (Nigg 2007). The centriole cycle is hallmarked by the four key events, centriole disengagement, procentriole formation (and subsequent procentriole elongation), centriole maturation and separation (Figure 2).

Proliferating somatic cells exit mitosis with one centrosome comprising two centrioles of which the younger procentriole ("daughter") has been assembled during the previous cell cycle and is strictly orthogonally engaged at the proximal end of the older ("mother") centriole.

'Centriole disengagement', licensed by parallel actions of separase and Plk1 (Tsou and Stearns 2006; Tsou et al. 2009), denotes the loosening of this tight daughter-centriole-to-mother-centriole connection during late mitosis/early G1 phase and results in the disorientation of the two centrioles. After disengagement the two centrioles are only tethered at their proximal ends by the linker protein rootletin via the docking site protein C-Nap1 (and most likely additional proteins), ensuring that the duplicated centrosome functions as one single MTOC until late G2 phase (Fry et al. 1998; Mayor et al. 2000; Bahe et al. 2005).

During 'procentriole formation', the centriole duplication step at the G1 to S phase transition, a new procentriole is assembled at the proximal ends of each existing centriole. This process is initiated by and crucially depends on the formation of an inner 'cartwheel (-like)' structure at the proximal procentriolar end which is composed of the conserved Sas-6 protein (the homologue of *Chlamydomonas* Bld12p) stabilizing the 9-fold symmetry of the canonical centriole (Matsuura et al. 2004; Hiraki et al. 2007; reviewed in Marshall 2007; Nakazawa et al. 2007). These procentrioles then grow in length throughout G2 phase ('procentriole elongation') by the addition of α-/β-tubulin dimers to the centriolar MTs and the assembly of further proteins. Eventually, the procentrioles reach a relatively constant length of approximately 400 nm in a typical human cell (Azimzadeh and Bornens 2007).

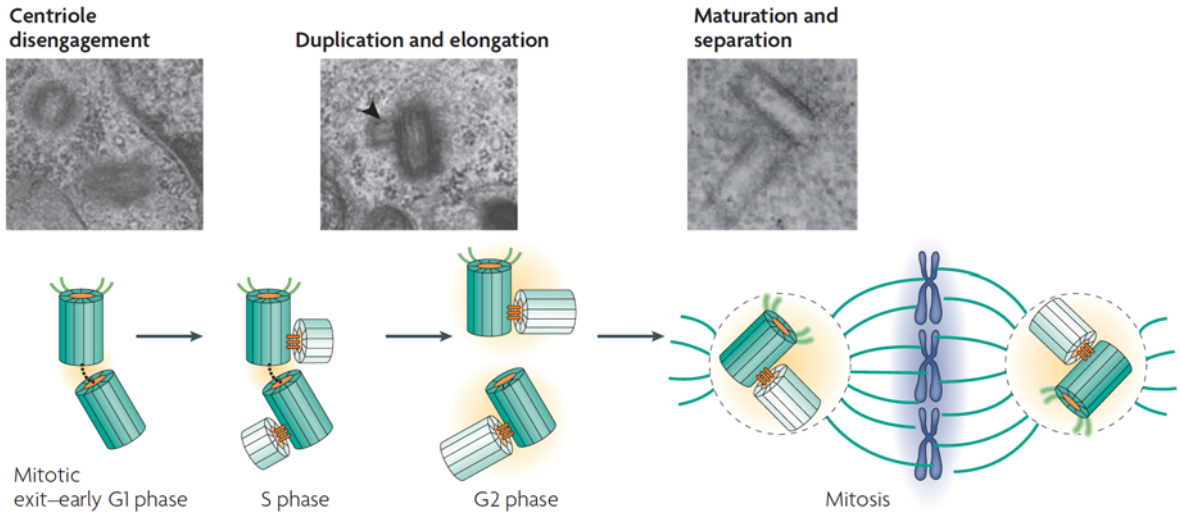

Figure 2: The centrosome cycle. Schematic illustration of the four major events of the centrosome cycle (centriole disengagement, centriole duplication and elongation, centriole maturation and centrosome separation). Mature centrioles are depicted with schematic green appendages at their distal ends. Procentrioles that have not yet acquired their final length are shown in light green. Representative transmission electron microscopy (TEM) images of centrioles are shown above the illustration in the respective cell cycle stage (adapted from Bettencourt-Dias and Glover 2007).

Concomitantly with the late steps of procentriole elongation, the second-oldest of the four centrioles within the cell acquires its maturity markers, the distal and subdistal appendages and the two centriolar pairs start to move apart from one another ('separation and maturation'), thereby generating two separate clouds of PCM (reviewed in Lim et al. 2009). Accordingly, the MT nucleation capacity and centrosome size substantially increase while further PCM proteins are recruited (reviewed in Palazzo et al. 2000; Hoyer-Fender 2009). At the onset of mitosis, the linker components C-Nap1 and rootletin are phosphorylated by the Nek2 kinase and the tether between the two parental centrioles is severed as a consequence of this modification (Mayor et al. 2000; Faragher and Fry 2003; Bahe et al. 2005; Yang et al. 2006). This allows the separated centrosomes to move further apart from one another and define the two opposed spindle poles to orchestrate chromosome separation and cell division during mitosis.

2.3 Centriole Biogenesis and Control of Centriole Length

A precise regulation of centriole duplication during the G1/S transition is essential to guarantee the accurate control of centriole copy numbers. Recent work in protists, invertebrates and vertebrates concurs to reveal an evolutionarily conserved pathway for the formation of centrioles and basal bodies (reviewed in Bettencourt-Dias and Glover 2007; Nigg 2007; Strnad and Gonczy 2008; Bettencourt-Dias and Glover 2009; Nigg and Raff 2009).

It has long been known that centriole duplication in cycling somatic cells occurs only during S phase of the cell cycle, in a timely synchronized fashion with DNA replication. Since this cell cycle stage is characterized by the rise of cyclin dependent kinase 2 (Cdk2) activity, comprehensive studies on its function in centriole replication were initiated already in the late 90's (reviewed in Hinchcliffe and Sluder 2002). Inhibition of *Xenopus* Cdk2 blocked centrosome duplication *in vivo* and *in vitro* (Hinchcliffe et al. 1999; Lacey et al. 1999). Thereafter, the requirement of Cdk2/Cyclin-E activity for mammalian procentriole formation was demonstrated (Matsumoto et al. 1999; Hinchcliffe et al. 2001). Moreover, Cyclin-A, was shown to be a pivotal positive regulator of centrosome duplication or reduplication (Lacey et al. 1999; Meraldi et al. 1999; De Boer et al. 2008). Orc1, which is recruited to the centrosome by a mechanism involving Cyclin-A, restricts Cyclin-E dependent centrosome reduplication (Hemerly et al. 2009). Nevertheless, $Cdk2^{-/-}$ knockout mice are viable and show no centriole duplication defects suggesting that Cdk1 activity might compensate for Cdk2 function (Berthet et al. 2003; Ortega et al. 2003).

2.3.1 Centriole Biogenesis in *Caenorhabditis elegans*

Similar to the process in human cells, several conserved gene products are crucial for centriole biogenesis in *C. elegans*. Despite the significantly shorter length of nematode centrioles (approximately 150 nm) and their tube composition of nine singlet (instead of nine triplet) MTs (O'Toole et al. 2003), the key duplication proteins are the same. Notably, the coiled-coil proteins SAS-5, SAS-6 and SAS-4 assemble sequentially in response to the activation of the protein kinase ZYG-1 (Figure 3; O'Connell et al. 2001; Kirkham et al. 2003; Leidel and Gonczy 2003; Delattre et al. 2004; Leidel et al. 2005; Delattre et al. 2006; Pelletier et al. 2006; Dammermann et al. 2008). Before the start of daughter

centriole formation, during meiosis of the embryonic one-cell stage, SPD-2 and ZYG-1, a functional analogue of Plk4, are Cdk2-dependently recruited to the centrioles (Cowan and Hyman 2006). At pronuclear appearance, coincident with the start of procentriole assembly, ZYG-1 recruits SAS-5 and SAS-6, two coiled-coil molecules that are necessary for the formation and elongation of the central tube of the juvenile centriole. Once the central tube is established, the latter two act together to recruit SAS-4, the homologue of human CPAP, which ultimately assembles nine singlet MTs onto the core structure (Pelletier et al. 2006). According to a recent study, the phosphorylation of SAS-6 by ZYG-1 is pivotal for procentriole formation in *C. elegans* (Kitagawa et al. 2009). Furthermore, homologues of nematode SAS-4 and SAS-6 are essential for centriole biogenesis in all organisms examined (Kilburn et al. 2007; Nakazawa et al. 2007; Rodrigues-Martins et al. 2007).

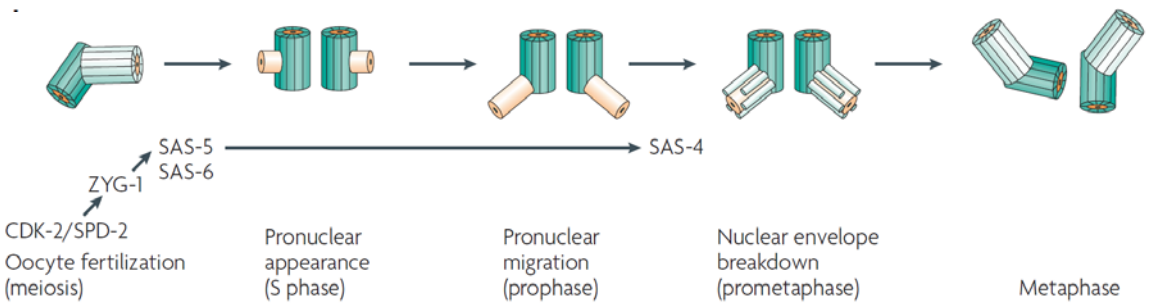

Figure 3: Centriole duplication in *Caenorhabditis elegans*. The schematic illustrates the key steps of nematode centriolar tube formation during the first mitotic division. Although *C. elegans* centrioles are built simpler and are smaller than the human ones, there are only few differences in the assembly process. Daughter centrioles (yellow) are nucleated in S phase and their elongation takes place during G2 phase and mitosis. CDK-2 is important for recruiting SPD-2 to the mother centriole, which is necessary for ZYG-1 recruitment. ZYG-1 in turn recruits the complex that is formed by SAS-5 and SAS-6, which is essential for formation of the inner centriole tube. Formation of the tube is a prerequisite for the action of SAS-4, the homologue of human CPAP, which is needed for the placement of the singlet outer MTs (light green) onto the central tube (adapted from Bettencourt-Dias and Glover 2007).

2.3.2 Centriole Biogenesis in Human Cells

Polo-like kinase 4 (Plk4) has been identified as the pivotal master regulator of centriole duplication in human cells (Habedanck et al. 2005). Depletion of Plk4 inhibits centriole duplication and its overexpression induces centriole amplification, indicating that its physiological levels need to be tightly regulated to ensure centriole copy number control (Habedanck et al. 2005; Duensing et al. 2007; Kleylein-Sohn et al. 2007). Autophosphorylation of active Plk4 at serine 305 primes the protein for its proteolytic degradation and thereby contributes to the precise control of its cellular levels (Sillibourne et al. 2009; Holland et al. 2010). Plk4 is functionally highly conserved and similarly, SAK, the *Drosophila* homologue of PLK4, was identified as a key regulator of centriole duplication (Bettencourt-Dias et al. 2005). Recently, it has been reported that protein expression levels of SAK are regulated by degradation via the SCF/Slimb ubiquitin ligase (Cunha-Ferreira et al. 2009; Rogers et al. 2009).

A first delineation of the human procentriole assembly pathway has been established by the combination of sequential depletion of proteins involved in centriolar duplication and by the analysis of their localization by electron microscopy (EM) and immunofluorescence (IF) microscopy. This study has been conducted in U2OS osteosarcoma cells carrying an inducible Plk4 transgene, showing procentriole amplification in a 'flower-like' pattern around the parental centriole (Kleylein-Sohn et al. 2007). Accordingly, at the transition from G1 to S phase, Plk4 recruits Sas-6, a protein solely found on immature centrioles, before γ-tubulin (Kleylein-Sohn et al. 2007), CPAP/CenpJ (Hung et al. 2000) and Cep135 (Ohta et al. 2002) are placed at the core procentriolar tube and CP110 at its distal end (Figure 4).

Two of these centriole duplication proteins are the subjects of the present study: First, CPAP (centrosomal P4.1-associated protein), the putative homologue of *C. elegans* SAS-4 (Hung et al. 2000; Leidel and Gonczy 2003), is of considerable medical interest as homozygous mutations in the corresponding gene (*CENPJ*) cause primary recessive microcephaly (Bond et al. 2005; Gul et al. 2006). Its structure comprises five coiled-coil domains, a glycine-rich C-terminus, several potential destruction motifs (seven putative D boxes and two putative KEN boxes) and a tubulin dimer binding domain (Hung et al. 2000; Hsu et al. 2008; Tang et al. 2009). CPAP was initially identified as an interactor of protein 4.1R which localizes to distal/subdistal regions of mature centrioles and displays MT-organizational functions *in vitro* (Hung et al. 2000; Perez-Ferreiro et al. 2004; Krauss

et al. 2008). Depletion of CPAP in Plk4-overexpressing human cells inhibits the formation of multiple daughter centrioles (Kleylein-Sohn et al. 2007).

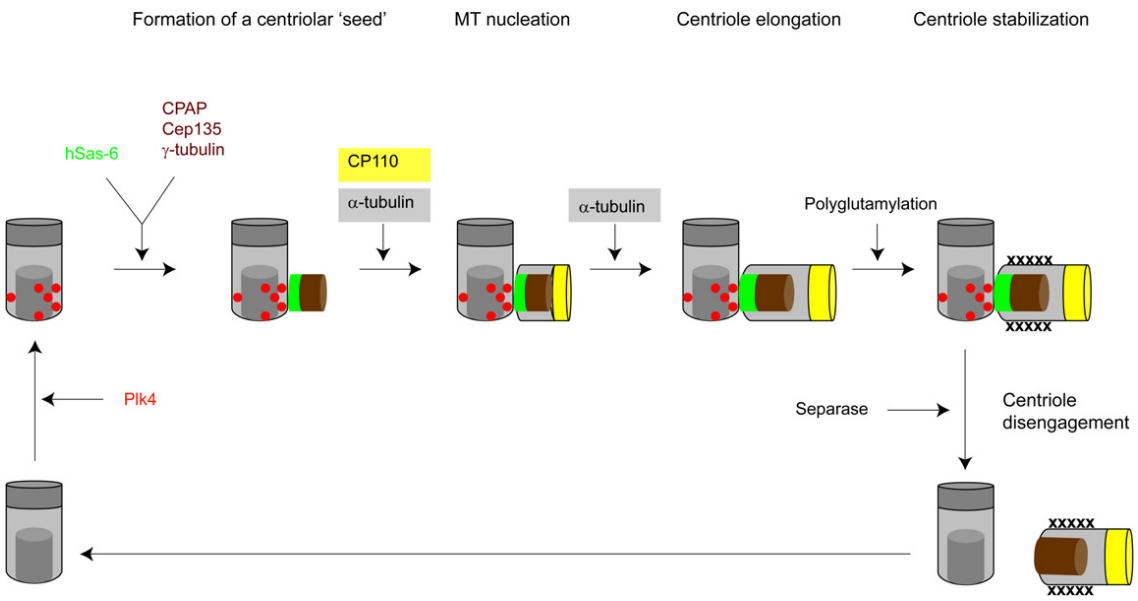

Figure 4: Centriole assembly in human cells. Nascent procentriolar structures are depicted coding Plk4 (red), Sas-6 (green), α-tubulin (gray), CP110 (yellow) and CPAP, Cep135, and γ-tubulin in brown. For simplicity the parental centriole is depicted in gray and polyglutamylation on the parental centriole is omitted (adapted from Kleylein-Sohn et al. 2007).

Second, CP110, which was originally identified as a substrate of Cdk2, contains a KEN box and a D box, and is highly conserved from mice to humans (Chen et al. 2002). Over the cell cycle, CP110 protein levels increase as cells progress into S phase and are diminished when cells complete mitosis or arrest in G0 (Chen et al. 2002). CP110 physically interacts with centrin and calmodulin *in vivo* and upon its depletion, cells display cytokinesis defects and binucleation after mitosis (Tsang et al. 2006). The protein specifically localizes to the distal tips of both parental and nascent centrioles, suggesting a capping function during centriole biogenesis (Kleylein-Sohn et al. 2007). In this regard, it is noteworthy that CP110 is recruited to nascent procentrioles very early during centriole duplication at a time when the procentrioles are very short and before the procentriolar MTs start to elongate (Kleylein-Sohn et al. 2007). Ultimately, after the MTs have

elongated by the addition of tubulin throughout G2 phase, they are stabilized by posttranslational polyglutamylation.

2.3.3 Control of Centriole Length during Procentriole Formation

Despite the rapidly advancing understanding of centriole duplication, it remains unknown how procentriole growth is promoted in human cells, how tubulins and other centriolar proteins are added to elongating procentrioles, which proteins control accurate centriolar length and how further growth is prevented once the final length has been achieved. In general, centriole length in mammals is considered to be highly constant throughout all tissues and developmetal stages, while it varies between different stages of *Drosophila* development, with centrioles reaching enormous lengths in spermatids (more than 10-fold increased compared to somatic cells; Gonzalez et al. 1998).

Within the past year, two studies identified the first two proteins that contribute to centriole elongation. Bornens and co-workers found that the Centrin2-binding centriolar protein POC5 (proteome of centrioles) is needed for the elongation of nascent procentrioles in human cells (Azimzadeh et al. 2009) and the Marshall laboratory reported that POC1 is required for the establishment of centriole length and that its overexpression leads to elongated centriole-like structures in U2OS cells (Keller et al. 2009). Homologues of both POC5 and POC1 had earlier been identified as basal body components in the algae *Chlamydomonas* (Keller et al. 2005). Human POC5 localizes to the distal end of centrioles, is not required for centriole duplication and reveals an evolutionary divergence between vertebrates and organisms like *Drosophila melanogaster* or *Caenorhabditis elegans* (which assemble modified shorter centrioles), raising the possibility that the loss of POC5 may correlate with the structural differences of their centrioles (Azimzadeh et al. 2009). POC1, in contrast, is essential for centriole duplication and is localized to centrioles via its WD40 domains (Keller et al. 2009).

2.4 Centrosome Abnormalities and Cancer

Almost one century ago, Theodor Boveri proposed a direct link between centrosomal aberrations, chromosome aneuploidy and tumorigenesis. Based on his observations in

horse nematode eggs, he proposed that aberrations in centrosome numbers might contribute to the development of cancer through malfunctional mitosis and the generation of multipolar spindles (Boveri 1914). Over the past years, Boveri's proposal has increasingly regained interest because it became clear that centrosome amplification is a hallmark of several tumor cells (Fukasawa et al. 1996; Lingle et al. 1998; Pihan et al. 1998; Carroll et al. 1999; Ghadimi et al. 2000; D'Assoro et al. 2002; Lingle et al. 2002; Nigg 2002; Pihan et al. 2003; Saunders 2005; Nigg and Raff 2009; Zyss and Gergely 2009). Especially human carcinomas show high incidences of numerical and structural centrosome aberrations, often already at early proliferative stages (Table 1; reviewed in Zyss and Gergely 2009). Intriguingly, in *Drosophila* experimental transplantation of tissue containing extra centrosomes can initiate aggressive tumors in wild-type host flies (Basto et al. 2008).

Cancer type	Centrosome analysis		Centrosome abnormalities	Early lesions
	Marker	Method		
Bladder cancer	γ-tubulin Aurora-A	IHC	N	
Breast (invasive)	Centrin γ-tubulin	IHC, EM	N, S	
Breast (DCIS)	Centrin	IHC	N	✓
Breast (DCIS, invasive)	γ-tubulin	IHC		✓
Hepatocellular carcinoma	Pericentrin	IHC	N, S	✓
Non-small cell lung cancer	Pericentrin γ-tubulin	IHC	N, S	
Pancreatic DC	Pericentrin γ-tubulin	IHC	N, S	✓
Prostate cancer	Pericentrin	IHC	N, S	
Breast, prostate, lung, colon	Pericentrin	IHC	N, S	
Breast, cervix, prostate (pre-invasive)	Pericentrin	IHC	N, S	✓
Myeloma	Centrin γ-tubulin Pericentrin	ICC	N	✓
B-CLL	γ-tubulin	ICC		
CML	Pericentrin	ICC	N, S	✓
AML	Pericentrin	ICC	S	
Non-Hodgkin's lymphoma	γ-tubulin Pericentrin	ICC	S	
Burkitt's lymphoma	γ-tubulin	ICC	N, S	

Table 1: Centrosome abnormalities in human cancers. Abbreviations: AML, acute myeloid leukaemia; B-CLL, B cell chronic lymphocytic leukaemia; CML, chronic myeloid leukaemia; DC, ductal carcinoma; DCIS, ductal carcinoma in situ; EM, electron microscopy; ICC, immunocytochemistry; IHC, immunohistochemistry; N, numerical; S, structural (adapted from Zyss and Gergely 2009).

In principle, five mechanisms exist how cells can accumulate additional centrosomes. First, they can arise by deregulation of centriole duplication, as it has been observed in transformed U2OS osteosarcoma or Chinese hamster ovary (CHO) cells, after the induction of S phase arrest by aphidicolin or hydroxyurea (Balczon et al. 1995; Meraldi et al. 1999). In addition, other studies have shown that the overexpression of the centrosomal kinase Plk4, Sas-6 or the human papillomavirus protein E7 induces centriole amplification in human cells (Duensing et al. 2000; Habedanck et al. 2005; Leidel et al. 2005). Second, failures during cell division can result in tetraploid G1 cells with twice the number of centrosomes. This could be caused either by delay of the spindle assembly checkpoint, by damaged and unrepaired DNA, or by deregulation of cytokinesis (Nigg 2002). A third scenario for the generation of supernumerary centrosomes is cell fusion. The ectopic expression of the RAD6 ubiquitin-conjugating enzyme, for example, leads to cell fusion-induced centrosome amplification (Shekhar et al. 2002). A fourth possible mechanism relates to the *de novo* formation of centrioles (Dirksen 1991; La Terra et al. 2005). In differentiated ciliated epithelia hundreds of centrioles can form from amorphous EM-dense granules composed of various centrosomal proteins (Dawe et al. 2007; Vladar and Stearns 2007). Although spontaneous *de novo* centriole formation in cycling somatic cells is normally prevented by the existing centrioles, it can also be artificially induced by the removal of existing centrioles via laser ablation or microsurgery (Khodjakov et al. 2002; La Terra et al. 2005; Uetake et al. 2007; Loncarek et al. 2008). Lastly, Khodjakov and co-workers have recently reported that PCM size may be a critical regulator of procentriole numbers. Overexpression of the PCM component pericentrin in CHO cells resulted in exaggerated PCM clouds containing two mature centrioles and many associated centrioles at different levels of maturation, challenging the long-standing view that centriole number is determined by a centriolar assembly template (Loncarek et al. 2008; reviewed in Salisbury 2008).

However, excessive numbers of centrioles/centrosomes do not inevitably lead to multipolar spindles in dividing cells (Acilan and Saunders 2008). Several mechanisms exist to limit the detrimental consequences of supernumerary centrosomes and enable the formation of a bipolar mitotic spindle. These include centrosome removal, centrosome inactivation, asymmetric segregation of centrosomes and centrosome clustering (Figure 5; reviewed in Godinho et al. 2009). Among these four mechanisms, centrosome clustering has attained much scientific interest over the past years. Several cell lines seem to

overcome spindle defects by mechanisms that cluster excess centrosomes at the two poles during mitosis (Quintyne et al. 2005; Saunders 2005; Basto et al. 2008; Kwon et al. 2008; Yang et al. 2008). An explanation for the generation of chromosomal instability (CIN) despite efficient centrosomal clustering was recently given by the analysis of transient 'multipolar spindle intermediates' (Ganem et al. 2009). Accordingly, merotelic kinetochore-MT attachment errors accumulate before the centrosomes are clustered and this leads to frequent lagging chromosomes during anaphase. This observation not only provides a possible reason for the high correlation between centrosome amplification and CIN, but furthermore gives a simple and unifying explanation for the observed high rates of merotely in these cancers.

Despite these recent advances in centrosome biology, the question whether supernumerary centrosomes are a cause or only a consequence of tumor formation remains unresolved until now (Nigg 2002).

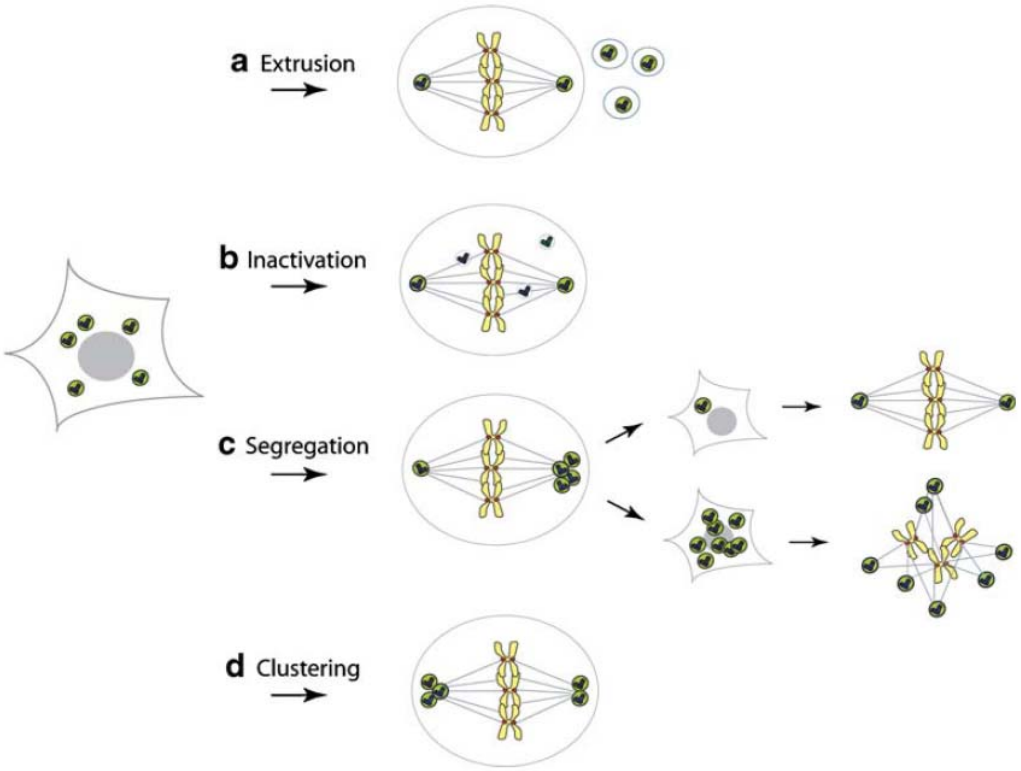

Figure 5: Mechanisms to suppress multipolar mitosis in cells with too many centrosomes. The schematic illustrates four distinct mechanisms how bipolar mitosis is enabled in cells with extra chromosomes. (a) Centrosome extrusion; cells can expel extra centrosomes by the formation of cytoplasts containing centrosomes. (b)

Centrosome inactivation; a bipolar mitosis is achieved in the presence of extra centrosomes by silencing MTOC activity. Some extra centrosomes are incapable of functioning as MTOC due to loss of PCM. (c) Asymmetric segregation of centrosomes into two daughter cells and potential clonal expansion. A daughter cell that inherits one centrosome forms a bipolar spindle in a subsequent mitosis. (d) Centrosome clustering at the two opposed spindle poles (adapted from Godinho et al. 2009).

2.5 Structure and Functions of Cilia

Cilia are conserved organelles that have appeared early in the evolution of eukaryotes. They have initially been recognized more than 100 years ago in rabbit and human kidney (Zimmermann 1898). In general, one can distinguish between immotile, singular primary cilia, motile cilia and flagella (reviewed in Dawe et al. 2007). Cilia are important for a wide variety of vertebrate developmental and cellular functions, including morphogenetic signaling during early embryogenesis, cell motility, the reception of mechanical and chemical cues and brain development (reviewed in Gerdes et al. 2009; Han and Alvarez-Buylla 2010; see also Figure 6). For instance, flagellar propulsion enables sperm motility or the motile cilia-covered surface of *Paramecium* allows its movement within its surrounding liquid environment. Motile ciliary epithelia are also required to clear the human airway duct or to propel oocytes forward in the oviduct.

Single primary cilia are sensory organelles that act as transducer of extracellular stimuli into intracellular signaling (Satir and Christensen 2007; Gerdes et al. 2009): The ciliary membrane is a specialized and close-meshed compartment for receptor signaling, which has been documented for the 12 trans-membrane receptor (TMR) Patched and the 7 TMR Smoothened receptors, both implicated in hedgehog signaling (Rohatgi et al. 2007; Kovacs et al. 2008), the receptor tyrosine kinase PDGFRα (Schneider et al. 2005) and the Wnt signaling pathways (Gerdes et al. 2007). Many essential downstream components of these pathways as well as for neurotransmission and extracellular matrix interaction uniquely localize to the cilium (reviewed in Michaud and Yoder 2006; Singla and Reiter 2006; Christensen and Ott 2007; Christensen et al. 2007; Berbari et al. 2009; Veland et al. 2009).

For example, primary cilia mechanically sense liquid flow in nephronal ducts. Furthermore, they are implicated in the development of the body's left-right asymmetry

(Nonaka et al. 1998). Lower plants, such as mosses and ferns that lack centrioles and cilia in most cells, suddenly form them during spermatogenesis (Marshall 2009).

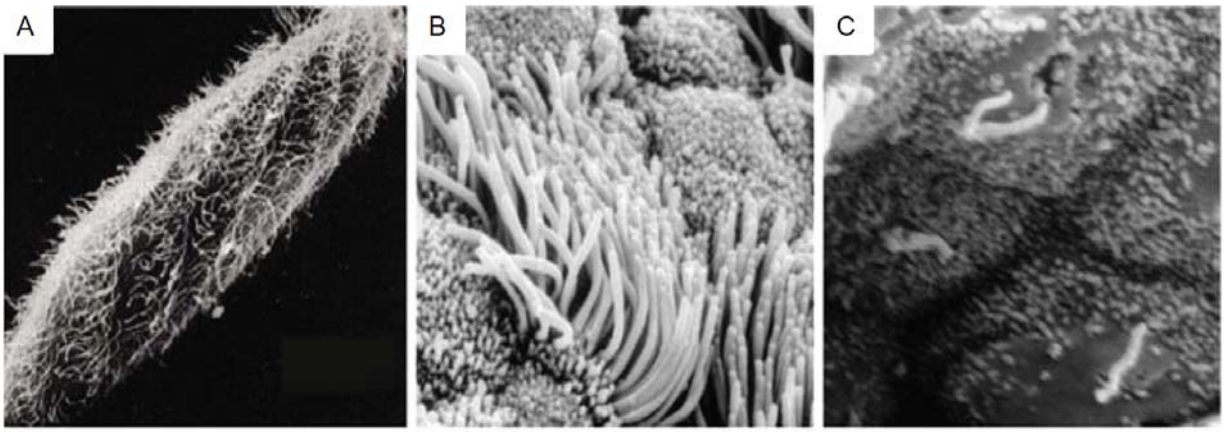

Figure 6: Motile and primary cilia in diverse organisms and cell types. Scanning electron micrographs showing different types of cilia. **(A)** The protozoan *Paramecium* is covered with motile cilia that enable swimming. **(B)** Motile cilia in the multi-ciliated mammalian trachea. **(C)** Primary cilia in renal tubule epithelia cells (adapted from Pazour et al. 2000; Rosenbaum and Witman 2002; Badano et al. 2006).

The ciliary/flagellar structure is based on a common building plan of membrane-covered MTs that protrude from the cell surface into the extracellular space. Each entity contains an outer cylindrical array of doublet axonemal MTs, arranged in a nine-fold symmetry continuing the centriole/basal body ultrastructure (Satir and Christensen 2007; Marshall 2008). The structure of a basal body itself is the same as the one of the centriole, but basal bodies additionally contain a transition zone at their distal end contiguous with the ciliary axoneme (Figure 7).

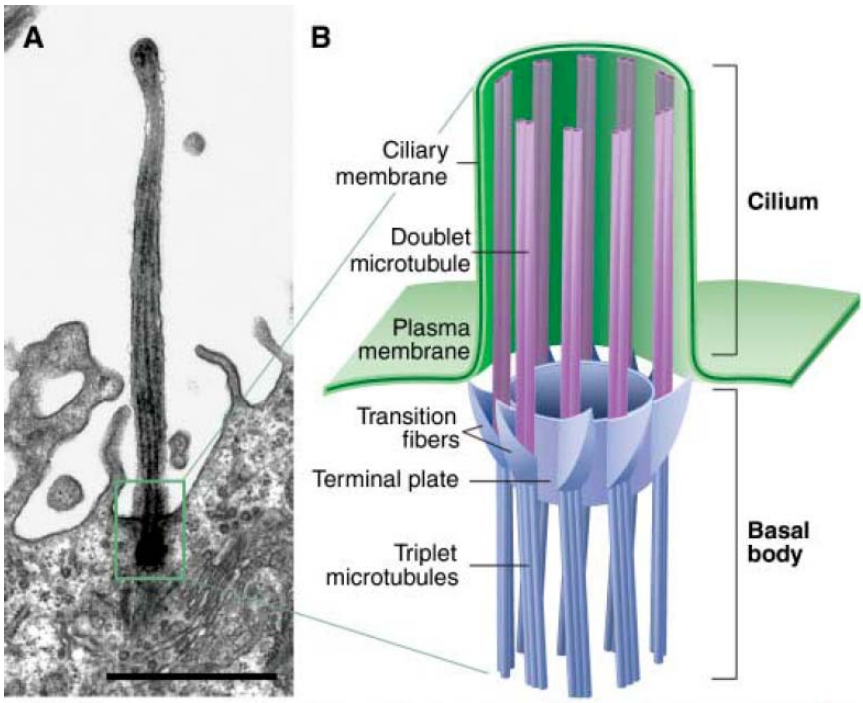

Figure 7: Structure of the basal body/ciliary transition zone. (A) Electron micrograph of a primary cilium of a canary brain radial glia cell. Scale bar represents 1 µm. **(B)** Shematic showing the structure of a basal body, the transition zone and the basal part of a primary cilium (adapted from Singla and Reiter 2006).

Primary and motile cilia fundamentally differ in their central structure and their occurrence. In contrast to the axonemes of non-motile primary cilia, which completely lack not only motor proteins but also the two central MTs (9+0), axonemes of motile cilia are composed of a central pair of singlet MTs surrounded by nine outer MT doublets (9+2) and contain axonemal dyneins that confer ciliary beating (Figure 8; reviewed in Salathe 2007; Satir and Christensen 2007). Their outer MTs are interconnected by nexin links and dynein arms (whose ATPase activity generates the beating) and radial spokes reach towards the two inner MTs (reviewed in Ibanez-Tallon et al. 2003). Furthermore, whereas primary cilia usually occur solitarily, epithelial cells may possess several hundreds of motile cilia and an according number of basal bodies (e.g. in the mammalian trachea or the female Fallopian tubes).

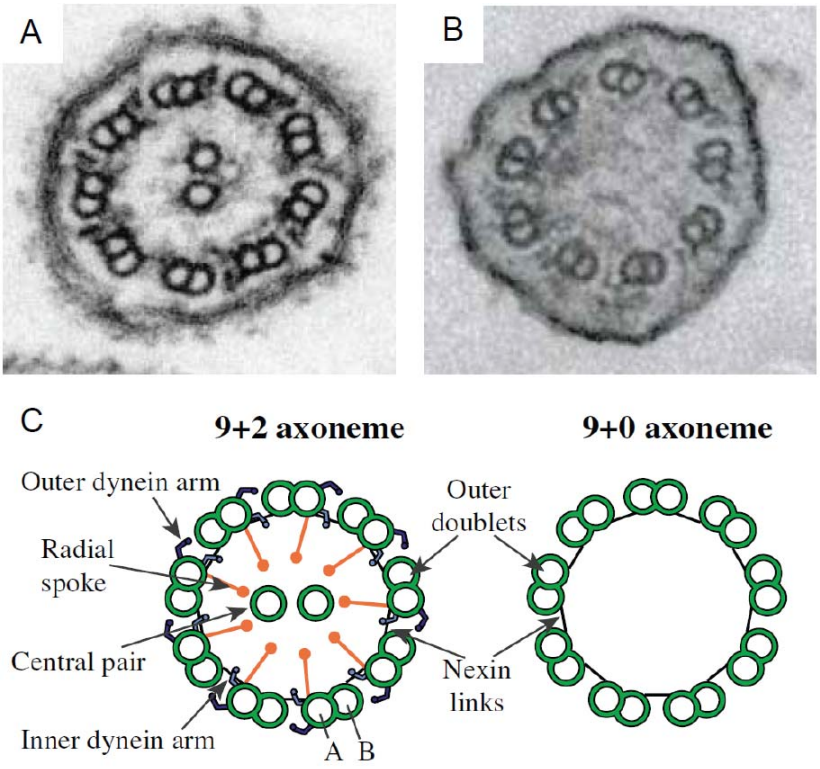

Figure 8: Structural difference between motile (9+2) and primary (9+0) cilia. TEM images of cross-sections through **(A)** a *Chlamydomonas* cilium and **(B)** a mouse nodal cilium. **(C)** Shematic comparing the structures of the canonical motile 9+2 axoneme and an immotile 9+0 axoneme (adapted from Takeda et al. 1999; Pazour and Rosenbaum 2002; Dawe et al. 2007).

Entailed by these structural differences it is plausible to think that motile cilia solely exert mechanical force whereas only primary cilia serve sensory functions. Contrary to this concept, however, human airway epithelium expresses sensory bitter taste receptors which localize on motile cilia, thereby unifying both attributes (Shah et al. 2009).

2.6 Formation and Disassembly of Primary Cilia

Assembly of cilia occurs either when cells exit mitosis and proceed into a quiescent/stationary state (G0) or when cells ultimately differentiate within specialized tissues. Cilia formation requires a signaling network that includes the translocation of the former centrioles (which are then called 'basal bodies') towards the plasma membrane, the fusion of Golgi-derived vesicles at the distal end of the mature basal body (see Figure 9; reviewed in Satir and Christensen 2007), the anchoring to the membrane presumably via centriolar distal appendage structures (Ishikawa et al. 2005; Graser et al. 2007) and the targeting of further proteins to the axonemal area (reviewed in Hoyer-Fender 2009). As a first candidate protein of the latter step, the conserved HYLS-1, for example, has recently been linked to the functionality of axonemal basal body extension (Dammermann et al. 2009). Ciliogenesis is furthermore dependent on the biogenesis of the ciliary membrane by the BBS proteins and Rab8 (Nachury et al. 2007) and on intraflagellular transport (IFT) proteins, which carry a broad range of proteins across the ciliary compartment border and along the axoneme to their functional assembly sites and *vice versa* (reviewed in Pedersen and Rosenbaum 2008).

Interestingly, primary cilia grow in a timely asynchronous fashion such that the sister cell receiving the older of the two mature centrioles after mitosis grows the cilium first (Anderson and Stearns 2009). Furthermore, this asynchronous fashion is also manifested in the cell's response to sonic hedgehog and PDGF signaling.

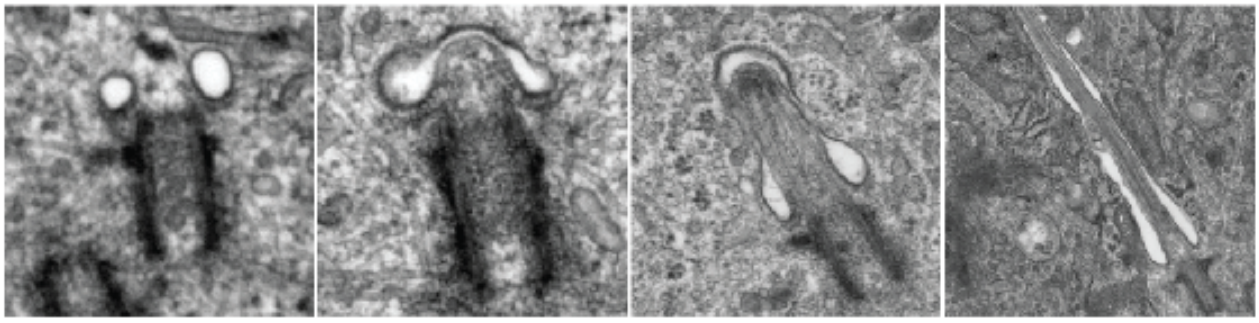

Figure 9: Fusion of Golgi-derived vesicles at the mature basal body during early ciliogenesis. TEM images showing four different stages of primary cilium formation in astrocytes. Note how vesicles are first placed at the distal end of the future basal body and then fuse prior to axoneme formation and cilia assembly (adapted from Moser et al. 2009).

In contrast to highly specialized cell types, G0-arrested cells have the capacity to resorb primary cilia and re-enter the cell cycle upon serum stimulation. It is known that the ciliary disassembly machinery in human cells is promoted by growth factor stimulation of HEF1, which activates Aurora kinase A and leads to the phosphorylation of the deacetylase HDAC6, which then deacetylates the ciliary axoneme, finally leading to ciliary resorption (Pugacheva et al. 2007). Several studies in the green algae *Chlamydomonas reinhardtii* (the last common ancestor of plants and animals), have begun to dissect flagellar resorption and have identified an altered IFT machinery (reviewed in Quarmby 2004; Bradley and Quarmby 2005; Pan and Snell 2005) as well as the ubiquitin conjugating system (Huang et al. 2009) as being essential for this process.

The mechanisms controlling vertebrate ciliary length are largely unknown, but recent studies claim that primary cilium length is, at least in part, controlled by the adenylate cyclase III-cAMP signaling pathway and can significantly be enhanced by treatment with lithium or with compounds that decrease intracellular calcium levels (Miyoshi et al. 2009; Ou et al. 2009; Besschetnova et al. 2010). Furthermore, primary cilium length, in particular in renal cells, may be adaptable depending on flow intensity (Besschetnova et al. 2010). Flagellar length has been intensively studied in *Chlamydomonas* and many genetic defects and changes of the extra- and intracellular environment have been identified contributing to its establishment (reviewed in Wemmer and Marshall 2007; Wilson et al. 2008). The ciliate *Tetrahymena thermophila* is an organism in which ciliary defects can be rather easily monitored, for instance showing that the motor complex component Dynein-2 is critical for the acquisition of genuine ciliary length (Rajagopalan et al. 2009).

2.7 Cilia-related Human Diseases

Cilium formation is a yet insufficiently understood process of high complexity that involves many steps such as the docking of basal bodies onto the plasma membrane, the extension of the ciliary axoneme and the functional bidirectional IFT system (reviewed in Pedersen and Rosenbaum 2008). Interference with any of these steps can either cause the formation of malfunctional cilia or even their complete lack. Not surprisingly, therefore, the number of human disorders known to relate to mutations in basal body or cilium-

associated genes is rapidly growing. Although these diseases, termed 'ciliopathies', are caused by the malfunction of one organelle, they encompass a variety of disorders and affected organs (reviewed in Badano et al. 2006; Fliegauf et al. 2007; Marshall 2008; Sharma et al. 2008; Lancaster and Gleeson 2009). The pleiotropic defects caused by gene products normally localizing to and fulfilling their function at either cilia or basal bodies are a characteristic of this class of diseases, as for example the Bardet-Biedl (Ansley et al. 2003), Meckel-Gruber (Frank et al. 2007), Joubert (Valente et al. 2006) and Senior-Løken (Omran et al. 2002) syndromes. Symptomes of these diseases, that result from mutations of ciliary genes, are defects in the development of left-right asymmetry, sperm infertility, obesity (BBS genes), hearing loss (ALMS1), retinal degeneration (RPGR), fibrocystic (NPHP genes) and polycystic kidneys (IFT/PKD genes), brain (Joubert syndrome-associated genes) and oral-facial-digital malformations (OFD1) or the respiratory tract (summarized in Table 2). Currently, most of the reports on these diseases are based on genome-wide sequencing of patients or on the phenotypic description of mouse models but their precise etiology is widely unknown.

	PKD	NPHP	MKKS	SLSN	EVC	JATD	OFD	ALMS	JS	BBS	MKS
CNS malformations					●	●	●	●	●	●	●
Cystic kidney	●	●		●		●	●	●	●	●	●
Diabetes								●		●	
Gonadal malformations			●		●					●	●
Heart disease			●		●			●		●	
Hepatic dysfunction	●	●		●		●	●	●	●	●	●
Mental retardation/Developmental delay					●	●	●		●	●	●
Obesity								●		●	
Polydactyly			●		●	●	●		●	●	●
Pulmonary dysfunction								●			
Retinal degeneration				●		●		●	●	●	
Left–right asymmetry defects		●		●		●			●	●	●
Skeletal defects					●	●	●				

PKD, polycystic kidney disease; NPHP, nephronophthisis; MKKS, McKusick–Kaufman syndrome; SLSN, Senior–Løken syndrome; EVC, Ellis-van Creveld; JATD, Jeune asphyxiating thoracic dystrophy; OFD, orofaciodigital syndrome; ALMS, Alström syndrome; JS, Joubert syndrome/Cerebello-oculo-renal syndrome; BBS, Bardet–Biedl syndrome; MKS, Meckel–Gruber syndrome; CNS, Central nervous system.

Table 2: Principal phenotypes observed in different ciliopathies. The table illustrates the broad pleiotropic appearance of the most prominent clinical symptoms across human diseases that are related to malfunctional cilia (adapted from Cardenas-Rodriguez and Badano 2009).

3. AIM OF THIS PROJECT

The aim of this study was, first, to scrutinize functions of the centriolar protein CP110. It was found to have crucial roles in the control of centriole length and ciliogenesis. During the course of these investigations, it became clear that CPAP/CenPJ is a key regulatory protein for the determination of centriole length in human cells as well. Based on these results, this study was extended to address the question how these two proteins control the length of human centrioles and to investigate which other centriolar/basal body proteins might be required for procentriole elongation and the control of centriole length.

4. RESULTS

Before I started my work in the laboratory, a proteomic search for novel human centrosomal proteins had been performed in the human T-lymphoblastoid cell line KE37 by our group (Andersen et al. 2003). Among the mammalian proteins found in this study were CP110 and CPAP, two proteins that had been implicated to have a function in centriole duplication and biogenesis. It was known that CP110, having been identified as a substrate of the kinase Cdk2, is required for centrosome duplication (Chen et al. 2002; Tsang et al. 2006). Human CPAP/CenPJ displays high homology to SAS-4, a protein required for centriole duplication in the nematode *C. elegans* and had been associated with the γ-tubulin complex and microtubular functions (Hung et al. 2000; Hung et al. 2004).

During the course of this work, antibodies and cell lines were first produced to address the questions mentioned above. Encouraged by immunoprecipitations (IPs) of CP110, we then examined changes of centriolar proteins that had been identified as interaction partners of CP110 during ciliogenesis. Moreover, we characterized the striking centriolar phenotypes observed upon the deregulation of the cellular levels of CP110 and CPAP, suggesting their involvement in centriolar length control. Further experiments aimed at dissecting the differences between the generated elongated centrioles in cycling cells and primary cilia forming upon serum starvation in quiescent cells. Finally, by utilization of an inducible myc-CPAP cell line in a small interfering RNA (siRNA)-based inventory screen, we identified further proteins with a role in the control of centriole length.

4.1 Generation of Anti-CP110 Antibodies and of a Cell Line to Induce CPAP Overexpression

4.1.1 Production of Polyclonal Anti-CP110 Antibodies

In order to study the centriolar functions of CP110, polyclonal antibodies were raised in rabbits against the N-terminal sequence of CP110. The purified His-tagged antigen comprised the first 150 residues of the protein (aa1-149; see Figure 10; A) and had previously been proven successful for antibody production in a different laboratory (Chen et al. 2002). Sera from two different animals were compared to the respective pre-immune sera, tested positive for a strong immune response and were affinity purified (only one of the two affinity purified sera is characterized and used for further experiments in this study). Antibody specificity was confirmed by Western blotting and IF microscopy after depletion of the protein for 48 hours. In Western blot analysis the antibody detected a band of approximately 125 kDa molecular weight. After siRNA-mediated protein depletion with two different oligonucleotides targeting CP110 (# 290 and # 291), CP110 protein levels were significantly reduced in U2OS, HEK293T (Figure 10; B) and HeLa S3 cells (data not shown). Analysis of U2OS cells by IF microscopy demonstrated a reduced detection of centriolar CP110 by the antibody after the depletion of the protein with siRNA oligonucleotides, while Cep135 remained present with an unaltered intensity at the centrioles (Figure 10; C). In centrosome purifications that were obtained by sucrose gradient centrifugations from human KE37 cell lysates (Kellogg et al. 1994; Bornens and Moudjou 1999; Andersen et al. 2003) the bulk of CP110 co-fractionated with the centriolar proteins Cep135 and Sas-6 (data not shown).

Furthermore, U2OS cells stained with anti-CP110 polyclonal antibodies showed specific variations in the appearance of the protein over the cell cycle when analyzed by IF microscopy. According to the number of centrioles present in each cell, the number of visible CP110-positive dots doubled early during procentriole formation between G1 phase (2 CP110 dots/cell) and S/G2 phase (4 CP110 dots/cell; Figure 10; D). This pattern confirmed previous studies showing that CP110 is recruited to nascent procentrioles at very early stages of centriole duplication during the G1/S transition and permanently remains at the distal ends of centrioles, irrespectively of their maturation state (Chen et al. 2002; Kleylein-Sohn et al. 2007).

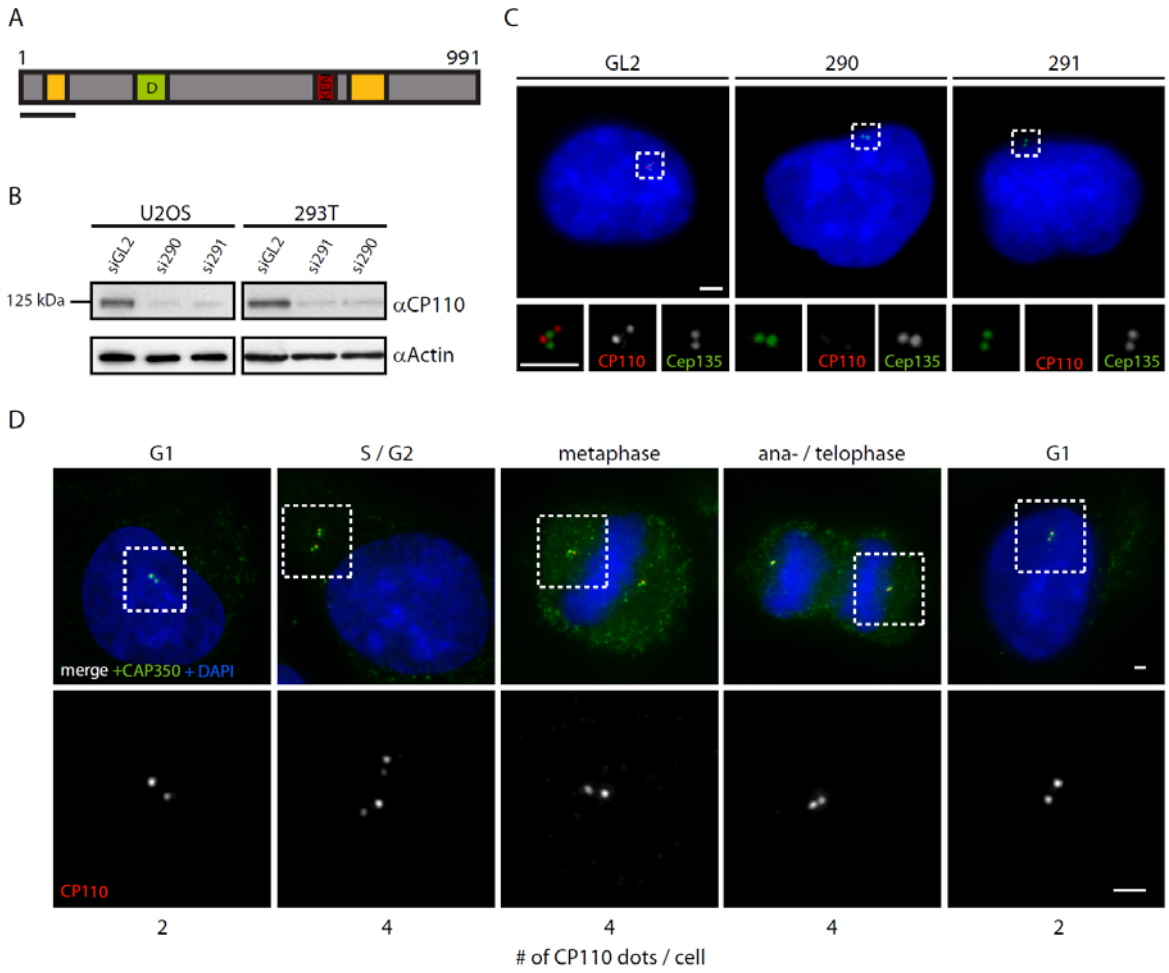

Figure 10: Specificity of polyclonal anti-CP110 antibodies. (A) Schematic representation of human CP110. Coiled-coil regions are illustrated in yellow, the D and KEN box destruction motifs in green and red, respectively. The region used as antigen for the generation of CP110 antibodies is depicted by the black bar below. **(B)** Western blot confirming the specificity of the antibodies raised in rabbits by siRNA-mediated CP110 protein depletion in U2OS and 293T cells. The cells were treated with two different siRNA oligonucleotides targeting CP110 and GL2 (control) for 48 hours, respectively. Cell lysates were probed with polyclonal anti-CP110 antibodies and anti-Actin as loading control. **(C)** IF analysis of U2OS cells after depletion with GL2 (control) and two different CP110 siRNA oligonucleotides for 48 hours. CP110 (red), Cep135 (green) and DAPI (blue) are visualized. The insets show a 3-fold magnification of the boxed areas. **(D)** Visualization of CP110 over the cell cycle. U2OS cells were fixed and stained with anti-CP110 (red) and anti-CAP350 (green) antibodies (DNA was stained with DAPI, blue). Note that cells in G1 phase show two distinct CP110 dots, whereas four centriolar CP110 dots are seen for every cell from S/G2 phases to cytokinesis. The lower panels show only the CP110 staining and represent 3-fold zooms of the boxed areas in the upper panel. All scale bars represent 1 µm.

4.1.2 Generation of Monoclonal Anti-CP110 Antibodies

In addition to the previously described polyclonal antibodies, a monoclonal antibody was raised against CP110 (with the extensive help of E. Bürgelt, E. Nigg and A. Baskaya). After mice had been injected with the HIS-tagged purified CP110 antigen (aa1-149) and an immune response had been monitored, mouse spleen cells were fused to myeloma cells. After initial hybridoma cell clone selections, the supernatants of two positive clones (140-195-5 and 140-195-38) were analyzed in more detail. Protein depletion by siRNA in U2OS cells confirmed the reactivity of the monoclonal anti-CP110 antibodies by Western blotting (Figure 11; A) and IF microscopy (Figure 11; B).

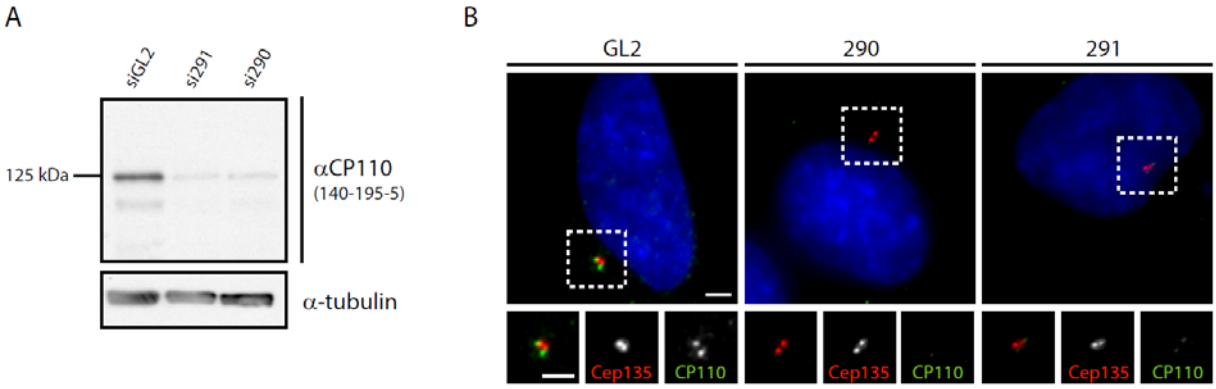

Figure 11: Characterization of the CP110 monoclonal antibody. (A and **B)** U2OS cells were treated with two siRNA oligonucleotides targeting CP110 or GL2 (control) for 48 hours. **(A)** Lysates were then probed with monoclonal CP110 antibodies (clone 140-195-5) to confirm the specificity of the antibody on Western blot level. **(B)** After fixation, U2OS cells were stained for IF microscopy with polyclonal antibodies against Cep135 (red) and monoclonal CP110 antibodies (green). Note that the signal of CP110 is strongly reduced after the depletion, while the IF intensity of Cep135 remains unaltered.

4.1.3 Generation of an U2OS T-REx myc-CPAP Stable Cell Line

To study the centriolar functions of CPAP with more accuracy and higher efficiency than possible by transient overexpression, U2OS T-REx cells (Invitrogen) were transfected with full-length myc-CPAP to obtain clones allowing the inducible overexpression of the protein (carried out by Dr. Jens Westendorf). After two weeks of antibiotic selection with

geneticin, growing colonies were individually selected and subsequently examined by IF microscopy for their myc-CPAP expression after tetracyclin induction. One clone (A7) was finally chosen for further experimental use based on minimal CPAP expression in the absence of tetracyclin. Western blotting demonstrated an increase in myc-CPAP levels over time of induction in the clone selected at a molecular weight of approximately 150 kDa (Figure 12; A). A rough estimate based on quantification of chemiluminescence suggested a 20- to 40-fold increase of CPAP over endogenous levels after tetracycline induction, whereas CP110 levels remained unchanged. IF analysis showed that the bulk of exogenous CPAP was cytoplasmic (data not shown). Fluorescent-activated cell sorting (FACS) was used to detect any cell cycle aberrations after the induction of protein expression. The cell cycle profile of myc-CPAP induced cells, however, remained unaltered after 24 hours of induction (Figure 12; B).

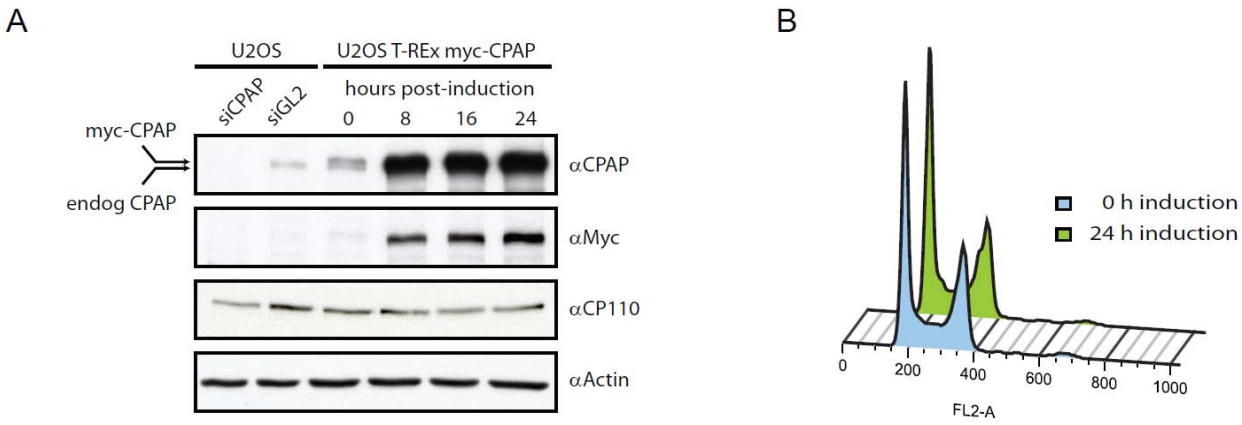

Figure 12: Characterization of the myc-CPAP U2OS T-REx cell line. (A) myc-CPAP was induced for 0 - 24 hours, and cell lysates were probed by Western blotting with the indicated antibodies. Actin was monitored as a loading control. Lysates from U2OS cells treated for 48 hours with GL2 or CPAP siRNA were analyzed in parallel for comparison of protein levels. Note that CP110 levels remain unaltered upon the induction of CPAP expression. **(B)** CPAP expression was induced in U2OS T-REx cells for 0 or 24 hours and cell cycle profiles were analyzed by FACS (both Figures were prepared by Dr. Jens Westendorf and are published in Schmidt et al. 2009).

4.2 CP110 in Ciliogenesis

4.2.1 CP110 and Cep97 are Absent from the Ciliated Basal Body

With the raised and characterized anti-CP110 antibodies IPs of endogenous CP110 were performed to identify novel interaction partners of the protein. To acquire a profound dataset of candidate proteins, samples from two independent IPs were separated on gels, excised and subsequently subjected to mass spectrometry (MS) analysis. Several proteins that had previously been reported to be part of the centrosomal proteome (Andersen et al. 2003) were found to co-precipitate with CP110 in these experiments (data not shown). Cep97 and Cep290 were the most prominent proteins found by this approach.

Cep97 (FLJ23047) had already been reported as a 'centrosome candidate' in the proteomic analysis of centrosomal components (Andersen et al. 2003), but further information had remained elusive. Overexpression of the gene product showed no centrosomal localization, but using anti-Cep97 antibodies the co-localization with CP110 at the distal ends of both mature and juvenile centrioles was confirmed (data not shown). Cep290 was known to localize to the centrosome (Valente et al. 2006) and to be a translation product of the NPHP6/CEP290 gene which is mutated in several ciliopathies (den Hollander et al. 2006; Valente et al. 2006; Frank et al. 2007). During the course of this study, both proteins were confirmed as interaction partners of CP110 by publications of Dynlacht and co-workers (Spektor et al. 2007; Tsang et al. 2008).

Because both CP110 and Cep97 localize to the distal ends of centrioles and because our MS analysis had revealed the interaction of CP110 with Cep290, we extended our studies onto hTERT-RPE1 cells. Upon serum starvation these human retinal cells become quiescent and as a result form primary cilia. Intriguingly, after serum starvation CP110 was not present at the mature and ciliated basal body any more, in contrast to its localization in proliferating cells. However, on the juvenile basal body, which is not competent of forming a primary cilium, CP110 remained at the distal tips as we had observed in cycling cells (Figure 13; A). This observation was confirmed by immunogold labelling with anti-CP110 antibodies followed by EM and the difference between the ciliated and the non-ciliated basal body was illustrated explicitly (Figure 13; C).

Accordingly, we asked whether the protein Cep97, which co-localizes and interacts with CP110 in proliferating cells, showed the same alteration in G0-arrested cell populations. Therefore, we fixed serum starved hTERT-RPE1 cells and stained them with

anti-Cep97 antibodies. Notably, Cep97 was also displaced from the ciliated (but not the juvenile) basal body, mirroring the situation we had observed for CP110 (Figure 13; B).

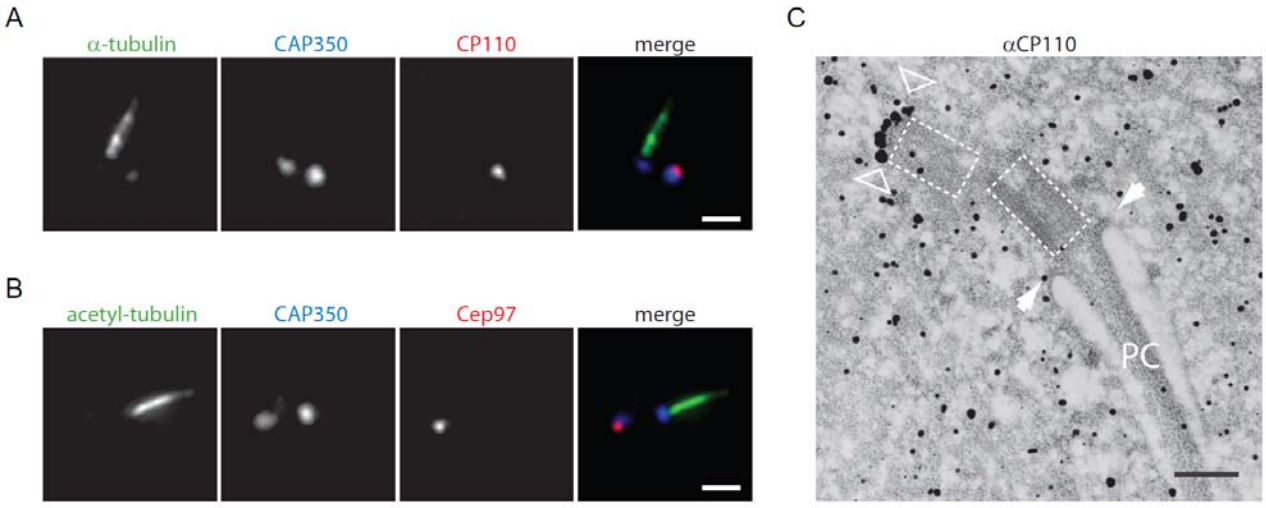

Figure 13: Removal of CP110 and Cep97 from the ciliated basal body. hTERT-RPE1 cells were serum starved for 60 hours and analyzed by IF microscopy with the antibodies indicated **(A** and **B)** or by pre-embedding immuno-EM staining with anti-CP110 antibodies **(C)**. Dashed lines indicate the positions of the two basal bodies in the EM image and arrowheads refer to the distal ends of the ciliated basal body (filled arrowheads) and of the juvenile non-ciliated basal body (open arrowheads), respectively. For clarity the primary cilium is indicated (PC). Note that CP110 and Cep97 are selectively displaced from the mature ciliated basal body and are present only at the non-ciliated centriole. Scale bars represent 1 µm in (A) and (B) and 250 nm in (C). The EM picture was kindly provided by Dr. York-Dieter Stierhof, University of Tübingen.

4.3 Centriole Elongation

4.3.1 Depletion of CP110 Causes the Elongation of Centrioles

To visualize centriolar MTs, which are stabilized by polyglutamylation and acetylation, the bulk of cytoplasmic tubulin can be extracted by combined cold and detergent treatment. Strikingly, when such treatment was applied to cells from which CP110 had been depleted, microtubular extensions from the distal end of the centrioles were observed. These centriolar extensions were observed in U2OS and HeLa S3 cells and were visualized with antibodies against acetylated-tubulin, while Cep192 was used to define

their proximal ends (Figure 14). Interestingly, both centrioles frequently showed such extended microtubular structures and their lengths often reached the three- to five-fold of genuine centriolar tubes (further experiments were conducted on this phenotype and are discussed later in this work from chapter 4.3.5 on).

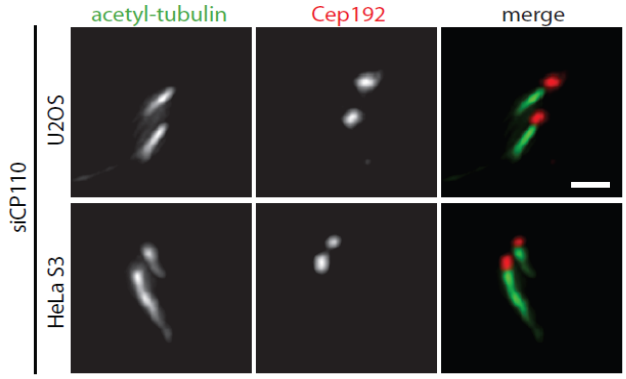

Figure 14: Depletion of CP110 causes elongated centriolar structures. IF microscopy showing U2OS and HeLa S3 cells after CP110 was depleted by siRNA treatment for 72 hours. Centrioles were stained with antibodies against acetylated-tubulin (green) and Cep192 (red) after the removal of cytoplasmic tubulin by cold and detergent treatment.

4.3.2 CPAP is Required for Centriole Duplication in Cycling Cells

The centriolar component CPAP binds MTs (Hung et al. 2000; Hsu et al. 2008) and associates with both parental centrioles and nascent procentrioles (Kleylein-Sohn et al. 2007), whereas its depletion compromises centrosome integrity, leads to the formation of multipolar spindles (Cho et al. 2006) and interferes with Plk4-induced centriole overduplication in human cells (Kleylein-Sohn et al. 2007). Accordingly, we asked whether *bona fide* centriole duplication was reduced after the depletion of CPAP. Therefore, we fixed S phase arrested cells after the transfection of siRNA oligonucleotides targeting the protein. As expected, CPAP depletion prevented centriole duplication in U2OS cells (Figure 15). Importantly though, while the recruitment of procentriolar CP110 and Cep135 was impaired, the procentriole precursor-specific Sas-6 was still recruited in thymidine arrested cells in S phase (Figure 15).

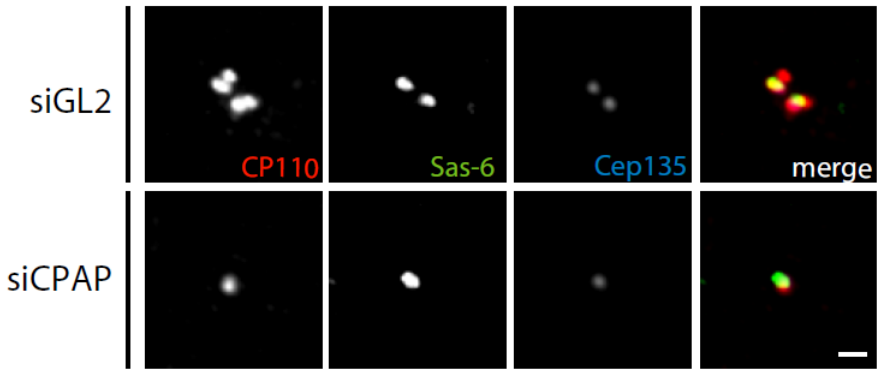

Figure 15: CPAP is required for centriole duplication in human cells. IF microscopy showing U2OS cells after the depletion of CPAP or GL2 (control) for 72 hours and an subsequent S phase arrest by a thymidine block during the final 16 hours of depletion. Cells were stained with antibodies against CP110 (red), Sas-6 (green) and Cep135 (blue). Note that cells depleted of CPAP fail to assemble procentrioles but recruit the cartwheel protein Sas-6. The scale bar represents 1 µm.

4.3.3 Overexpression of CPAP Leads to Centriole Elongation

As the CPAP homologue SAS-4 is required for the addition of centriolar MTs to the core centriolar tube in nematodes (Pelletier et al. 2006), we transiently overexpressed CPAP in U2OS and hTERT-RPE1 cells to investigate the role of CPAP in human centriole assembly. After removal of the cytoplasmic tubulin we observed that elevated cellular levels of CPAP caused the formation of strikingly elongated centriolar structures in both cell lines (Figure 16; A, B and C; initially reported in U2OS osteosarcoma cells by Dr. Mikael LeClech and Dr. Julia Kleylein-Sohn by personal communication). Staining of U2OS cells with antibodies against α-tubulin and CP110 revealed that CP110 was positioned at the distal end as in genuine-sized centrioles (Figure 16; B). Cep192, in contrast, was confined to the proximal end of the centrioles (Figure 16; A), hence showing high similarity to the elongated centriolar structures after the depletion of CP110 (Figure 14). Despite low transfection rates in non-quiescent hTERT-RPE1 cells, we observed cells that showed centriolar elongations at both centrioles upon the overexpression of full-length CPAP cDNA (Figure 16; C). Even though primary cilia can also be found to a low extent in serum fed cell populations due to high cell confluency and look similar to centriolar elongations described here (Figure 16; C, lower right panel), the observed centriolar extensions do not resemble genuine primary cilia. In contrast to primary cilia,

which form only at the mature basal body, the population of CPAP-mediated elongated centrioles mostly appeared on both centrioles (Figure 16; C, left panels).

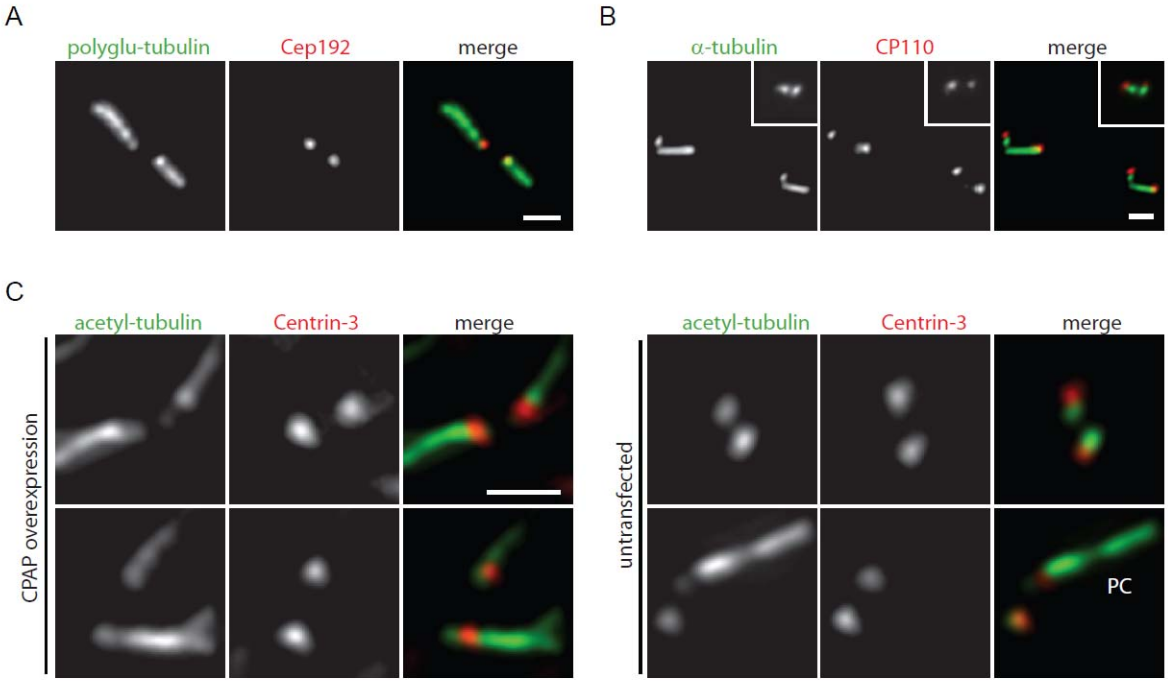

Figure 16: Formation of elongated centriolar structures upon overexpression of CPAP. Full length myc-CPAP was transiently expressed for 72 hours in asynchronously growing U2OS cells. After extraction of cytoskeletal MTs, centrioles were stained with antibodies **(A)** against acetylated-tubulin (green) and Cep192 (red)**,** or **(B)** against α-tubulin (green) and CP110 (red) and analyzed by IF microscopy. Note that two of the four centrioles in **(B)** are longer than 0.5 µm but decorated at their distal ends by CP110 protein. The insets show a pair of normal size G2 phase centrioles for comparison. **(C)** hTERT-RPE1 cells were transiently transfected with full-length GFP-CPAP, fixed by cold and detergent treatment and stained with antibodies against acetylated tubulin (green) and Centrin-3 (red). Left panels show MT extension structures emanating from both centrioles. Although not shown here, we emphasize that some of these extensions reached lengths of several µm. For comparison, the right panels show an untransfected cell lacking MT extensions (upper right panel) and an untransfected cell showing spontaneous formation of a primary cilium (PC) due to confluency (lower right panel). All scale bars represent 1 µm.

4.3.4 Mapping of the CPAP Region Required for Centriole Elongation

Having been intrigued by the capacity of full-length CPAP to generate elongated centrioles, we consequently asked which fragment of the 1338 amino acid protein was necessary and sufficient for the induction of these structures. In a first approach an amino-terminal (CPAP-3; aa1-422), a carboxy-terminal fragment (CPAP-5; aa898-1338) and a truncation covering the central region (CPAP-4; aa429-890) of CPAP were cloned into myc-tagged expression vectors (successful expression of these fragments was monitored by Western blotting; data not shown). To map the region required for the generation of centriole elongation, these expression constructs were transiently overexpressed in U2OS cells. The cells were then cold and detergent treated before fixation and then stained for IF microscopy to visualize possible centriolar extensions. Interestingly, expression of the C-terminal truncation (CPAP-5) induced centriole elongation, even though transfection rates were low and the elongation was only observed in less than 5 % of the cell population (Figure 17). This region was therefore further investigated and smaller fragments were cloned to map the essential region. cDNA truncations spanning the very C-terminus including the glycine-rich G-box region (CPAP-6; aa1070-1338) and another fragment covering only the region of the two far most C-terminal coiled-coil domains of CPAP (CPAP-8; aa898-1065) were generated (Figure 17). We found that elongation of centrioles was observed after the transient overexpression of the fragment comprising only the two C-terminal coiled-coil domains (CPAP-8; Figure 17).

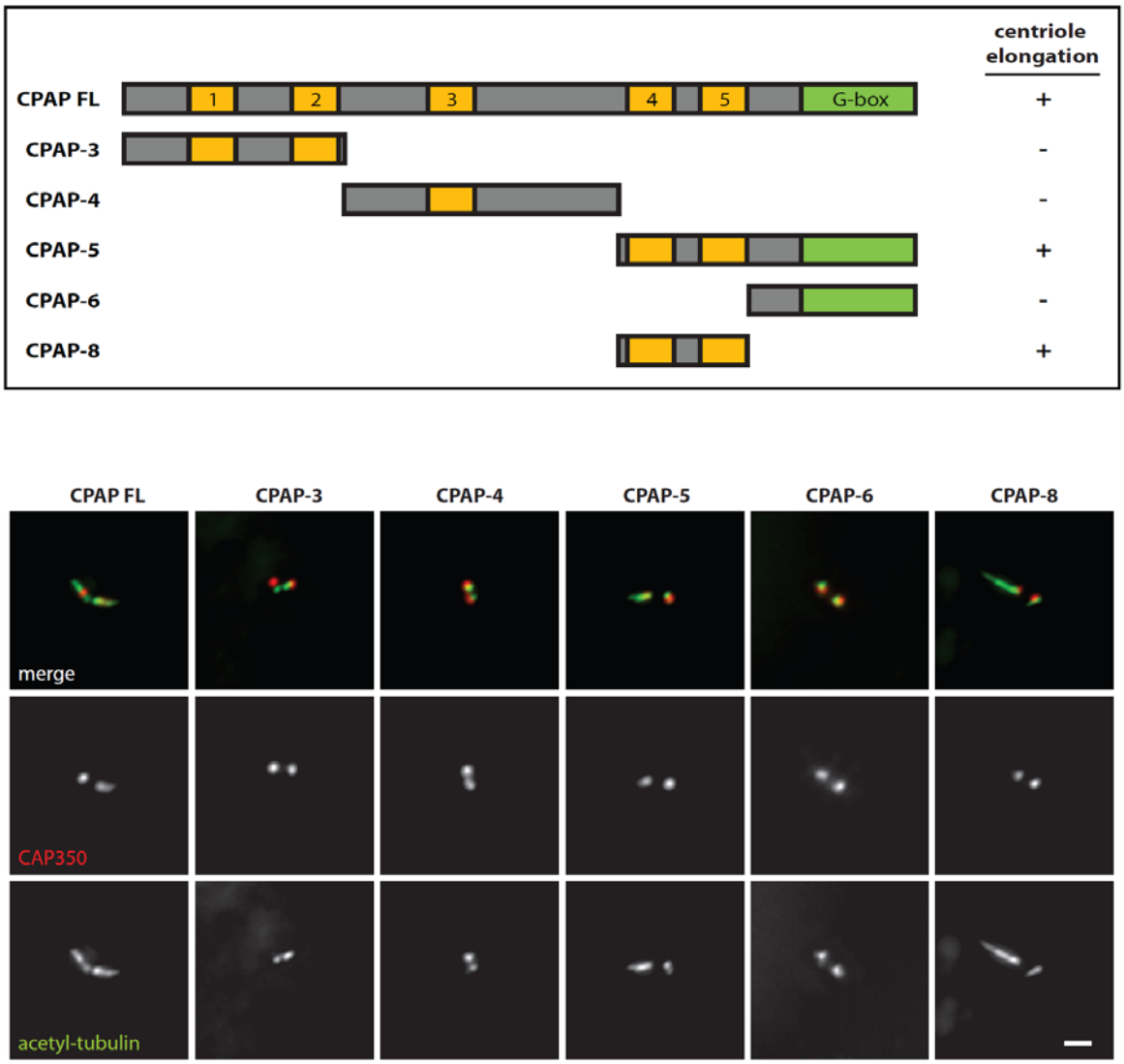

Figure 17: Overexpression of the N-terminal coiled-coil region of CPAP is sufficient for centriole elongation. (A) Schematic indicating different truncated fragments of CPAP that were transiently overexpressed in U2OS cells to determine the fragment sufficient to induce centriole elongation. Yellow areas indicate coiled-coil regions and the glycine-rich C-terminus is depicted in green. + : observation of elongated centrioles, - : no elongated centrioles. **(B)** IF images of U2OS cells after the transient overexpression of the exemplified CPAP truncations.

4.4 Delineation of CPAP-mediated Procentriole Elongation

4.4.1 Analysis of Centriole Elongation with the myc-CPAP Inducible Cell Line

To analyze the function of CPAP in centriole length control in more detail, we used the previously described U2OS T-REx A7 clone expressing myc-CPAP under control of a tetracycline inducible promoter (Figure 12; A and B). We examined the cell line for various parameters such as centriole length, centriole numbers and spindle morphology after tetracycline addition. CPAP overexpression did not have an effect on cell cycle progression, nor did it interfere with centrosome function as spindle poles during mitosis. The cell cycle pattern was unaltered after 24 hours of induction (Figure 12; B) and G2 centrosomes with elongated centrioles were able to separate and to move apart from another in preparation for mitotic cell division (Figure 18; A and C). Moreover, mitotic cells induced to overexpress CPAP showed a similar incidence of mono- or multipolar spindles as control populations and cell in which CPAP and Plk4 were co-overexpressed did not differ from cells in which Plk4 only was expressed (Figure 18; C).

Next, the elongated structures were visualized by IF microscopy after staining with antibodies against acetylated-tubulin and against myc. This analysis revealed that myc-CPAP decorated the elongations in their entirety (Figure 18; A). The length of these centriolar extensions increased with the time of induction and eventually surpassed 1 μm and reached 2-3 times the length of normal centrioles (Figure 18; B). After 24 hours more than 50 % and after 48 hours approximately 65 % of the cells, respectively, showed significantly elongated centrioles (Figure 18; B). However, CPAP induction did not cause a detectable increase in centriole numbers (data not shown).

We then asked whether the ultrastructure of genuine centrioles and the localization of known centriolar proteins were maintained upon increased elongation of the MTs after CPAP overexpression. We could show that the centriole linker protein C-Nap1 was present only at the proximal ends (Fry et al. 1998) and CP110 only at the distal ends (Kleylein-Sohn et al. 2007), as predicted for the ultrastructure of genuine centrioles (Figure 18; D). This observation suggested that increased tubulin incorporation onto the centriolar MTs caused the elongation of the centrioles without changing the localization of proteins specifically confined to either end of the cylinder.

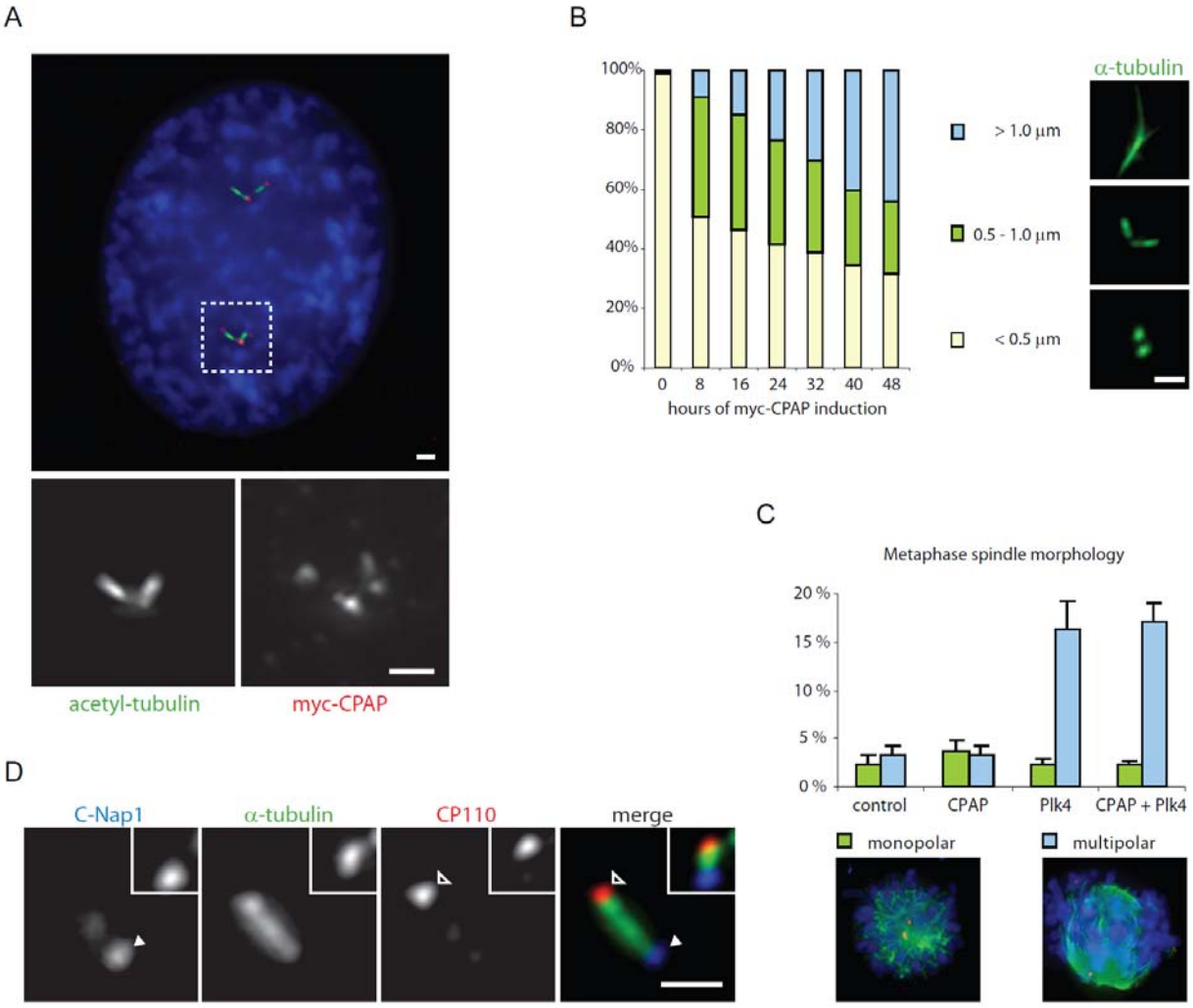

Figure 18: CPAP overexpression leads to centriole elongation. (A) myc-CPAP expression was induced in U2OS T-REx cells and the association of myc-CPAP with elongated centrioles was visualized in a prophase cell by staining with anti-myc antibodies (red). Centrioles were counter-stained with antibodies against acetylated-tubulin (green) and DNA was visualized by DAPI (blue). The upper panel shows that all four centrioles are elongated and stain positive for exogenous myc-CPAP. Lower panels show magnifications of the boxed area. **(B)** CPAP was induced for 0 to 48 hours before cells were stained with anti-α-tubulin antibodies and the lengths of centriolar extensions were measured. As illustrated by representative fluorescence images of α-tubulin stained centriolar structures (right), these were classified into three categories according to their length (< 0.5 µm, 0.5 - 1.0 µm and > 1 µm). As shown in the histogram, the length of centriolar structures increases with time of CPAP induction. **(C)** U2OS T-REx myc-CPAP cells were either transfected for 4 hours with full length Plk4 cDNA or left untreated before myc-CPAP was induced (or remained uninduced for controls) for 20 hours under aphidicolin arrest. Cells were then released into fresh medium and collected in metaphase 16 hours later by the addition of MG132 for 1 hour. To assess spindle morphology cells were stained with antibodies against α-tubulin and CAP350 and chromosomes were visualized by DAPI staining. Histograms illustrate the frequency of abnormal (mono- or multi-polar)

spindles, as illustrated in representative IF images. Data are from 3 independent experiments (n = 100) and bars indicate standard errors. **(D)** Visualization of an elongated centriole after induction of myc-CPAP expression in a U2OS T-REx Tet-on cell line. Centrioles were stained with antibodies against the proximal marker C-Nap1 (blue; filled arrowhead), the distal marker CP110 (red; open arrowhead) and α-tubulin (green). Insets show a normal size centriole for comparison. Scale bar represent 1 µm in (A) and (B) and 500 nm in (D).

4.4.2 CPAP Overexpression Causes Enhanced Tubulin Accumulation at Centrioles

Having shown that induction of CPAP causes elongated centrioles that resemble the ultrastructure of centrioles of normal size, we were interested if excess CPAP had an effect on tubulin recruitment to growing centrioles, similar to the function of SAS-4 in *C. elegans*. Therefore, the fluorescence intensity of centriolar tubulin was measured by IF microscopy in fixed cells relative to the fluorescence intensity of CAP350 in myc-CPAP induced U2OS T-REx cells at short induction times. Interestingly, a significant increase of α-tubulin recruitment to centrioles could be detected eight hours after tetracycline induction, already before any obvious centriole elongation became apparent (Figure 19). The fluorescent intensity of CAP350 was not altered by the induction of CPAP overexpression or the increased tubulin recruitment.

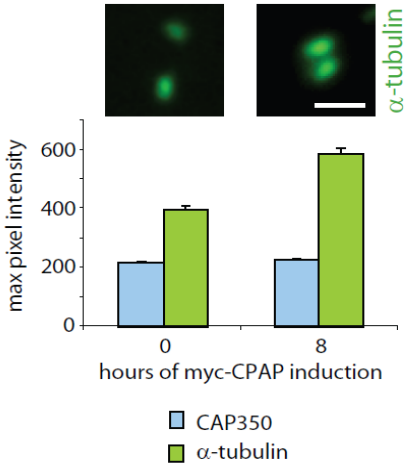

Figure 19: Increase of tubulin at centrioles after the overexpression of CPAP. After induction of myc-CPAP for 0 or 8 hours, cells were stained with antibodies against α-tubulin and the centriolar protein CAP350. The histogram shows the maximal pixel intensity of α-tubulin and CAP350 (control) staining. Insets show

representative fluorescence images of α-tubulin staining (scale bar = 1 μm). Results are from 3 independent experiments (n = 100) and bars indicate the standard errors.

4.4.3 Both Procentrioles and Mature Centrioles are Elongation-Competent

To determine whether parental centrioles or procentrioles or both are competent to elongate in response to excess CPAP, we counted the number of elongated centrioles relative to the number of C-Nap1 dots per cell. After 24 hour induction of CPAP expression in asynchronously growing cells, most cells showed a 2:2 ratio between C-Nap1 dots and elongated centrioles, but about 15 % - 20 % of cells showed a 2:3 or 2:4 ratio (Figure 20; A). Because only parental centrioles stain positively for C-Nap1 (Fry et al. 1998), this latter population must represent G2 cells in which parental centrioles as well as new procentrioles were elongated, demonstrating that both mature centrioles and procentrioles are elongation competent. In further support of this conclusion, co-overexpression of CPAP with Plk4 resulted in the formation of flower-like structures in which the parental centriole as well as several of the newly formed (engaged) procentrioles were clearly elongated (Figure 20; B).

Overall, many of the elongated centriolar structures formed in response to CPAP overexpression appeared to represent compact cylinders (Figure 16; A, B and 18; D). When we induced CPAP expression for more than 48 hours and subsequently stained the cells for IF microscopy or immuno-EM analysis, however, we observed that the longest structures frequently showed splayed MTs, whose distal ends were invariably decorated by CP110 (Figure 20; C and D). This suggests that although CPAP overexpression did not always result in a homogenous extension of centriolar walls, each of the MT extensions was recognized by the distal end-capping protein CP110.

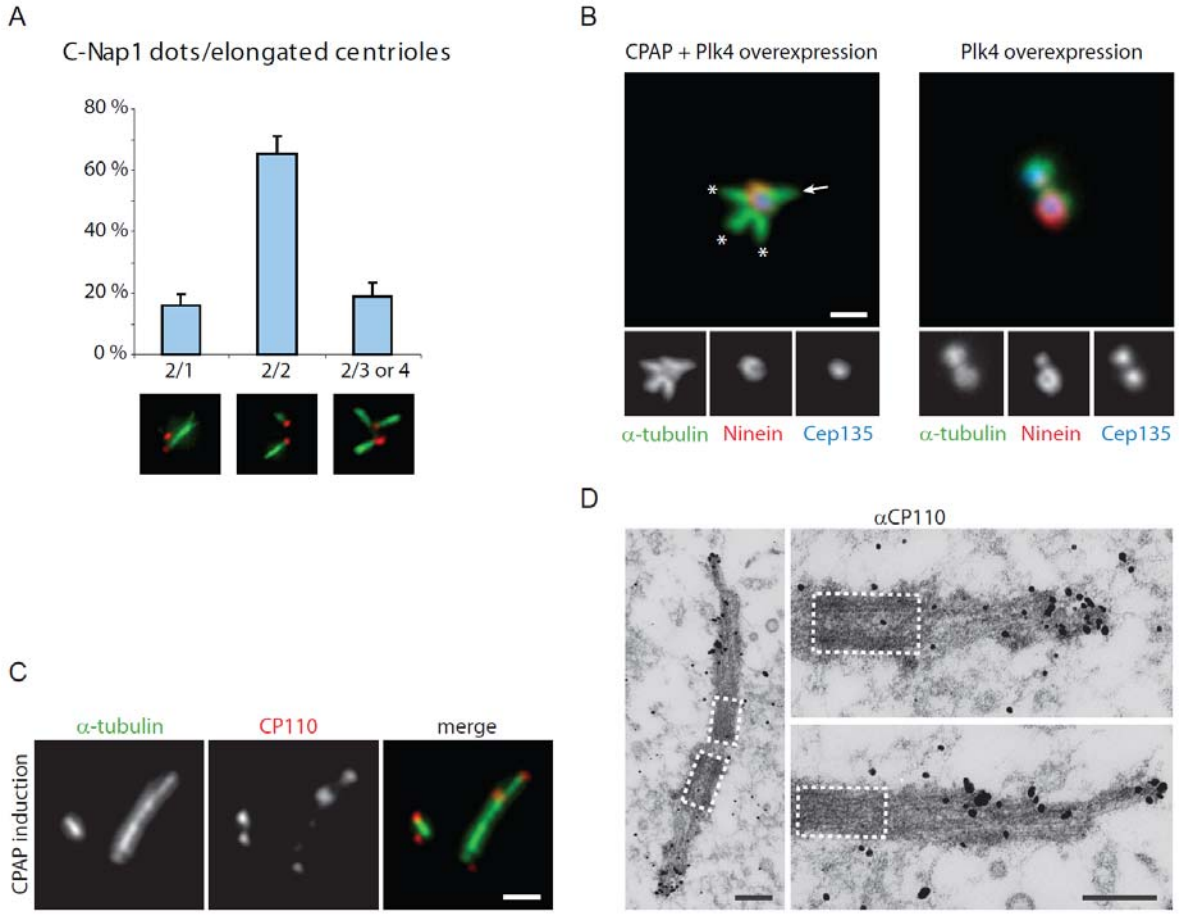

Figure 20: Procentrioles and mature centriole are elongation competent by overexpression of CPAP; CP110 decorates the distal ends of elongated centriolar MTs. (A) Asynchronously growing U2OS T-REx cells were induced for myc-CPAP expression for 24 hours and stained with antibodies against α-tubulin and the proximal marker C-Nap1. The histogram shows the ratio between the number of C-Nap1 dots and the number of elongated centrioles present in each cell. The fluorescence images show representative examples of cells counted under each column of the histogram (C-Nap1 red, α-tubulin green). Results are from 3 independent experiments (n = 100) and bars indicate the standard error. **(B)** Elongation of multiple daughter centrioles after CPAP and Plk4 co-overexpression. Plk4 was transiently expressed for 16 hours before CPAP expression was induced for 24 hours in U2OS cells (left), before multiple elongating centrioles were stained with antibodies against α-tubulin (green), Ninein (red) and Cep135 (blue). Arrow points to elongated parental centriole, whereas elongated procentrioles are indicated by asterisks. For comparison, two centrioles are shown after induction of Plk4 only (right). (**C)** Staining of centrioles after CPAP overexpression with anti-α-tubulin and anti-CP110 antibodies shows two parental centrioles of differing length and a newly growing procentriole at each of their proximal ends (hence presumably an S phase cell). Note that CP110 decorates the tips of splayed centriolar MTs on the same centriole. Scale bars in (B) and (C) represent 1 μm. **(D)** Pre-embedding immuno-EM visualizes CP110 at two centrioles after CPAP induction for 24 hours. Note that these

centrioles are disengaged (and thus presumably occur in a G1 phase cell). The bottom images show 2-fold magnifications of the two centrioles. White dashed lines mark the normal sizes of centrioles and scale bars represent 250 nm. The EM picture was kindly provided by Dr. York-Dieter Stierhof, University of Tübingen.

4.5 Comparison of Centriolar Elongations

4.5.1 Elongated Centrioles after CP110 Depletion and CPAP Overexpression are Highly Similar

We had previously observed that depletion of CP110 caused microtubular extensions from the distal ends of centrioles (Figure 15) and were intrigued by their similarity to the elongated centrioles produced by CPAP overexpression (Figure 17; A). This prompted us to compare the two structures in more detail. Therefore, we determined the localization of various centriolar proteins on the microtubular structures induced by either CP110 depletion or CPAP overexpression (Figure 21). Elongated structures were visualized by co-staining with GT335 antibody, recognizing polyglutamylated tubulin, or by staining with antibodies against α-tubulin or acetylated tubulin. In contrast to Cep192 (Figure 14 and 16; A), which was confined to the expected proximal ends of all structures, the proteins CAP350, Cep135 and Cep290 additionally spread over the elongated structures, particularly well visible in the case of CPAP overexpression (Figure 21; further information on the protein localization is available in chapter 4.6). Interestingly, both types of microtubular extensions were stabilized by acetylation and polyglutamylation (Figure 21), consistent with their resistance to cold treatment and detergent extraction.

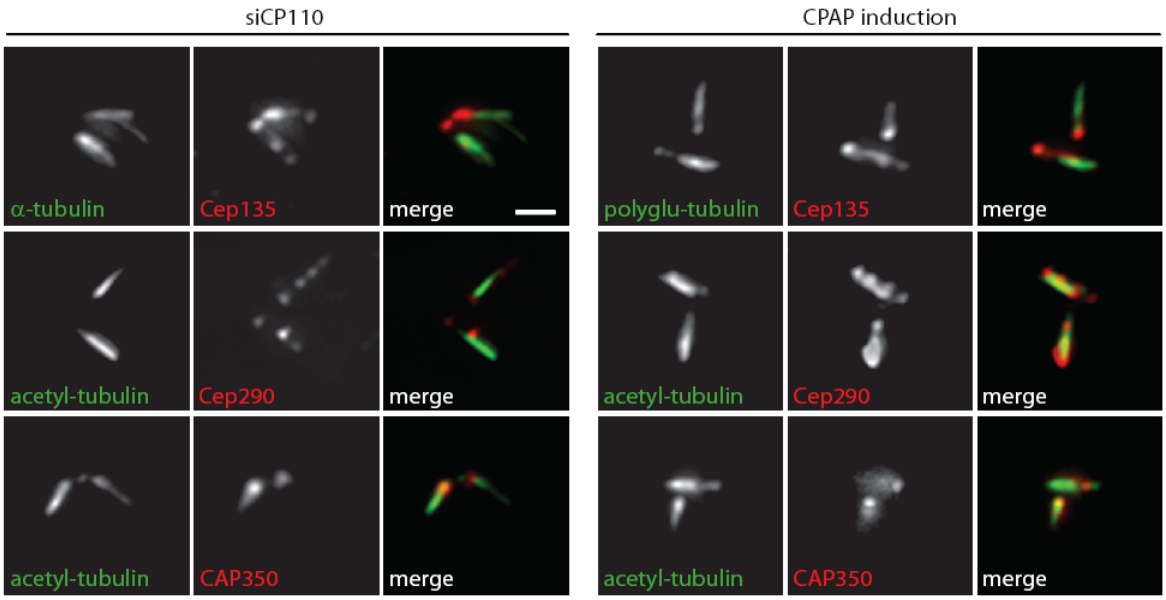

Figure 21: Elongated centriolar structures are decorated by various centriolar proteins. Following siRNA-mediated depletion of CP110 (left panel) and CPAP induction (right panel), centrioles and elongated microtubular structures were stained with the indicated antibodies. Scale bar represents 1 µm.

Many further centriolar proteins were tested for their localizations on the elongated centrioles by IF analysis. Among these Plk4, Sas-6, pericentrin, chTog and Cep170 remained confined to their genuine positions (data not shown) as shown previously for Cep192, while Centrin-2, Centrin-3 and PCM-1 were clearly distributed across the elongated centrioles (data not shown) as shown above for Cep135.

4.5.2 Positioning of Distal and Subdistal Appendages on Elongated Centrioles

Having shown that both mature parental centrioles and procentrioles are competent to elongate in response to CPAP overexpression (Figure 21; A and B) or CP110 depletion (Figure 14), we asked whether the positions of subdistal or distal appendages were affected by centriole elongation. Cells overexpressing CPAP or depleted of CP110 were stained with antibodies against Ninein and Cep164, markers of subdistal and distal appendages, respectively (Mogensen et al. 2000; Graser et al. 2007). As shown by IF microscopy for both treatments (Figure 22; A) or by immuno-EM for CPAP overexpression (Figure 22; B), the distances between the proximal ends of centrioles and

appendages were unchanged when comparing elongated centrioles with control centrioles. Considering that CP110 associates early with nascent procentrioles and then stays associated with the distal tips of elongating centrioles (Kleylein-Sohn et al. 2007), these results suggest that under conditions of CPAP-induced elongation, tubulin insertion into the growing centriolar cylinder occurs within a relatively narrow region located between appendages and a CP110 cap.

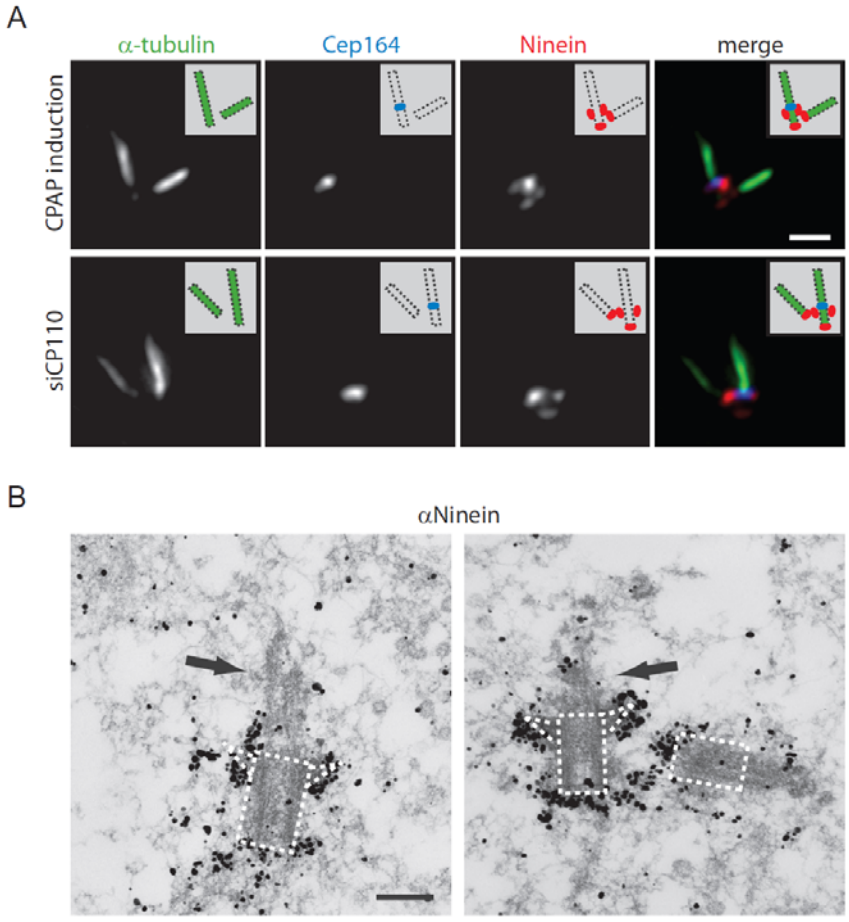

Figure 22: Centriole elongation does not affect positioning of distal and sub-distal appendages. (A) After induction of myc-CPAP expression or CP110 depletion pairs of elongated parent and progeny centrioles were stained with antibodies against α-tubulin (green), Cep164 (blue) and Ninein (red). Insets show corresponding drawings to facilitate data interpretation. Scale bar represents 1 µm. **(B)** Pre-embedding immuno-EM performed after 24 hours of CPAP induction. Sub-distal appendages were visualized with anti-Ninein antibodies, followed by Nanogold-labelled secondary antibodies. White dashed lines mark the normal sizes of centrioles and the positions of sub-distal appendages on mature centrioles, and dark arrows point to extensions. Scale bar represents 250 nm. The EM picture was kindly provided by Dr. York-Dieter Stierhof, University of Tübingen.

4.6 Centriolar Elongations are Fundamentally Different from Primary Cilia

During the course of this work, it had been reported that depletion of the centriolar proteins CP110 promotes the formation of primary cilia in proliferating U2OS cells (Spektor et al. 2007). This finding was contrary to our observation that both the depletion of CP110 and the overexpression of CPAP leads to the generation of elongated centrioles but does not promote cilium formation in these cells. To compare the structures induced by CPAP overexpression or CP110 depletion in U2OS cells to *bona fide* primary cilia (in hTERT-RPE1 cells), we searched for proteins that would associate differentially with the two structures. We found that Centrin-3 readily decorated the extended structures formed in U2OS cells by either CPAP overexpression or CP110 depletion, but the protein was confined to the basal bodies when primary cilia formation was induced by serum starvation of hTERT-RPE1 cells (Figure 23; A; left columns).

Conversely, the intraflagellar transport protein Polaris/IFT88 (Pazour et al. 2000) was detectable on genuine cilia but not on the microtubular extensions seen in cells that were induced for myc-CPAP overexpression or were depleted of CP110 (Figure 23; A, central columns). Finally, CP110 was conspicuously absent from the basal body underlying the single primary cilium in serum starved hTERT-RPE1 cells (Figure 17; A, right columns; see also Figure 13; A and C), consistent with previous results (Spektor et al. 2007). In contrast, it decorated the distal tips of the two elongated centrioles that were frequently seen in cells overexpressing CPAP (Figure 17; A, right columns). Similarly Cep97, the interaction partner of CP110 (Spektor et al. 2007), was removed selectively from the ciliated basal body (Figure 13; C) but persisted on both centrioles upon CPAP-induced centriole elongation (Figure 23; B).

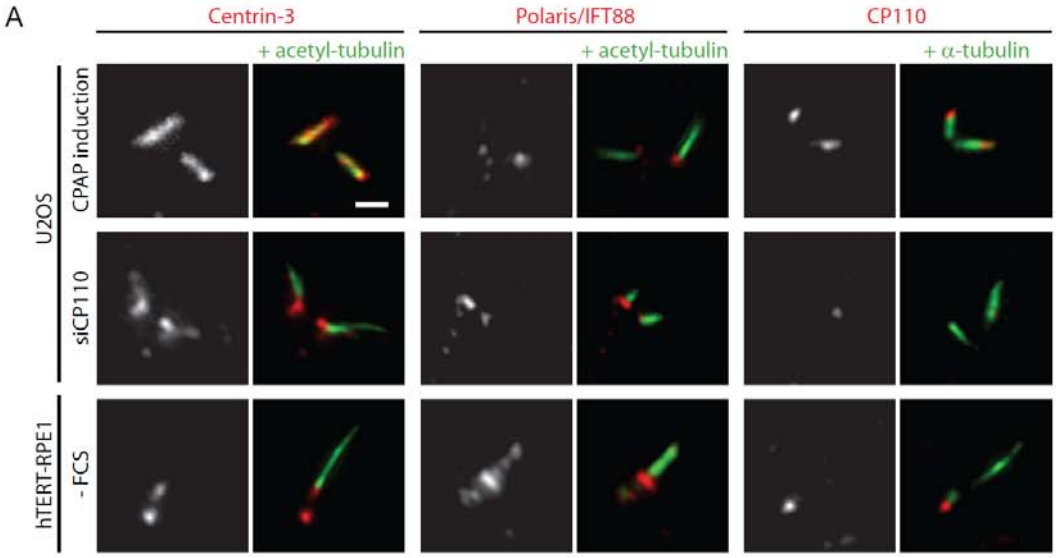

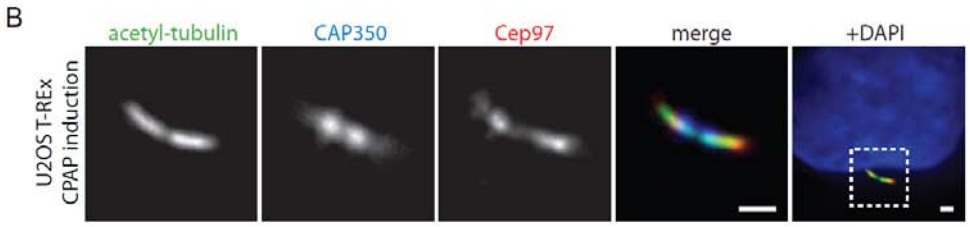

C

	U2OS T-REx CPAP ind	U2OS siCP110	hTERT-RPE1 - FCS
α-tubulin	+	+	+
acetyl. tubulin	+	+	+
polygl. tubulin	+	+	+
Centrin-3	+	+	-
Cep290	+	+	-
CAP350	(+)	(+)	-
Cep135	(+)	(+)	-
CP110	+	-	-
Cep97	+	-	-
Polaris/IFT88	-	-	+

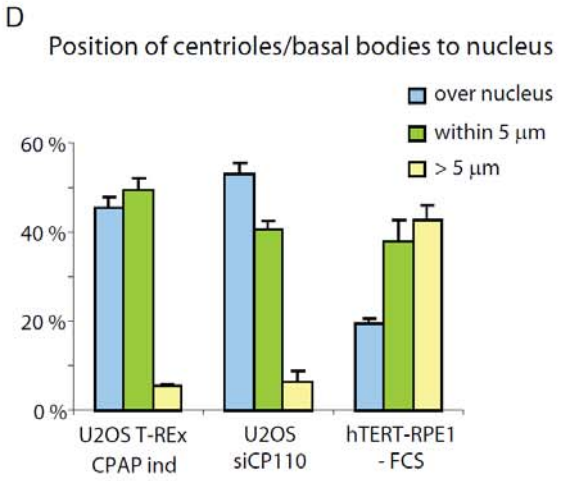

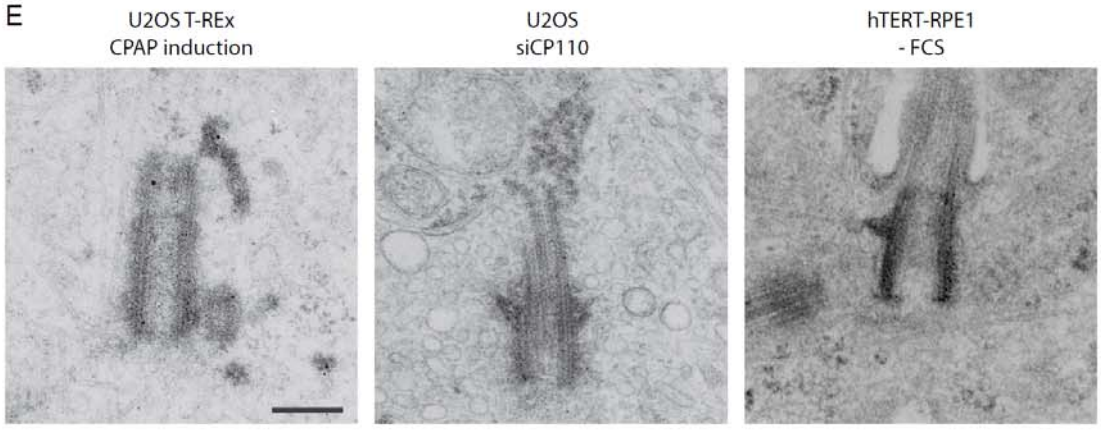

Figure 23: Elongated centrioles are fundamentally different from primary cilia. **(A)** Using immunofluorescent staining with the indicated antibodies, the centriolar extensions produced in U2OS cells by either CPAP overexpression (upper row) or CP110 depletion (central row) were compared with primary cilia formed in quiescent hTERT-RPE1 cells (bottom row). Note that Centrin-3 stains microtubular elongation in cells overexpression CPAP or lacking CP110, but not primary cilia. Conversely, Polaris/IFT88 only stains primary cilia. Finally, CP110 is present at the distal ends of both elongated centrioles in cells overexpressing CPAP but absent from the mature basal body in the ciliated hTERT-RPE1 cells. **(B)** U2OS T-REx cells were induced for CPAP overexpression and elongated centrioles were stained as indicated. Note that Cep97 is present on both elongating centrioles. Scale bar represents 1 μm in (A) and (B). **(C)** Table comparing the localization of various centriolar and ciliary markers on centriolar structures produced in U2OS cells by CPAP overexpression or CP110 depletion and on primary cilia in hTERT-RPE1 cells [+ : protein localizes to extended MT structures; (+) positive localization detectable on some but not all structures; - : protein not found on extended structures] **(D)** Histogram comparing the distance between centrioles/basal bodies and the nucleus after overexpression of CPAP in U2OS cells, CP110 depletion from U2OS cells, or induction of ciliogenesis in hTERT-RPE1 cells. Results are from 3 independent experiments (n = 100) and bars indicate standard errors. **(E)** Transmission EM was used to compare centriolar extensions produced in U2OS cells by either CPAP overexpression (left) or CP110 depletion (middle) with primary cilia formed in quiescent hTERT-RPE1 cells (right). Note the increased length of an apparent solid cylinder after CPAP overexpression (left) and the presence of membranous sheaths surrounding the axoneme of primary cilia (right). Scale bar represents 250 nm. The EM picture was kindly provided by Dr. York-Dieter Stierhof, University of Tübingen.

Thus, the structures induced by overexpression of CPAP or depletion of CP110 resemble each other, but both can readily be distinguished from genuine primary cilia (as summarized in Figure 23; C), implying that the removal of CP110 from basal bodies is most likely required but not sufficient for ciliogenesis.

In further support of this conclusion, we noted that elongated centrioles and microtubular structures produced by CPAP overexpression or CP110 depletion were generally located in close vicinity to the nucleus, as recognized as a distinguishing mark of genuine centrioles (Doxsey 2001), whereas most of the basal bodies giving rise to primary cilia in quiescent cells had migrated to the plasma membrane (Figure 23; D).

The three microtubular structures were also compared by TEM. The structures seen after overexpression of CPAP often resembled genuine centrioles of extended length (Figure 23; E, left image), but centrioles showing partial extensions of their cylindrical wall could also be seen. Similarly, partially extended microtubular structures were

commonly seen in response to CP110 depletion, but these often protruded distally from a centriole of normal length (Figure 23; E, middle). In contrast, primary cilia were characterized by the presence of membranous sheaths surrounding the axonemal MTs and a clear structural transition between the basal body and the cilium (Figure 23; E, right).

4.7 Antagonistic Actions of CPAP and CP110 in Centriole Length Control

To further address the relationship between CPAP and CP110, we asked whether depletion of CP110 would synergize with CPAP overexpression. Therefore, cells were depleted of CP110, induced for CPAP expression or first treated with siRNA oligonucleotides against CP110 and then additionally induced for CPAP expression by tetracycline addition. Although combined treatment resulted in significant cell death (data not shown), surviving cells showed exceptionally long MT structures emanating from centrioles that considerably exceeded the lengths of the singular treatments, reaching an average length that was more than 10-fold larger than the size of genuine centrioles (Figure 24; A and B).

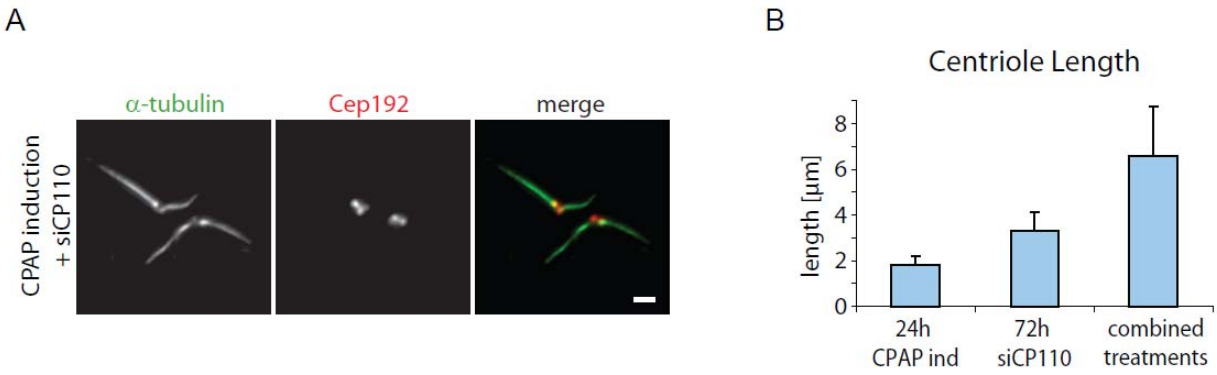

Figure 24: CP110 depletion and CPAP overexpression synergize to produce extraordinarily long MT extensions. (A) U2OS cells were depleted of CP110 for 24 hours before CPAP was induced for 24 hours and centriolar structures were stained with antibodies against α-tubulin (green) and Cep192 (red). Scale bar represents 1µm. **(B)** Histogram illustrating the maximal length of centriolar MTs seen in U2OS cells after CPAP induction for 24 hours, CP110 depletion for 72 hours and combined

treatments (48 hours CP110 siRNA, followed by 24 hours of CPAP induction). Error bars indicate +/- SD (n = 25).

4.8 Screen for Further Proteins Involved in Centriole Length Control

Intrigued by our investigations on the functions of CP110 and CPAP in centriolar length control, we asked which other centrosomal proteins regulate procentriole elongation. To this end, we depleted various candidate proteins for 24 hours and then induced CPAP expression for 48 hours by tetracycline addition in the U2OS T-REx myc-CPAP cell line (for experimental setup see Figure 25; A). Each candidate protein assayed was depleted with two different siRNA oligonucleotides and centrioles of more than 1 µm length were counted after fixation by IF microscopy. These numbers were compared to cells in which elongated centrioles were induced after GL2 control siRNA treatment. Further negative controls included cells only induced for CPAP expression or cells additionally depleted of C-Nap1 or CPAP itself. Moreover, the previously described depletion of CP110 was used as positive control.

Using this approach the centrosomal components Cep76, CAP350 and Cep70 were identified to promote centriole growth in human cells (Figure 25; B, yellow bars). The depletion of Cep76 even reduced the number of elongated centrioles to a degree similar to CPAP depletion. Apart from that, our results suggested that the MT-depolymerising kinesin MCAK has an important function opposing tubulin addition at centriolar MTs because its depletion led to a significant increase in elongated centrioles (Figure 25; B, blue bar), as also demonstrated for CP110 in this assay (Figure 25; B, light blue bar).

A

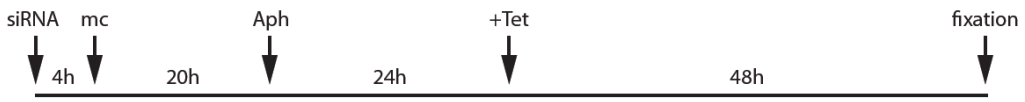

B

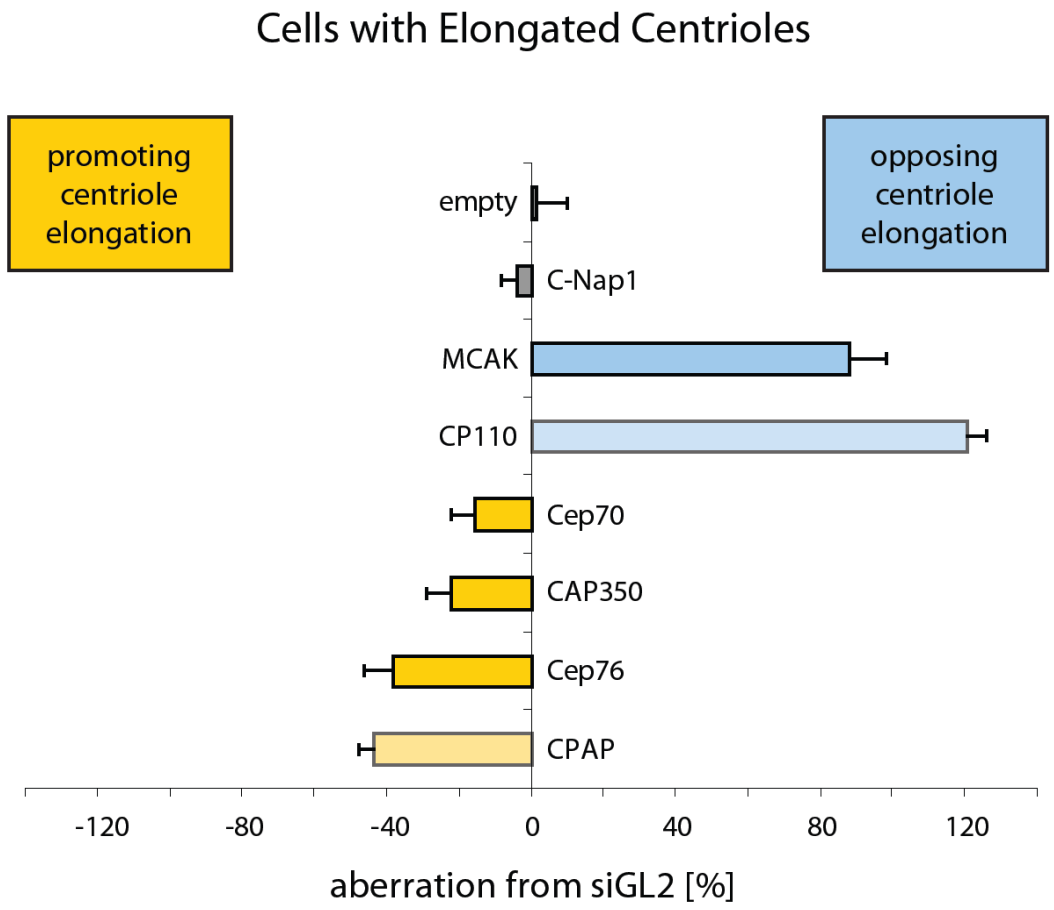

Figure 25: Identification of novel key regulatory proteins of centriole length. (A) Schematic indicating the experimental setup of the siRNA inventory screen using the U2OS T-REx myc-CPAP cell line. **(B)** Histogram showing the number of cells with centrioles longer than 1 µm after treatment with two different siRNA oligonucleotides for each protein annotated in comparison to GL2 treated cells. CP110 and CPAP siRNA treated cells were used as positive and negative control, respectively and C-Nap1 and cells without siRNA oligonucleotide treatment as neutral controls. Data from 3 independent experiments (n = 50).

5. DISCUSSION

Centrosome biology has gained increased scientific interest within the last two decades due to novel insights into the roles centrosomes play in the development of cancer and ciliopathies. Since then, pronounced effort has been undertaken to gain information about the organelle's proteomic composition and to understand the regulation of centriole duplication. As a result of advanced proteomic and microscopic techniques, presumably most of the key human centrosomal proteins are now known and functional homologues have been identified in many other organisms (reviewed in Bettencourt-Dias and Glover 2007). Nevertheless, how the fundamental centrosomal functions are coordinated on a molecular level and how the closely related ciliary functions are controlled is just starting to be unravelled.

Here, two important topics have been addressed: First, we have described that displacement of CP110 and Cep97 from the mature basal body is needed to allow cilium formation. Second, we have asked how the length of centrioles is controlled during centriole biogenesis and have found several centriolar proteins that contribute to this process.

5.1 Ciliogenesis is Dependent on a Multi-Step Regulatory Process which Includes the Removal of CP110/Cep97 from the Mature Basal Body

Human CP110 is known to be a target of cyclin dependent kinase 2 and its cellular protein levels are highly regulated within the cell cycle (Chen et al. 2002; Tsang et al. 2006). However, it remains unclear whether its centriole duplication function depends on Cdk phosphorylation and how its degradation is controlled. To gain further insight into the centriolar functions of CP110 on a molecular level we performed IPs followed by MS analysis and thereby identified Cep97 and Cep290 as two novel interaction partners of CP110.

In an independent study the interaction of Cep97 with CP110 was confirmed and Cep97 was shown to be co-recruited to centrioles with CP110 and to promote its stability

at centrioles, surprisingly without having any importance for centriole duplication (Spektor et al. 2007). Cep290 cooperates with PCM-1 and the GTPase Rab8a, an integral component of primary cilia, to promote ciliogenesis (Kim et al. 2008; Tsang et al. 2008). Cep290 localizes to centrosomes and is of considerable medical interest because mutations of the encoding gene have been implicated in several ciliopathic syndromes (Hildebrandt and Otto 2005; Badano et al. 2006; Chang et al. 2006; den Hollander et al. 2006; Sayer et al. 2006; Valente et al. 2006; Baala et al. 2007; Helou et al. 2007; Leitch et al. 2008; Travaglini et al. 2009). Brian Dynlacht and co-workers have suggested that the interaction of CP110 with Cep290 is essential to suppress Cep290-dependent primary cilium formation in human retinal pigment epithelial cells (Tsang et al. 2008). Cep97 and Cep290, however, do not interact, suggesting that they form distinct complexes with CP110 (Tsang et al. 2008). Another centrosomal component, Cep76, has recently been found to be an additional interaction partner of CP110 as well as Cep97 (Tsang et al. 2009). However, Cep76 was not identified in the MS IP approach that we performed, presumably due to the low abundance of co-immunoprecipitated Cep76 in IPs of endogenous CP110. Its depletion has been implicated with the generation of "centriolar intermediate structures" containing different centriolar proteins but no additional mature centrioles (Tsang et al. 2009). In the future, the role of Cep76 and its involvement in centriole duplication will need to be determined more precisely.

Overall, the proteins that we found to interact with CP110 pointed towards a potential function of CP110 in cilia-related cellular processes, in addition to previously known interaction partners and its requirement for centriole duplication (Chen et al. 2002). This led us to examine the function of CP110 in the context of ciliogenesis. Interestingly, we found that CP110 is removed specifically from the mature basal body, from which the ciliary axoneme is built during ciliogenesis in G0-arrested hTERT-RPE1 cells (Figure 13). Concerning this point, our data are consistent with a different study by the Dynlacht laboratory (Spektor et al. 2007). In addition, we showed that Cep97, the proposed recruiting factor of CP110, is displaced from the mature basal body in ciliated cells. Both data sets indicate that the removal of CP110 (and Cep97) from the distal tip of the mature basal body is a key regulatory event for the formation of a primary cilium (Spektor et al. 2007; Tsang et al. 2008). Other essential steps in this process include the translocation of the centrosome from the nucleus to the cell surface, the encapsulation of a Golgi-derived vesicle at the distal end of the mature centriole (Satir and Christensen 2007), the anchoring

of the basal body to the membrane via Cep164 and ODF-2 (Ishikawa et al. 2005; Graser et al. 2007), formation of the axonemal transition zone (Dammermann et al. 2009) and the ciliary membrane (Nachury et al. 2007; Loktev et al. 2008) and the subsequent establishment of various ciliary transport processes (reviewed in Pazour and Bloodgood 2008; Pedersen and Rosenbaum 2008; Pedersen et al. 2008). In their work, Spektor *et al*. additionally provide plausible information that CP110 overexpression interferes with primary cilium formation in NIH 3T3 mouse fibroblasts and that the depletion of both CP110 and Cep97 increases the number of cilia formed in hTERT-RPE1 cells (Spektor et al. 2007). Taken together, these results strengthen the observation that cilia formation is hindered by the presence of CP110/Cep97 at the future axonemal transition zone and that their removal is essential to enable the assembly of a primary cilium.

Intriguingly, the spatially distinct regulation of CP110 and Cep97 between the two basal bodies of one ciliated cell (removal only from the mature basal body and persistence on the juvenile basal body) is the first reported variation between the two basal bodies in the process of primary cilium formation. Therefore, a multitude of questions arise by this observation: First, in which way does the molecular environment change at the mature basal body while remaining intact at the juvenile basal body? Is CP110 locally primed for degradation at one basal body, e.g. by the APC/C complex (CP110 contains one KEN box and one D box; Chen et al. 2002), and may the appendage structures contribute to the selectivity between the two different basal bodies? Do CP110/Cep97 prevent the recruitment of molecules required for cilium formation (discussed in Bettencourt-Dias and Carvalho-Santos 2008), or is the equilibrium of tubulin turnover rates kept under control at the distal end of centrioles by the presence of these “caps” so that axoneme formation is inhibited? Either way, the identification of the molecular changes of CP110 and Cep97 during ciliogenesis will pave the way for a better understanding of the differences that account for the dual functions of centrioles/basal bodies. Due to technical intricacies in the biochemical separation of the two centrioles, first from the plasma membrane and second from each other, investigations on posttranslational CP110 or Cep97 modifications (and potential differences between the centrioles) have not been approached in the course of this study.

The depletion of many different centriolar/ciliary proteins has been linked to defects in the formation of primary or motile cilia. The centrosomal component pericentrin, for example, which is related to primordial dwarfism, is essential for

ciliogenesis and for the localization of IFT components and polycystin-2 to cilia (Jurczyk et al. 2004; Miyoshi et al. 2009). The MT plus end-binding protein EB1, that localizes to the flagellar tip in *Chlamydomonas* (Pedersen et al. 2003), is yet another example (Schroder et al. 2007), just as several other constituents of the centrosomal proteome (Graser et al. 2007). Despite the accumulation of data about proteins needed for canonical ciliogenesis, it is yet unknown how most of these proteins relate to one another and how their functions are orchestrated on a molecular level.

Besides the process of ciliogenesis, our results also raise questions about the reverse mechanism that has to be initiated when cells re-enter the cell cycle and cilia are resorbed. For instance, how are CP110/Cep97 re-localized to the basal body after or during ciliary disassembly? Whether this process is promoted by and closely coordinated with the signaling pathway of HEF1 - Aurora A - HDAC6 that drives ciliary resorption (Pugacheva et al. 2007) will be an interesting question in the future. HDAC6 physically interacts with BBIP10, a small subunit of the BBSome implicated in tubulin acetylation, which is essential for ciliogenesis and a conserved protein within ciliated organisms (Loktev et al. 2008). Conceivably, BBIP could counteract HDAC6-mediated ciliary deacetylation and thereby prevent premature ciliary resorption. Despite many recent advances in the understanding of cilium biology, the molecular mechanisms that coordinate cilia assembly and disassembly processes remain largely obscure.

5.2 Centriolar Microtubules Elongate in the Absence of CP110

After the initiation of procentriole formation during the G1/S phase transition, procentriolar MTs need to be elongated throughout G2 phase in order for the centriole to reach the full length of approximately 400 nm by the ongoing addition of tubulin dimers, a process not finished until the following cell cycle (Azimzadeh and Bornens 2007). Surprisingly, when CP110 was depleted in proliferating U2OS cells, we noticed the formation of long MT structures extending from both centrioles, which were stabilized by polyglutamylation and acetylation. These structures had previously been interpreted as ciliary axonemes (Spektor et al. 2007) with the implication that CP110 serves as the only suppressor of a default pathway of ciliogenesis in proliferating cells (Pearson et al. 2007;

Spektor et al. 2007). We, in contrast, carefully examined those centriolar MT extensions by high resolution imaging and came to the conclusion that they rather represented elongated centriolar structures: First, we did not detect the ciliary marker Polaris/IFT88 on these extensions and found several associated centrosomal proteins that did not localize to primary cilia. Second, primary cilia are well known to assemble only at mature centrioles in a one-cilium-per-cell fashion. But the observed centriolar elongations commonly occurred at both mature and juvenile centrioles. Third, the majority of elongated centrioles remained in close vicinity to the nucleus and did not show any association with the plasma membrane in CP110 depleted cells. Last, electron microscopy illustrated clear morphological differences between elongated centriolar MTs and genuine primary cilia.

In support of this conclusion, it is known that α-/β-tubulin dimers assemble onto purified centrioles *in vitro*, preferentially to the distal ends (Gould and Borisy 1977; see Figure 26; A). Very similar centriolar phenotypes have been detected in γ-tubulin depleted, mitotic *Drosophila* S2 cells (Raynaud-Messina et al. 2004; see Figure 26; B) and in taxol-treated Chinese hamster ovary cells (Kuriyama et al. 1986; see Figure 26; C).

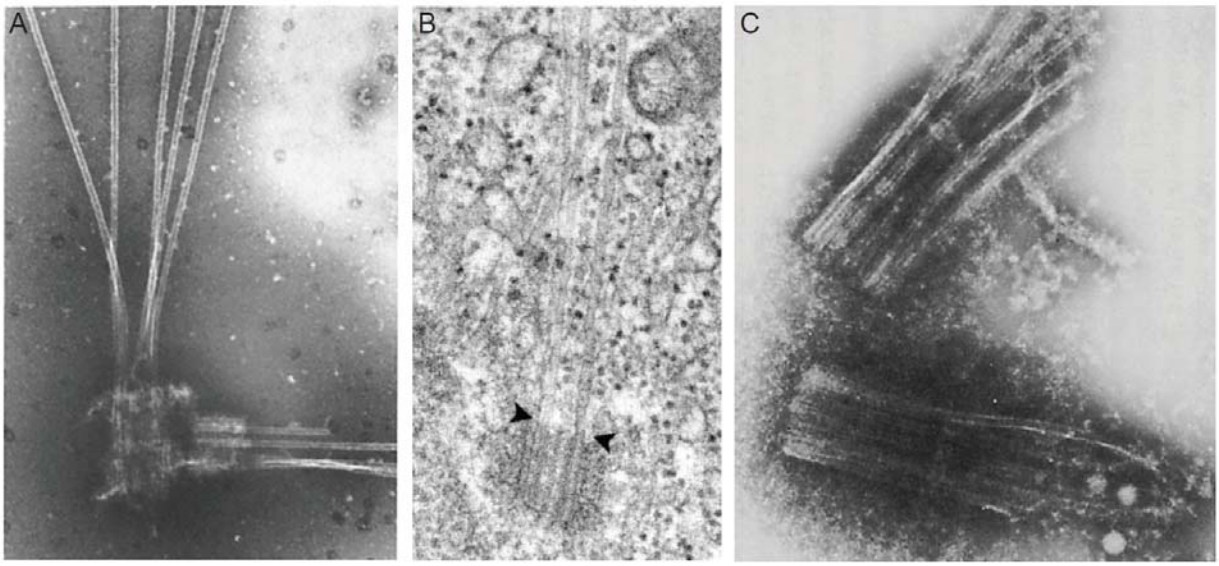

Figure 26: Electron micrographs of distally elongated centriolar MTs. (A) Isolated interphase centrioles from CHO cells were incubated with tubulin polymerization buffer. Note that the centriole and procentriole shown both show tubulin polymerization at the distal end (adapted from Gould and Borisy 1977). **(B)** Mitotic *Drosophila* centriole after γ-tubulin depletion (adapted from Raynaud-Messina et al. 2004). **(C)** Isolated centrioles from taxol-treated CHO cells (adapted from Kuriyama et al. 1986).

To date, it remains unclear whether centriolar length is perturbed in any pathologic symptoms or whether unphysiological centriole extensions occur *in vivo*. However, strikingly elongated basal bodies have been detected by TEM studies of disorganized human renal tissue of a patient suffering from systemic lupus erythematosus, a severe chronic autoimmune disease (Larsen and Ghadially 1974; Figure 27). In *Drosophila* imaginal wing disc cells, in which Cdk1 is inactivated, the length of mother and daughter centrioles is increased but the underlying molecular mechanisms remain elusive (Vidwans et al. 2003).

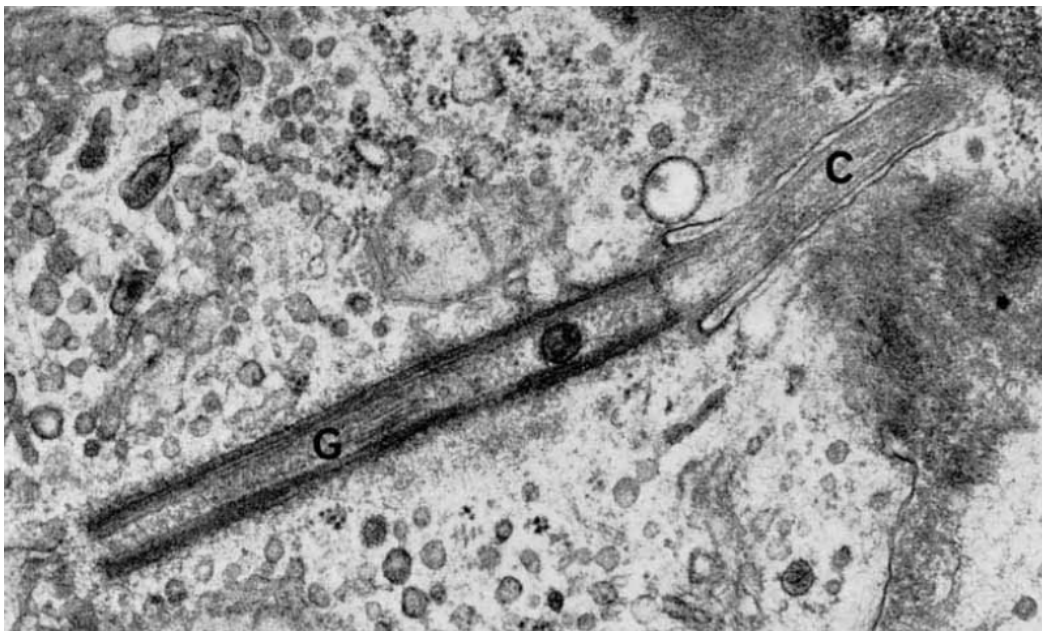

Figure 27: Electron micrograph of a giant renal basal body (G), giving rise to a primary cilium (C) in the nephronal tissue of a lupus nephritis patient, x 41.000 (adapted from Larsen and Ghadially 1974).

5.3 CPAP Controls Centriole Length during Procentriole Elongation

The homology to *C. elegans* SAS-4 suggested that human CPAP may account for an essential role in procentriole biogenesis. Although the depletion of CPAP inhibited procentriole formation, we found that the essential centriole duplication factor Sas-6 was still recruited under these conditions. This suggests that CPAP acts downstream of Sas-6 in a procentriole assembly pathway, resembling the situation in *C. elegans* and in Plk4 overexpressing human cells (Kirkham et al. 2003; Pelletier et al. 2006; Kleylein-Sohn et al. 2007). Intriguingly, in human cells the endogenous expression of both proteins, CPAP and Sas-6, are under careful cell cycle control. Their protein levels gradually increase from S phase on and suddenly decrease in late mitosis (Strnad et al. 2007; Tang et al. 2009). Accordingly, the degradation of both CPAP and human Sas-6 is promoted by the E3 ubiquitin ligase anaphase promoting complex/cyclosome (APC/C). The cell cycle regulation of CPAP is dependent on the first KEN box and the fourth D box and both proteins are degradaded by the 26S proteasome in an APC/C-Cdh1 dependent manner (Strnad et al. 2007; Tang et al. 2009).

Based on these data we set out to characterize the function of human CPAP in centriole biogenesis in more detail. We found that overexpression of human CPAP promoted the extension of the centriolar cylinder, presumably via its ability to recruit tubulin to the nascent structure (Pelletier et al. 2006; Hsu et al. 2008). The resulting elongated centrioles demonstrated striking similarity to the phenotype observed in CP110 deficient cells. Interestingly, juvenile and mature centrioles were elongation competent in response to high levels of CPAP, indicating that the levels of the protein have to be kept under stringent control at genuine centrioles at any time, even when they are fully grown. Otherwise even mature centrioles maintain/regain the ability to further incorporate tubulin and grow in length. Similar conclusions on the function of human CPAP have independently been reached by the groups of Pierre Gönczy and Tang Tang (Kohlmaier et al. 2009; Tang et al. 2009). Moreover, the expression of a degradation-resistant CPAP mutant displayed an enhanced occurrence of this phenotype (Tang et al. 2009).

To gain a better understanding of the molecular mechanisms by which tubulin dimers polymerize on growing procentrioles, we carefully analyzed the positions of distal and subdistal appendages on artificially elongated maternal centrioles and found them unchanged compared to genuine organelles (Figure 22). Taking into account that CP110

localized properly to centriolar ends upon centriole elongation, independently of the length of the MTs (even under a severely disrupted centriolar architecture; see Figure 20), our analysis bears two implications: First, CP110 does not entirely prevent the elongation of centriolar MTs by capping their tips if CPAP is overexpressed (combined overexpression of CPAP and depletion of CP110, however, generates even longer centrioles). Second, our results suggest that tubulin heterodimers are added distally to growing procentrioles, underneath a cap consisting of CP110/Cep97, regardless of the current centriole length (Figure 28; left illustration). Therefore, even mature centrioles kept their appendages in position while the MTs elongated more distally upon CPAP overexpression (Figure 28; right illustration). We therefore conclude that the distal incorporation of α-/β-tubulin dimers represents the genuine molecular mechanism of centriole elongation that is dependent on the action of CPAP and that occurs during procentriole growth from early S phase and throughout G2 phase.

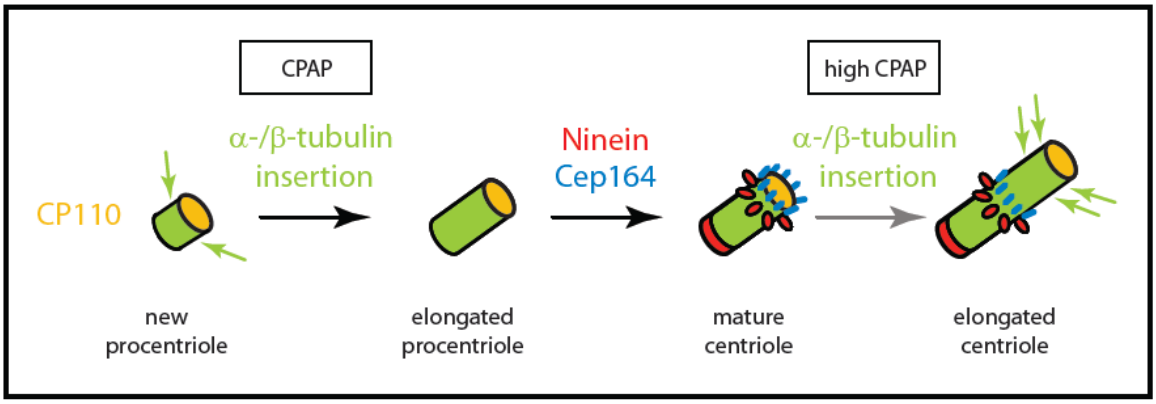

Figure 28: Mode of tubulin insertion at elongating centrioles. Schematic indicating the putative sites of CPAP-mediated α-/β-tubulin dimer insertion (green arrows) underneath a distal cap of CP110 (yellow) at elongating procentrioles. Once the genuine length of approximately 400 nm is established, another cell cycle has been completed and the centriole has itself given rise to a new procentriole, the centriole matures and is henceforth characterized by appendages. The unchanged positions of these distal (Cep164; blue) and sub-distal (Ninein; red) appendages on elongated mature centrioles after the overexpression of CPAP are schematically indicated (as experimentally shown in Figure 22). For simplicity only one centriole (without the respective adjacent centriole) is depicted in this figure.

One of the recent studies on CPAP reported the occurrence of mitotic defects upon the generation of elongated centrioles and additional Sas-6 foci adjacent to these elongated

structures promoting granddaughter centriole growth (Kohlmaier et al. 2009). Similar observations on centriolar triplets comprising grandmother, mother and daughter centrioles have been reported for a severely disorganized centriolar architecture in Cdk1-inactivated flies (Vidwans et al. 2003). However, neither the Tang laboratory nor our laboratory was able to support the conclusions by Kohlmaier and co-workers. It is not clear how the differences regarding the mitotic fate and additional Sas-6 foci can be explained, but it is conceivable that they originate from the use of different methods regarding plasmid integration into cells or the induction of expression. The discrepancies might furthermore arise from the fact that live cell imaging may have allowed a more precise assessment of the cellular fate than the analysis of fixed cells.

An examination of CPAP truncation mutants revealed that overexpression of the region comprising the two most C-terminal coiled-coil domains of the protein (aa898-1065) is sufficient to generate elongated centrioles. Interestingly, it has been recently shown that CPAP homodimerizes via its most C-terminal coiled-coil domain (aa978-1150) and that cells in which a CPAP deletion mutant of this region is expressed show reduced tubulin accumulation at centrosomes (Zhao et al. 2009). Whether CPAP dimerization is a prerequisite for its function to recruit tubulin during procentriole elongation or if CPAP monomers are sufficient to exert this task will need to be answered in future.

Our observation that tubulin accumulation is enhanced at centrioles within a short period of time after the overexpression of CPAP strengthens the conclusion that human CPAP recruits α-/β-tubulin dimers to enable procentriole elongation in a fashion similar to nematode SAS-4 (Pelletier 2006). This idea is further strengthened by the identification of a polypeptide MT-binding domain in CPAP that shows significantly diminished capacities of binding tubulin heterodimers when its charge properties are altered by a KR377EE mutation (Hung et al. 2004; Hsu et al. 2008). Importantly, excess CPAP-KR377EE strongly perturbed normal mitosis with a significant percentage of cells undergoing mono-, multi- or asymmetric bipolar mitosis (Tang et al. 2009). How the action of CPAP at the centriolar level fits with the identification of a MT-destabilizing motif in CPAP (referred to as PN2-3; residues 311-422) and its importance for tubulin sequestration on a molecular level remains obscure (Hung et al. 2004; Cormier et al. 2009).

5.4 Centriole Length is Equilibrated by Antagonistic Actions of CPAP and CP110

The astonishing similarity of the centriolar phenotypes after the two described distinct treatments (CP110 depletion and CPAP overexpression) led us to examine synergistic effects of CP110 and CPAP. From the obtained results we conclude that CPAP and CP110 exert opposite effects on the length of centrioles. Our data suggest that both proteins need to be kept at equilibrium at every centriole to prevent a deregulation of MT length (Figure 29). Importantly though, during procentriole elongation, the presence of CP110 does not hinder the addition of tubulins to the growing centriole, but may help to control the amount of integrated α-/β-dimers. CPAP, however, is presumably the essential component driving this process forward. How exactly the activities of CPAP and CP110 are equilibrated so that each centriole reaches and maintains a defined length requires further analysis.

In addition, our results as well as elegant data by Brian Dynlacht and co-workers revealed that the removal of CP110 (and its interaction partner Cep97) from the distal tip of the mature centriole is required for the formation of a primary cilium (Spektor et al. 2007; as reviewed in Bettencourt-Dias and Carvalho-Santos 2008; Tsang et al. 2008), implying that CP110 acts also as a suppressor of ciliogenesis in G0 arrested cells (as summarized in Figure 29). Moreover, our results bear on the question of whether ciliogenesis represents a default pathway. At least for non-quiescent U2OS cells they lend no support for the idea that removal of CP110 is sufficient to trigger ciliogenesis (Pearson et al. 2007; Spektor et al. 2007).

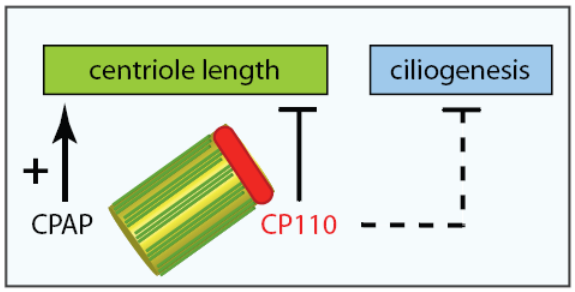

Figure 29: Schematic indicating the antagonistic actions of CPAP and CP110 in the control of centriole length. High levels of CPAP promote an increase in centriole length, whereas CP110 antagonizes MT elongation from the distal ends of

centrioles. In addition, removal of CP110 from the mature basal body is required for the growth of a primary cilium in quiescent cells, suggesting that CP110 suppresses ciliogenesis.

5.5 Novel Proteins Controling Centriole Length

After the identification of CPAP and CP110 as antagonising key regulators of centriole length we extended our analysis and aimed to discover further proteins involved in this process. Interestingly, we found further candidate proteins that either enhance centriole elongation or inhibit MT polymerization at the centriolar cap.

Among the proteins evaluated that may have a function promoting centriole elongation, Cep76 showed the most striking effect. The depletion of this protein resulted in a significant reduction of centriole elongation in the U2OS T-Rex A7 cell line in which CPAP overexpression had been induced. This effect nearly resembled the depletion of CPAP. Detailed information on Cep76 functions remain elusive, but it has been identified as a protein interacting with CP110 and is known to accumulate during S phase coinciding with procentriole formation (Tsang et al. 2009). CAP350 is a second candidate possibly involved in the promotion of centriole elongation. It localizes to the centrosome throughout the cell cycle and interacts with FOP to facilitate MT anchoring at the centrosome in cooperation with the MT-plus end binding protein EB1 (Yan et al. 2006; Schroder et al. 2007). More specifically, CAP350 is important for early procentriole stability and shields the centriolar MTs from the tubulin depolymerising activity of nocodazole (Le Clech 2008). The third protein identified, human Cep70, is a yet uncharacterized centrosomal protein, but has been indicated to contribute to ciliogenesis in zebrafish embryos (Wilkinson et al. 2009).

In this screen for regulators of centriole length, the protein MCAK was discovered whose depletion led to an increase in elongated centrioles in the combination with CPAP overexpression. MCAK is a mammalian kinesin-13 family member and is a potent MT-depolymerising molecule *in vivo* (Wordeman and Mitchison 1995; Hunter et al. 2003; Helenius et al. 2006; Cooper et al. 2010), which competitively binds to EB1 at MT plus ends (Lee et al. 2008). A related protein, the MCAK-like protein LmjKIN13-2, is involved

in length control of the eukaryotic flagellum and its overexpression results in flagellar shortening (Blaineau et al. 2007).

We conclude that along with CPAP and CP110, these additional proteins (Cep76, CAP350, Cep70 and MCAK) are novel candidates regulating the formation of cylindrical centrioles of defined length and may contribute to the opposing roles that CPAP and CP110 play in the control of centriole length. It is an intriguing observation that two of these newly identified potential regulators, MCAK and CAP350, are centrosomal molecules that execute tasks at MT ends not only of centriolar MTs but also in a more general cellular context.

In addition to the proteins identified in this screen, several other centriolar proteins have recently emerged as important regulators of centriole length. POC1 and POC5 are both required for centriole length control in human cells (Azimzadeh et al. 2009; Keller et al. 2009). Furthermore, Ofd1 localizes to the distal central region between CP110 and POC5 in procentrioles and parental centrioles, but in the absence of that protein centrioles elongate abnormally (Singla et al. 2010). These elongated centrioles are characterized by an ultrastructure similar to those of normal centrioles but their MTs are destabilized and often lack polyglutamylation and the recruitment of Ift88 is impaired. Ofd1 is required for the development of left-right asymmetry and for primary cilia formation (Ferrante et al. 2006). The corresponding gene, OFD1, is of particular medical interest because mutations are linked to lethal males and a variable phenotype in females including polycystic kidney disease and digital or oral malformations (Ferrante et al. 2001; Romio et al. 2004).

With the many newly identified centriolar proteins that either contribute to or are essential for the control of centriole length future research should aim to delineate the underlying molecular mechanisms and to generate a deeper understanding of the relevant protein interactions.

5.6 Are Ciliogenesis and the Control of Centriole Length Mechanistically Linked?

In addition to the role of CP110 displacement from the basal body in cilium formation, which has been discussed earlier (see chapter 5.1), all proteins that regulate centriole length are potentially important for ciliogenesis. In *C. elegans* and *Xenopus* SAS-4 does not only control procentriole formation but is indirectly needed for cilia assembly because it recruits the conserved protein HYLS-1. This protein is essential for the anchoring of the basal body to the plasma membrane, without being needed for centriole duplication (Dammermann 2009). A single amino acid change in HYLS-1 impairs ciliogenesis and leads to hydroethalus syndrome, a lethal perinatal disorder. However, an interaction between human CPAP and HYLS-1 has not been reported. In general, in human cells no compelling evidence has yet been found that an increase of CPAP levels may directly be required for cilia assembly and potentially the extension of the axonemal MTs. Even though CPAP depletion has been shown to reduce primary cilium formation, this might as well be a consequence of the underlying centriole duplication defects (Graser et al. 2007).

The *Tetrahymena* homologue of human POC1, which localizes to basal bodies and nascent centrioles (Keller et al. 2009), is the first protein identified that is required for both ciliogenesis and basal body stability (Pearson et al. 2009).

It is an interesting question whether CPAP is essential for ciliogenesis or if the elongation of axonemal MTs is driven by proteins completely unrelated to centriole elongation. It is an intriguing and plausible thought that those molecules assigned to the elongation of growing centrioles could also promote early axoneme formation and possibly contribute to the extension of the ciliary MT scaffold.

6. MATERIALS AND METHODS

Antibodies

Polyclonal rabbit antibodies against His-tagged CP110 (aa1-149) and Cep192 (aa1441-1938) and MBP-tagged Cep290 (aa584-1203) were raised at Charles River Laboratories (Elevages Scientifique des Dombes, Charles River Laboratories, Romans, France) and then purified according to standard protocols, using GST-tagged antigens bound to Affigel (Bio-Rad Laboratories, Hercules, CA, USA). A monoclonal antibody was raised against an HIS-tagged purified CP110 protein (aa1-149) in mice and after hybridoma cell fusion clones were analyzed and selected (the subclass was determined as IgG1; production of this monoclonal antibody was largely carried out by Elisabeth Bürgelt, Alicija Baskaja and Elena Nigg). Anti-c-myc (Evan et al. 1985), anti-CAP350 and anti-Ninein (Yan et al. 2006), anti-CPAP, anti-Plk4 and anti-Cep135 (Kleylein-Sohn et al. 2007), anti-Centrin-3 (Thein et al. 2007), anti-Cep164 (Graser et al. 2007), anti-C-Nap1 (Fry et al. 1998), and anti-GT335 antibodies (Wolff et al. 1992) were described previously. Antibodies against acetylated-tubulin as well as FITC-labeled anti-α-tubulin antibodies were purchased from Sigma (Taufkirchen, Germany). All primary antibodies used in this study are listed in Table 3 in this section. AlexaRed-555 and AlexaGreen-488 labeled secondary anti-mouse and anti-rabbit antibodies were purchased from Invitrogen (Carlsbad, CA, USA). Anti-Polaris and anti-Cep97 antibodies were generously provided by Dr. B. K. Yoder (University of Alabama, Birmingham, USA) and Dr. B. D. Dynlacht (New York University Cancer Institute, New York, USA). To simultaneously visualize different polyclonal rabbit antibodies, these were directly labelled by AlexaRed-555 and AlexaCy5-647 fluorophores, using the corresponding Antibody Labeling Kits (Invitrogen, Carlsbad, CA).

Chemicals and Materials

All chemicals were purchased from Merck, Sigma-Aldrich Chemical Company (Sigma, St Louis, MO), Fluka-Biochemika (Buchs, Switzerland) or Roth (Karlsruhe, Germany) unless otherwise stated. Components of growth media for *E. coli* and yeast were from Difco Laboratories (Lawrence, KS) or Merck (Darmstadt, Germany). The Minigel system was purchased from Bio-Rad., tabletop centrifuges were from Eppendorf.

Plasmids and Cloning

A plasmid encoding CPAP (Hung et al. 2000) was kindly provided by Dr. T. K. Tang (Institute of Biomedical Sciences, Academia Sinica, Taipei 115, Taiwan) and first subcloned into a pFBT9 vector by Dr. Sébastien B. Lavoie (MPI of Biochemistry) to then facilitate further cloning into a pcDNA3.1 vectors providing N-terminal FLAG- or myc-tags. Cloning of the CP110, Cep192 and Plk4 plasmids has been described previously (Andersen et al. 2003; Habedanck et al. 2005). Human Plk4 cDNA was constructed and kindly provided by Dr. Jens Westendorf (MPI of Biochemistry). All cloning procedures were performed according to standard techniques as described in "Molecular Cloning: A Laboratory Manual" (Sambrook, 1989; 2nd edition) and "Current Protocols in Molecular Biology" (Wiley, 1999) Restriction enzymes were purchased from Fermentas (Burlington, Ontario, Canada) and ligation reactions were performed using T4 DNA ligase (NEB, Ipswich, MA). Plasmid purifications and DNA extractions from agarose gels were done as specified by the supplier (QIAGEN). All initial plasmids were checked by DNA sequencing at Medigenomix (Martinsried, Germany).

Cell Culture and Transfections

All cells were grown at 37 °C in a 5 % CO_2 atmosphere. U2OS or HeLaS3 cells were cultured in Dulbecco's modified Eagle's medium (DMEM), supplemented with 10 % heat-inactivated fetal calf serum (FCS, PAN Biotech, Aidenbach, Germany) and penicillin-streptomycin (100 µg/ml, GIBCO-BRL, Karlsruhe, Germany). hTERT-RPE1 cells were cultured in DMEM Nutrient Mixture F-12 Ham (Sigma, Munich, Germany) supplemented with 10 % FCS (as above), penicillin/streptomycin (as above), 1 % glutamine (PAN Biotech, Aidenbach, Germany; 200 mM), and 0.35 % sodium bicarbonate (Sigma, Munich, Germany). Primary cilium formation was induced by serum starvation for 60 hours (Graser et al. 2007).

Cells adherent on acid treated glass coverslips were transiently transfected with full-length N-terminally myc-tagged and GFP-tagged CPAP, FLAG-tagged CP110 and Plk4 (as listed in Table 5), or corresponding pcDNA3.1 vector controls, using TransIT-LT1 transfection reagents (Mirus Bio; Madison, Wisconsin, USA) according to the manufacturers protocol. A tetracyclin-inducible cell-line expressing myc-tagged CPAP was generated by Dr. Jens Westendorf by transfection of U2OS T-REx cells (Invitrogen).

Stable transformants were established by clone selection for 2 weeks with 1 mg ml^{-1} G418 (Invitrogen) and 50 µg ml^{-1} hygromycin (Merck). Claudia Szalma largely contributed to the generation of the cell line and to initial clone selection. myc-CPAP expression was induced by the addition of 1 µg ml^{-1} of tetracyclin. To induce S phase arrests cells were incubated with 1.6 µg/ml aphidicolin and cells were synchronized in metaphase to assay spindle morphologies by the proteasome inhibitor MG132 (20 µM) for 1 hour after previously being release from aphidicolin.

siRNA-Mediated Protein Depletion

Proteins were depleted using the listed siRNA duplex oligonucleotides (Qiagen, Hilden, Germany and Dharmacon Research Inc, Lafayette, CO; target sequences are listed below in Table 4), and the luciferase duplex GL2 was used for control (Elbashir et al. 2001). Transfections were performed using Oligofectamin (Invitrogen) according to the manufacturer's protocol and the transfection mix was then replaced after 4 hours by fresh medium in order to improve cell viability.

Microscopic Techniques

To maximize visualization of centrioles, cytoplasmic MTs were depolymerized by a 40 min cold treatment (4 ^{o}C) before cells were permeabilized by incubation for 40 sec in PBS, 0.5 % Triton X-100, followed by methanol fixation for 20 min at -20 °C (or, in the case of staining for Polaris, 3.7 % formaldehyde). Antibody incubations and washings were performed as described previously (Meraldi et al. 1999), DNA was visualized by staining with DAPI (200 ng/ml). Slides were analyzed using a Deltavision microscope on a Nikon TE200 base (Applied Precision, Issaquah, WA), equipped with an APOPLAN x100/1.4 n.a. oil-immersion objective. Serial optical sections obtained 0.2 µm apart along the Z axis were processed using a deconvolution algorithm and projected into one picture using Softworx (Applied Precision). Images were processed with Adobe Photoshop CS2 (Adobe Systems, Mountain View, CA). For immuno-EM, cells were grown on coverslips, fixed with 4 % paraformaldehyde for 10 min, and permeabilized with PBS, 0.5 % Triton X-100 for 2 min. Blocking in PBS, 2 % BSA was performed for 30 min, primary antibody incubations were performed for 60 min and followed by incubation with goat anti-rabbit IgG-Nanogold (1:50 Nanoprobes; Yaphank, USA) for 60 min. Goat anti-rabbit IgG-Nanogold was silver enhanced with HQ Silver (Nanoprobes) for 8.5 min. Cells were

further processed as described previously (Fry et al. 1998). For transmission EM cells were fixed in 2.5 % glutaraldehyde for 2 h. All electron microscopy work was kindly performed by Dr. York-Dieter Stierhof and colleagues (ZMBP, University of Tübingen, Germany).

Cell Extracts, Immunoblotting and Immunoprecipitations

For immunoprecipitations, HEK293 cells were trypsinized and collected, washed with PBS and lysed on ice for 20 min in lysis buffer (50 mM HEPES pH 7.0, 250 mM NaCl, 5 mM EDTA pH 8.0, 0.1% NP40, 1 mM DTT, 10 mM NaF, 50 mM β-glycerophosphate, 10 % glycerol, Complete Mini protease inhibitor cocktail (Roche Diagnostics, Mannheim, Germany). Lysates were cleared by centrifugation for 15 min at 16,000 g, 4 °C, and incubated with anti-CP110 antibodies (raised in mouse or rabbit) coupled to proteinG beads for 2 hours at 4 °C. Immunocomplexes bound to beads were washed three times with wash buffer (50 mM HEPES pH 7.0, 400 mM NaCl, 5 mM EDTA pH 8.0, 0.1 % NP40, 1 mM DTT, 10 mM NaF, 50 mM β-glycerophosphate, 10 % glycerol). Immunoprecipitated proteins were eluted into Laemmli buffer, separated by SDS-PAGE and transferred by wet transfer with TOWBIN buffer to PVDF membranes using a blotting apparatus (Bio-Rad). For Western blot analysis, membranes were incubated for 1 hour in blocking buffer (5 % low-fat dry milk in PBS, 0.1 % Tween-20). All antibody incubations were either carried out in blocking buffer overnight at 4 °C or for 1 hour at room temparature. Membranes were probed with indicated antibodies in blocking buffer, followed by incubation with HRP conjugated goat anti-mouse or anti-rabbit antibodies (Jackson Immunoresearch). Signals were detected by enhanced chemoluminescence using SuperSignal® West Femto ECL reagents diluted 1:10 in dH_2O (Thermo Scientific, Rockford, IL).

Mass Spectrometry

Proteins were isolated by immunoprecipitation and separated on a NuPAGE Bis-Tris gel (4-12 %; Invitrogen). The separated proteins were stained with Coomassie Blue and bands were excised and in-gel digested using trypsin (Promega, sequencing-grade). Peptides were desalted and concentrated using C18 extraction tips. Samples were analyzed by online C18 reversed-phase nanoscale liquid chromatography tandem mass spectrometry on a NanoAcquity UPLC system (Waters) connected to an LTQ-Orbitrap (Thermo

Electron) equipped with a nanoelectrospray ion source (Proxeon). MaxQuant software (version 1.0.12.5) was used for data analysis using default parameters. Data was searched against IPI_human (version 3.48) using MASCOT (version 2.204). All mass spectrometry analyses were kindly performed by Dr. Roman Körner and his group (Max-Planck Institute of Biochemistry, Martinsried, Germany).

FACS Analysis, Quantification of Protein Levels and Statistical Approaches

For cell cycle distribution analysis, cells were trypsinized and fixed in 70 % ethanol, followed by an incubation for 30 min in PBS, 10 µg/ml RNase A (Sigma-Aldrich) and 5 µg/ml propidium iodide (Sigma-Aldrich). Analysis was performed using a FACScan cytometer (Becton Dickinson) and FlowJo software (TreeStar Inc., Ashland, Oregon, USA). Ratios of induced myc-CPAP over endogenous CPAP were roughly estimated based on pixel intensity measurements of chemiluminescent western blot signals using the ImageJ software. The mean pixel value for each band was divided by the number of pixels to give an absolute intensity for each band. Fold inductions refer to the absolute intensity of endogenous CPAP. Quantification of maximal pixel intensities and distance measurements in IF images were performed after image acquisition using Softworx software (Applied Precision). The data presented in Figure 12 were kindly provided by Dr. Jens Westendorf (Max-Planck Institute of Biochemistry, Martinsried, Germany).

Table 3: List of Primary Antibodies Used

Number	Antigen	Made in	Dilution	Comment	Distributor/Reference
6-11B-1	acetylated-tubulin	Mouse	1:1000	affinity purified	Sigma
DM1A	α-tubulin	Mouse	1:1000	affinity purified	Sigma
G01	CAP350	Goat	1:2000	affinity purified	Yan et al. 2006
R67	Centrin2	Rabbit	1:500	affinity purified	Kleylein-Sohn et al. 2007
G03	Centrin3	Goat	1:100	affinity purified	Thein et al. 2007
R738	Cep135	Rabbit	1:1000	affinity purified	Kleylein-Sohn et al. 2007
R171	Cep164	Rabbit	1:1000	affinity purified	Graser et al. 2007
R113	Cep170	Rabbit	1:1000	affinity purified	Guarguaglini et al. 2005
R775	Cep192	Rabbit	0.2 µg/ml	affinity purified	this work
R180	Cep290	Rabbit	1:200	affinity purified	Kindly provided by X. Yan (MPI of Biochemistry)
n.a.	Cep97	Rabbit	1:250	affinity purified	Kindly provided by B.D. Dynlacht (Spektor et al. 2007)
R63	C-Nap1	Rabbit	0.2 µg/ml	affinity purified	Fry et al. 1998
140-195-5	CP110	Mouse	undiluted	hybridoma supernatant	this work
R766	CP110	Rabbit	0.2 µg/ml	affinity purified	this work
R729	CPAP	Rabbit	1:500	affinity purified	Kleylein-Sohn et al. 2007
95-381	CPAP	Mouse	undiluted	hybridoma supernatant	Kindly provided by M. LeClech (MPI of Biochemistry)
9E10	Myc	Mouse	1:5	hybridoma supernatant	Evan et al. 1985
R154	Ninein	Rabbit	1:2000	affinity purified	Yan et al. 2006
Ab4448	Pericentrin	Rabbit	1.0 µg/ml		Abcam
R689	Plk4	Rabbit	1:500	affinity purified	Kleylein-Sohn et al. 2007
B1700	Polaris/IFT88	Rabbit	1:500	affinity purified	Kindly provided by B.K. Yoder (Taulman et al. 2001)
GT335	polyglutamylated-tubulin	Mouse	1:500	affinity purified	Wolff et al.1992
91-390	Sas-6	Mouse	undiluted	hybridoma supernatant	Kleylein-Sohn et al. 2007

Table 4: List of Relevant siRNA Oligonucleotides Used

Gene	Target sequence (all 5´-3´)	Oligo #	Reference
CP110	TAGACTTATGCAGACAGATAA	290	Kleylein-Sohn et al. 2007
CP110	CCCGAAATTATGCCAAAGTTA	291	Kleylein-Sohn et al. 2007
CP110	AAGCAGCATGAGTATGCCAGT	550	Spektor et al. 2007
CPAP	AAGGAAGATTGCACCAGTCAA	250	Kleylein-Sohn et al. 2007
CPAP	CCCAATGGAACTCGAAAGGAA	251	Kleylein-Sohn et al. 2007
CAP350	ATGAACGATATCAGTGCTATA	300	Yan et al. 2006
CAP350	CAGGTAGTAGTCATCTTATAA	301	Yan et al. 2006
Cep76	CTCGGTATTATAGGGCCAATA	268	Graser et al. 2007
Cep76	GACGGCTTCTTGATACTCCAA	819	Graser et al. 2007
Cep97	GATGAGAAGTGAAATCAATTT	542	Spektor et al. 2007
Cep97	TGAGAAAGCTGGACTATTATT	543	Spektor et al. 2007
Cep70	CCGGCGACTGAGTAAGATGAA	264	Graser et al. 2007
Cep70	GAAGATCGCATTGTCACTCAA	265	Graser et al. 2007
MCAK	AAGCTATCTGCTGGCTCTAAA	639	Thein, Kerstin 2007
MCAK	AAGATCCAACGCAGTAATGGT	643	Holmfeldt et al. 2004, Cassimeris et al. 2004
C-Nap1	CTGGAAGAGCGTCTAACTGAT	225	Bahe et al. 2005
C-Nap1	GCGGAGCTCTCTGAAGTTAAA	238	Bahe et al. 2005

Table 5: List of Plasmids Relevant to This Study

Name	Gene	Insert	Vector/Tag
pTS10	CP110	aa1-149	pET28b(+)/N+CHIS
pTS24	CP110	aa1-991	pcDNA3.1/NFLAG
N/A	Cep192	aa1441-1938	pET28b(+)/N+CHIS
pTS36	CPAP	aa1-1338	pcDNA3.1/3xmyc-A
pTS38	CPAP	aa1-1338	pcDNA3.1/NFLAG-TO
pTS39	CPAP	aa1-1338	pcDNA3.1/NMyc-TO
pTS40	CPAP	aa1-1338	pcDNA4/TO
pTS53	CPAP	aa1-132	pcDNA3.1/NFLAG-TO
pTS54	CPAP	aa311-422	pcDNA3.1/NFLAG-TO
pTS55	CPAP	aa1-422	pcDNA3.1/NFLAG-TO
pTS56	CPAP	aa430-890	pcDNA3.1/NFLAG-TO
pTS57	CPAP	aa898-1338	pcDNA3.1/NFLAG-TO
pTS58	CPAP	aa1070-1338	pcDNA3.1/NFLAG-TO
pTS59	CPAP	aa1150-1338	pcDNA3.1/NFLAG-TO
pTS60	CPAP	aa1-1338	pEGFP-C2
pTS68	CPAP	aa898-1065	pcDNA3.1/NFLAG-TO
pTS86	Cep97	aa1-865	pcDNA3.1/NFLAG
pJW127	Plk4	aa1-889	pcDNA3.1/NFLAG

Table 6: List of Primers Relevant to This Study

Name	Purpose	Sequence (5' - 3')
oTS6	cloning of CP110 aa1-149	CCGGATCCCCATGGAGGAGTATGAGAAGTTCTGTG
oTS7		CCCTCGAGATCCAATGGCAAAATCCCAGC
oTS32	cloning of CP110 aa1-991	ATTGGATCCACCATGGAGGAGTATGAGAAGTTCTGTG
oTS33		ATTCTCGAGTTATCCTAATGAATGTTGTCTTCTTAAATTGTCG
oTS64	cloning of Cep97 aa1-866	ATATGGATCCTGGCGGTGGCGCGCGTGGACG
oTS65		ATGGCTCGAGCTACACAGTAACACCAACATGC
oSL74	cloning of CPAP aa1-1338	ATATGGATCCTGTTCCTGATGCCAACCTCTTC
oSL75		ATATGTCGACTCACAGCTCCGTGTCCATTAGC
M3346	cloning of CPAP aa1-132	GGGATCCCCATGTTCCTGATGCCAACCTCTTC
M3351		CGTCGACTTCACTCGCACGATCTGGGATGAAG
M3347	cloning of CPAP aa311-422	GGGATCCCCCAAAAACATGATGATTCCTCAG
M3352		CGTCGACCCGCTGGAGTTGCTGTCTATCC
M3346	cloning of CPAP aa1-422	GGGATCCCCATGTTCCTGATGCCAACCTCTTC
M3352		CGTCGACCCGCTGGAGTTGCTGTCTATCC
M3348	cloning of CPAP aa430-890	GGGATCCCCGAGCTGTGTGCAGACAACCCTATC
M3353		CGTCGACGTTTAACTTGAGTTCATTTCCCAAGTG
M3349	cloning of CPAP aa898-1338	GGGATCCCCGGTGACAATGCTCGATCCCAG
M3354		CGTCGACCAGCTCCGTGTCCATTGACACATTAC
M3350	cloning of CPAP aa1070-1338	GGGATCCCCCTTGCGAACACATCTGTTCG
M3354		CGTCGACCAGCTCCGTGTCCATTGACACATTAC
oTS47	cloning of CPAP aa1150-1338	GGGATCCCCGGAGAAATCAGTCATCCTGATG
M3354		CGTCGACCAGCTCCGTGTCCATTGACACATTAC
M3349	cloning of CPAP aa898-1065	GGGATCCCCGGTGACAATGCTCGATCCCAG
oTS48		ATATGTCGACTCACACCTCGAGGCTGCTCTCTAT

7. ABBREVIATIONS

all units are abbreviated according to the International Unit System

aa	amino acid(s)
ALMS	Alström Syndrome
BBS	Bardet Biedl Syndrome
BSA	bovine serum albumin
Cdk	cyclin-dependent kinase
Cep	centrosomal protein
CHO	Chinese hamster ovary
CIN	chromosomal instability
EM	electron microscopy
FACS	fluorescent-activated cell sorting
FCS	fetal calf serum
GFP	green fluorescent protein
HRP	horse raddish peroxidase
IF	immunofluorescence
IFT	intraflagellular transport
IgG	immunoglobulin G
IP	immunoprecipitation
LCA	Leber Congenital Amaurosis
MBP	maltose binding protein
MS	mass spectrometry
MT	microtubule
MTOC	microtubule organizing centre
NPHP	nephronophthisis
OFD	oral-facial disease
PBS	phosphate buffered saline
PCM	pericentriolar material
PKD	polycystic kidney disease
RPGR	retinitis pigmentosa GTPase regulator
siRNA	small interfering ribonucleic acid
TEM	transmission electron microscopy
TMR	trans-membrane receptor

8. REFERENCES

Acilan C. and Saunders W.S. (2008). A tale of too many centrosomes. *Cell* 134: 572-5.

Andersen J.S., Wilkinson C.J., Mayor T., Mortensen P., Nigg E.A. and Mann M. (2003). Proteomic characterization of the human centrosome by protein correlation profiling. *Nature* 426: 570-4.

Anderson C.T. and Stearns T. (2009). Centriole Age Underlies Asynchronous Primary Cilium Growth in Mammalian Cells. *Curr Biol*

Ansley S.J., Badano J.L., Blacque O.E., Hill J., Hoskins B.E., Leitch C.C., Kim J.C., Ross A.J., Eichers E.R., Teslovich T.M., et al. (2003). Basal body dysfunction is a likely cause of pleiotropic Bardet-Biedl syndrome. *Nature* 425: 628-33.

Azimzadeh J. and Bornens M. (2007). Structure and duplication of the centrosome. *J Cell Sci* 120: 2139-42.

Azimzadeh J., Hergert P., Delouvee A., Euteneuer U., Formstecher E., Khodjakov A. and Bornens M. (2009). hPOC5 is a centrin-binding protein required for assembly of full-length centrioles. *J Cell Biol* 185: 101-14.

Baala L., Audollent S., Martinovic J., Ozilou C., Babron M.C., Sivanandamoorthy S., Saunier S., Salomon R., Gonzales M., Rattenberry E., et al. (2007). Pleiotropic effects of CEP290 (NPHP6) mutations extend to Meckel syndrome. *Am J Hum Genet* 81: 170-9.

Badano J.L., Mitsuma N., Beales P.L. and Katsanis N. (2006). The ciliopathies: an emerging class of human genetic disorders. *Annu Rev Genomics Hum Genet* 7: 125-48.

Bahe S., Stierhof Y.D., Wilkinson C.J., Leiss F. and Nigg E.A. (2005). Rootletin forms centriole-associated filaments and functions in centrosome cohesion. *J Cell Biol* 171: 27-33.

Balczon R., Bao L., Zimmer W.E., Brown K., Zinkowski R.P. and Brinkley B.R. (1995). Dissociation of centrosome replication events from cycles of DNA synthesis and mitotic division in hydroxyurea-arrested Chinese hamster ovary cells. *J Cell Biol* 130: 105-15.

Basto R., Brunk K., Vinadogrova T., Peel N., Franz A., Khodjakov A. and Raff J.W. (2008). Centrosome amplification can initiate tumorigenesis in flies. *Cell* 133: 1032-42.

Beisson J. and Wright M. (2003). Basal body/centriole assembly and continuity. *Curr Opin Cell Biol* 15: 96-104.

Berbari N.F., O'Connor A.K., Haycraft C.J. and Yoder B.K. (2009). The primary cilium as a complex signaling center. *Curr Biol* 19: R526-35.

Berthet C., Aleem E., Coppola V., Tessarollo L. and Kaldis P. (2003). Cdk2 knockout mice are viable. *Curr Biol* 13: 1775-85.

Besschetnova T.Y., Kolpakova-Hart E., Guan Y., Zhou J., Olsen B.R. and Shah J.V. (2010). Identification of Signaling Pathways Regulating Primary Cilium Length and Flow-Mediated Adaptation. *Curr Biol*

Bettencourt-Dias M. and Carvalho-Santos Z. (2008). Double life of centrioles: CP110 in the spotlight. *Trends Cell Biol* 18: 8-11.

Bettencourt-Dias M. and Glover D.M. (2007). Centrosome biogenesis and function: centrosomics brings new understanding. *Nat Rev Mol Cell Biol* 8: 451-63.

Bettencourt-Dias M. and Glover D.M. (2009). SnapShot: centriole biogenesis. *Cell* 136: 188-188 e1.

Bettencourt-Dias M., Rodrigues-Martins A., Carpenter L., Riparbelli M., Lehmann L., Gatt M.K., Carmo N., Balloux F., Callaini G. and Glover D.M. (2005). SAK/PLK4 is required for centriole duplication and flagella development. *Curr Biol* 15: 2199-207.

Blaineau C., Tessier M., Dubessay P., Tasse L., Crobu L., Pages M. and Bastien P. (2007). A novel microtubule-depolymerizing kinesin involved in length control of a eukaryotic flagellum. *Curr Biol* 17: 778-82.

Bond J., Roberts E., Springell K., Lizarraga S.B., Scott S., Higgins J., Hampshire D.J., Morrison E.E., Leal G.F., Silva E.O., et al. (2005). A centrosomal mechanism involving CDK5RAP2 and CENPJ controls brain size. *Nat Genet* 37: 353-5.

Bornens M. (2002). Centrosome composition and microtubule anchoring mechanisms. *Curr Opin Cell Biol* 14: 25-34.

Bornens M. (2008). Organelle positioning and cell polarity. *Nat Rev Mol Cell Biol* 9: 874-86.

Bornens M. and Moudjou M. (1999). Studying the composition and function of centrosomes in vertebrates. *Methods Cell Biol* 61: 13-34.

Boveri T. (1887). Ueber die Befruchtung der Eier von Ascaris megalocephala. *SitzBer Ges Morph Phys München* 71-80.

Boveri T. (1914). Zur Frage der Entstehung maligner Tumoren. *(English Translation: The Origin of Malignant Tumors, Williams and Wilkins, Baltimore, Maryland, 1929)*

Bradley B.A. and Quarmby L.M. (2005). A NIMA-related kinase, Cnk2p, regulates both flagellar length and cell size in Chlamydomonas. *J Cell Sci* 118: 3317-26.

Cardenas-Rodriguez M. and Badano J.L. (2009). Ciliary biology: understanding the cellular and genetic basis of human ciliopathies. *Am J Med Genet C Semin Med Genet* 151C: 263-80.

Carroll P.E., Okuda M., Horn H.F., Biddinger P., Stambrook P.J., Gleich L.L., Li Y.Q., Tarapore P. and Fukasawa K. (1999). Centrosome hyperamplification in human cancer: chromosome instability induced by p53 mutation and/or Mdm2 overexpression. *Oncogene* 18: 1935-44.

Chang B., Khanna H., Hawes N., Jimeno D., He S., Lillo C., Parapuram S.K., Cheng H., Scott A., Hurd R.E., et al. (2006). In-frame deletion in a novel centrosomal/ciliary

protein CEP290/NPHP6 perturbs its interaction with RPGR and results in early-onset retinal degeneration in the rd16 mouse. *Hum Mol Genet* 15: 1847-57.

Chang P., Giddings T.H., Jr., Winey M. and Stearns T. (2003). Epsilon-tubulin is required for centriole duplication and microtubule organization. *Nat Cell Biol* 5: 71-6.

Chen Z., Indjeian V.B., McManus M., Wang L. and Dynlacht B.D. (2002). CP110, a cell cycle-dependent CDK substrate, regulates centrosome duplication in human cells. *Dev Cell* 3: 339-50.

Cho J.H., Chang C.J., Chen C.Y. and Tang T.K. (2006). Depletion of CPAP by RNAi disrupts centrosome integrity and induces multipolar spindles. *Biochem Biophys Res Commun* 339: 742-7.

Chretien D., Buendia B., Fuller S.D. and Karsenti E. (1997). Reconstruction of the centrosome cycle from cryoelectron micrographs. *J Struct Biol* 120: 117-33.

Christensen S.T. and Ott C.M. (2007). Cell signaling. A ciliary signaling switch. *Science* 317: 330-1.

Christensen S.T., Pedersen L.B., Schneider L. and Satir P. (2007). Sensory cilia and integration of signal transduction in human health and disease. *Traffic* 8: 97-109.

Cooper J.R., Wagenbach M., Asbury C.L. and Wordeman L. (2010). Catalysis of the microtubule on-rate is the major parameter regulating the depolymerase activity of MCAK. *Nat Struct Mol Biol* 17: 77-82.

Cormier A., Clement M.J., Knossow M., Lachkar S., Savarin P., Toma F., Sobel A., Gigant B. and Curmi P.A. (2009). The PN2-3 domain of centrosomal P4.1-associated protein implements a novel mechanism for tubulin sequestration. *J Biol Chem* 284: 6909-17.

Cowan C.R. and Hyman A.A. (2006). Cyclin E-Cdk2 temporally regulates centrosome assembly and establishment of polarity in Caenorhabditis elegans embryos. *Nat Cell Biol* 8: 1441-7.

Cunha-Ferreira I., Rodrigues-Martins A., Bento I., Riparbelli M., Zhang W., Laue E., Callaini G., Glover D.M. and Bettencourt-Dias M. (2009). The SCF/Slimb ubiquitin ligase limits centrosome amplification through degradation of SAK/PLK4. *Curr Biol* 19: 43-9.

D'Assoro A.B., Lingle W.L. and Salisbury J.L. (2002). Centrosome amplification and the development of cancer. *Oncogene* 21: 6146-53.

Dammermann A., Maddox P.S., Desai A. and Oegema K. (2008). SAS-4 is recruited to a dynamic structure in newly forming centrioles that is stabilized by the gamma-tubulin-mediated addition of centriolar microtubules. *J Cell Biol* 180: 771-85.

Dammermann A., Pemble H., Mitchell B.J., McLeod I., Yates J.R., 3rd, Kintner C., Desai A.B. and Oegema K. (2009). The hydrolethalus syndrome protein HYLS-1 links core centriole structure to cilia formation. *Genes Dev* 23: 2046-59.

Dawe H.R., Farr H. and Gull K. (2007). Centriole/basal body morphogenesis and migration during ciliogenesis in animal cells. *J Cell Sci* 120: 7-15.

De Boer L., Oakes V., Beamish H., Giles N., Stevens F., Somodevilla-Torres M., Desouza C. and Gabrielli B. (2008). Cyclin A/cdk2 coordinates centrosomal and nuclear mitotic events. *Oncogene* 27: 4261-8.

Delattre M., Canard C. and Gonczy P. (2006). Sequential protein recruitment in C. elegans centriole formation. *Curr Biol* 16: 1844-9.

Delattre M., Leidel S., Wani K., Baumer K., Bamat J., Schnabel H., Feichtinger R., Schnabel R. and Gonczy P. (2004). Centriolar SAS-5 is required for centrosome duplication in C. elegans. *Nat Cell Biol* 6: 656-64.

den Hollander A.I., Koenekoop R.K., Yzer S., Lopez I., Arends M.L., Voesenek K.E., Zonneveld M.N., Strom T.M., Meitinger T., Brunner H.G., et al. (2006). Mutations in the CEP290 (NPHP6) gene are a frequent cause of Leber congenital amaurosis. *Am J Hum Genet* 79: 556-61.

Dirksen E.R. (1991). Centriole and basal body formation during ciliogenesis revisited. *Biol Cell* 72: 31-8.

Doxsey S. (2001). Re-evaluating centrosome function. *Nat Rev Mol Cell Biol* 2: 688-98.

Doxsey S., McCollum D. and Theurkauf W. (2005). Centrosomes in cellular regulation. *Annu Rev Cell Dev Biol* 21: 411-34.

Duensing A., Liu Y., Perdreau S.A., Kleylein-Sohn J., Nigg E.A. and Duensing S. (2007). Centriole overduplication through the concurrent formation of multiple daughter centrioles at single maternal templates. *Oncogene* 26: 6280-8.

Duensing S., Lee L.Y., Duensing A., Basile J., Piboonniyom S., Gonzalez S., Crum C.P. and Munger K. (2000). The human papillomavirus type 16 E6 and E7 oncoproteins cooperate to induce mitotic defects and genomic instability by uncoupling centrosome duplication from the cell division cycle. *Proc Natl Acad Sci U S A* 97: 10002-7.

Elbashir S.M., Harborth J., Lendeckel W., Yalcin A., Weber K. and Tuschl T. (2001). Duplexes of 21-nucleotide RNAs mediate RNA interference in cultured mammalian cells. *Nature* 411: 494-8.

Evan G.I., Lewis G.K., Ramsay G. and Bishop J.M. (1985). Isolation of monoclonal antibodies specific for human c-myc proto-oncogene product. *Mol Cell Biol* 5: 3610-6.

Faragher A.J. and Fry A.M. (2003). Nek2A kinase stimulates centrosome disjunction and is required for formation of bipolar mitotic spindles. *Mol Biol Cell* 14: 2876-89.

Ferrante M.I., Giorgio G., Feather S.A., Bulfone A., Wright V., Ghiani M., Selicorni A., Gammaro L., Scolari F., Woolf A.S., et al. (2001). Identification of the gene for oral-facial-digital type I syndrome. *Am J Hum Genet* 68: 569-76.

Ferrante M.I., Zullo A., Barra A., Bimonte S., Messaddeq N., Studer M., Dolle P. and Franco B. (2006). Oral-facial-digital type I protein is required for primary cilia formation and left-right axis specification. *Nat Genet* 38: 112-7.

Fliegauf M., Benzing T. and Omran H. (2007). When cilia go bad: cilia defects and ciliopathies. *Nat Rev Mol Cell Biol* 8: 880-893.

Frank V., den Hollander A.I., Bruchle N.O., Zonneveld M.N., Nurnberg G., Becker C., Bois G.D., Kendziorra H., Roosing S., Senderek J., et al. (2007). Mutations of the CEP290 gene encoding a centrosomal protein cause Meckel-Gruber syndrome. *Hum Mutat*

Fry A.M., Mayor T., Meraldi P., Stierhof Y.D., Tanaka K. and Nigg E.A. (1998). C-Nap1, a novel centrosomal coiled-coil protein and candidate substrate of the cell cycle-regulated protein kinase Nek2. *J Cell Biol* 141: 1563-74.

Fukasawa K., Choi T., Kuriyama R., Rulong S. and Vande Woude G.F. (1996). Abnormal centrosome amplification in the absence of p53. *Science* 271: 1744-7.

Gadde S. and Heald R. (2004). Mechanisms and molecules of the mitotic spindle. *Curr Biol* 14: R797-805.

Ganem N.J., Godinho S.A. and Pellman D. (2009). A mechanism linking extra centrosomes to chromosomal instability. *Nature*

Gerdes J.M., Davis E.E. and Katsanis N. (2009). The vertebrate primary cilium in development, homeostasis, and disease. *Cell* 137: 32-45.

Gerdes J.M., Liu Y., Zaghloul N.A., Leitch C.C., Lawson S.S., Kato M., Beachy P.A., Beales P.L., DeMartino G.N., Fisher S., et al. (2007). Disruption of the basal body compromises proteasomal function and perturbs intracellular Wnt response. *Nat Genet* 39: 1350-60.

Ghadimi B.M., Sackett D.L., Difilippantonio M.J., Schrock E., Neumann T., Jauho A., Auer G. and Ried T. (2000). Centrosome amplification and instability occurs exclusively in aneuploid, but not in diploid colorectal cancer cell lines, and correlates with numerical chromosomal aberrations. *Genes Chromosomes Cancer* 27: 183-90.

Godinho S.A., Kwon M. and Pellman D. (2009). Centrosomes and cancer: how cancer cells divide with too many centrosomes. *Cancer Metastasis Rev* 28: 85-98.

Gonzalez C., Tavosanis G. and Mollinari C. (1998). Centrosomes and microtubule organisation during Drosophila development. *J Cell Sci* 111 (Pt 18): 2697-706.

Gould R.R. and Borisy G.G. (1977). The pericentriolar material in Chinese hamster ovary cells nucleates microtubule formation. *J Cell Biol* 73: 601-15.

Graser S., Stierhof Y.D., Lavoie S.B., Gassner O.S., Lamla S., Le Clech M. and Nigg E.A. (2007). Cep164, a novel centriole appendage protein required for primary cilium formation. *J Cell Biol* 179: 321-30.

Guarguaglini G., Duncan P.I., Stierhof Y.D., Holmstrom T., Duensing S. and Nigg E.A. (2005). The forkhead-associated domain protein Cep170 interacts with Polo-like kinase 1 and serves as a marker for mature centrioles. *Mol Biol Cell* 16: 1095-107.

Gul A., Hassan M.J., Hussain S., Raza S.I., Chishti M.S. and Ahmad W. (2006). A novel deletion mutation in CENPJ gene in a Pakistani family with autosomal recessive primary microcephaly. *J Hum Genet* 51: 760-4.

Habedanck R., Stierhof Y.D., Wilkinson C.J. and Nigg E.A. (2005). The Polo kinase Plk4 functions in centriole duplication. *Nat Cell Biol* 7: 1140-6.

Han Y.G. and Alvarez-Buylla A. (2010). Role of primary cilia in brain development and cancer. *Curr Opin Neurobiol*

Helenius J., Brouhard G., Kalaidzidis Y., Diez S. and Howard J. (2006). The depolymerizing kinesin MCAK uses lattice diffusion to rapidly target microtubule ends. *Nature* 441: 115-9.

Helou J., Otto E.A., Attanasio M., Allen S.J., Parisi M.A., Glass I., Utsch B., Hashmi S., Fazzi E., Omran H., et al. (2007). Mutation analysis of NPHP6/CEP290 in patients with Joubert syndrome and Senior-Loken syndrome. *J Med Genet* 44: 657-63.

Hemerly A.S., Prasanth S.G., Siddiqui K. and Stillman B. (2009). Orc1 controls centriole and centrosome copy number in human cells. *Science* 323: 789-93.

Hildebrandt F. and Otto E. (2005). Cilia and centrosomes: a unifying pathogenic concept for cystic kidney disease? *Nat Rev Genet* 6: 928-40.

Hinchcliffe E.H., Li C., Thompson E.A., Maller J.L. and Sluder G. (1999). Requirement of Cdk2-cyclin E activity for repeated centrosome reproduction in Xenopus egg extracts. *Science* 283: 851-4.

Hinchcliffe E.H., Miller F.J., Cham M., Khodjakov A. and Sluder G. (2001). Requirement of a centrosomal activity for cell cycle progression through G1 into S phase. *Science* 291: 1547-50.

Hinchcliffe E.H. and Sluder G. (2002). Two for two: Cdk2 and its role in centrosome doubling. *Oncogene* 21: 6154-60.

Hiraki M., Nakazawa Y., Kamiya R. and Hirono M. (2007). Bld10p constitutes the cartwheel-spoke tip and stabilizes the 9-fold symmetry of the centriole. *Curr Biol* 17: 1778-83.

Holland A.J., Lan W., Niessen S., Hoover H. and Cleveland D.W. (2010). Polo-like kinase 4 kinase activity limits centrosome overduplication by autoregulating its own stability. *J Cell Biol* 188: 191-8.

Hoyer-Fender S. (2009). Centriole maturation and transformation to basal body. *Semin Cell Dev Biol*

Hsu W.B., Hung L.Y., Tang C.J., Su C.L., Chang Y. and Tang T.K. (2008). Functional characterization of the microtubule-binding and -destabilizing domains of CPAP and d-SAS-4. *Exp Cell Res* 314: 2591-602.

Huang K., Diener D.R. and Rosenbaum J.L. (2009). The ubiquitin conjugation system is involved in the disassembly of cilia and flagella. *J Cell Biol* 186: 601-13.

Hung L.Y., Chen H.L., Chang C.W., Li B.R. and Tang T.K. (2004). Identification of a novel microtubule-destabilizing motif in CPAP that binds to tubulin heterodimers and inhibits microtubule assembly. *Mol Biol Cell* 15: 2697-706.

Hung L.Y., Tang C.J. and Tang T.K. (2000). Protein 4.1 R-135 interacts with a novel centrosomal protein (CPAP) which is associated with the gamma-tubulin complex. *Mol Cell Biol* 20: 7813-25.

Hunter A.W., Caplow M., Coy D.L., Hancock W.O., Diez S., Wordeman L. and Howard J. (2003). The kinesin-related protein MCAK is a microtubule depolymerase that forms an ATP-hydrolyzing complex at microtubule ends. *Mol Cell* 11: 445-57.

Ibanez-Tallon I., Heintz N. and Omran H. (2003). To beat or not to beat: roles of cilia in development and disease. *Hum Mol Genet* 12 Spec No 1: R27-35.

Ishikawa H., Kubo A. and Tsukita S. (2005). Odf2-deficient mother centrioles lack distal/subdistal appendages and the ability to generate primary cilia. *Nat Cell Biol* 7: 517-24.

Jurczyk A., Gromley A., Redick S., San Agustin J., Witman G., Pazour G.J., Peters D.J. and Doxsey S. (2004). Pericentrin forms a complex with intraflagellar transport proteins and polycystin-2 and is required for primary cilia assembly. *J Cell Biol* 166: 637-43.

Keller L.C., Geimer S., Romijn E., Yates J., 3rd, Zamora I. and Marshall W.F. (2009). Molecular architecture of the centriole proteome: the conserved WD40 domain protein POC1 is required for centriole duplication and length control. *Mol Biol Cell* 20: 1150-66.

Keller L.C., Romijn E.P., Zamora I., Yates J.R., 3rd and Marshall W.F. (2005). Proteomic analysis of isolated chlamydomonas centrioles reveals orthologs of ciliary-disease genes. *Curr Biol* 15: 1090-8.

Kellogg D.R., Moritz M. and Alberts B.M. (1994). The centrosome and cellular organization. *Annu Rev Biochem* 63: 639-74.

Khodjakov A., Rieder C.L., Sluder G., Cassels G., Sibon O. and Wang C.L. (2002). De novo formation of centrosomes in vertebrate cells arrested during S phase. *J Cell Biol* 158: 1171-81.

Kilburn C.L., Pearson C.G., Romijn E.P., Meehl J.B., Giddings T.H., Jr., Culver B.P., Yates J.R., 3rd and Winey M. (2007). New Tetrahymena basal body protein components identify basal body domain structure. *J Cell Biol* 178: 905-12.

Kim J., Krishnaswami S.R. and Gleeson J.G. (2008). CEP290 interacts with the centriolar satellite component PCM-1 and is required for Rab8 localization to the primary cilium. *Hum Mol Genet* 17: 3796-805.

Kirkham M., Muller-Reichert T., Oegema K., Grill S. and Hyman A.A. (2003). SAS-4 is a C. elegans centriolar protein that controls centrosome size. *Cell* 112: 575-87.

Kitagawa D., Busso C., Fluckiger I. and Gonczy P. (2009). Phosphorylation of SAS-6 by ZYG-1 is critical for centriole formation in C. elegans embryos. *Dev Cell* 17: 900-7.

Kleylein-Sohn J., Westendorf J., Le Clech M., Habedanck R., Stierhof Y.D. and Nigg E.A. (2007). Plk4-induced centriole biogenesis in human cells. *Dev Cell* 13: 190-202.

Kohlmaier G., Loncarek J., Meng X., McEwen B.F., Mogensen M.M., Spektor A., Dynlacht B.D., Khodjakov A. and Gonczy P. (2009). Overly Long Centrioles and Defective Cell Division upon Excess of the SAS-4-Related Protein CPAP. *Curr Biol*

Kovacs J.J., Whalen E.J., Liu R., Xiao K., Kim J., Chen M., Wang J., Chen W. and Lefkowitz R.J. (2008). Beta-arrestin-mediated localization of smoothened to the primary cilium. *Science* 320: 1777-81.

Krauss S.W., Spence J.R., Bahmanyar S., Barth A.I., Go M.M., Czerwinski D. and Meyer A.J. (2008). Downregulation of protein 4.1R, a mature centriole protein, disrupts centrosomes, alters cell cycle progression, and perturbs mitotic spindles and anaphase. *Mol Cell Biol* 28: 2283-94.

Kuriyama R. and Borisy G.G. (1981). Centriole cycle in Chinese hamster ovary cells as determined by whole-mount electron microscopy. *J Cell Biol* 91: 814-21.

Kuriyama R., Dasgupta S. and Borisy G.G. (1986). Independence of centriole formation and initiation of DNA synthesis in Chinese hamster ovary cells. *Cell Motil Cytoskeleton* 6: 355-62.

Kwon M., Godinho S.A., Chandhok N.S., Ganem N.J., Azioune A., Thery M. and Pellman D. (2008). Mechanisms to suppress multipolar divisions in cancer cells with extra centrosomes. *Genes Dev* 22: 2189-203.

La Terra S., English C.N., Hergert P., McEwen B.F., Sluder G. and Khodjakov A. (2005). The de novo centriole assembly pathway in HeLa cells: cell cycle progression and centriole assembly/maturation. *J Cell Biol* 168: 713-22.

Lacey K.R., Jackson P.K. and Stearns T. (1999). Cyclin-dependent kinase control of centrosome duplication. *Proc Natl Acad Sci U S A* 96: 2817-22.

Lancaster M.A. and Gleeson J.G. (2009). The primary cilium as a cellular signaling center: lessons from disease. *Curr Opin Genet Dev* 19: 220-9.

Larsen T.E. and Ghadially F.N. (1974). Cilia in lupus nephritis. *J Pathol* 114: 69-73.

Le Clech M. (2008). Role of CAP350 in centriolar tubule stability and centriole assembly. *PLoS One* 3: e3855.

Lee T., Langford K.J., Askham J.M., Bruning-Richardson A. and Morrison E.E. (2008). MCAK associates with EB1. *Oncogene* 27: 2494-500.

Leidel S., Delattre M., Cerutti L., Baumer K. and Gonczy P. (2005). SAS-6 defines a protein family required for centrosome duplication in C. elegans and in human cells. *Nat Cell Biol* 7: 115-25.

Leidel S. and Gonczy P. (2003). SAS-4 is essential for centrosome duplication in C elegans and is recruited to daughter centrioles once per cell cycle. *Dev Cell* 4: 431-9.

Leitch C.C., Zaghloul N.A., Davis E.E., Stoetzel C., Diaz-Font A., Rix S., Alfadhel M., Lewis R.A., Eyaid W., Banin E., et al. (2008). Hypomorphic mutations in syndromic encephalocele genes are associated with Bardet-Biedl syndrome. *Nat Genet* 40: 443-8.

Lim H.H., Zhang T. and Surana U. (2009). Regulation of centrosome separation in yeast and vertebrates: common threads. *Trends Cell Biol* 19: 325-33.

Lingle W.L., Barrett S.L., Negron V.C., D'Assoro A.B., Boeneman K., Liu W., Whitehead C.M., Reynolds C. and Salisbury J.L. (2002). Centrosome amplification drives chromosomal instability in breast tumor development. *Proc Natl Acad Sci U S A* 99: 1978-83.

Lingle W.L., Lutz W.H., Ingle J.N., Maihle N.J. and Salisbury J.L. (1998). Centrosome hypertrophy in human breast tumors: implications for genomic stability and cell polarity. *Proc Natl Acad Sci U S A* 95: 2950-5.

Loktev A.V., Zhang Q., Beck J.S., Searby C.C., Scheetz T.E., Bazan J.F., Slusarski D.C., Sheffield V.C., Jackson P.K. and Nachury M.V. (2008). A BBSome subunit links ciliogenesis, microtubule stability, and acetylation. *Dev Cell* 15: 854-65.

Loncarek J., Hergert P., Magidson V. and Khodjakov A. (2008). Control of daughter centriole formation by the pericentriolar material. *Nat Cell Biol* 10: 322-8.

Marshall W.F. (2007). Centriole assembly: the origin of nine-ness. *Curr Biol* 17: R1057-9.

Marshall W.F. (2008). Basal bodies platforms for building cilia. *Curr Top Dev Biol* 85: 1-22.

Marshall W.F. (2008). The cell biological basis of ciliary disease. *J Cell Biol* 180: 17-21.

Marshall W.F. (2009). Centriole evolution. *Curr Opin Cell Biol* 21: 14-9.

Matsumoto Y., Hayashi K. and Nishida E. (1999). Cyclin-dependent kinase 2 (Cdk2) is required for centrosome duplication in mammalian cells. *Curr Biol* 9: 429-32.

Matsuura K., Lefebvre P.A., Kamiya R. and Hirono M. (2004). Bld10p, a novel protein essential for basal body assembly in Chlamydomonas: localization to the cartwheel, the first ninefold symmetrical structure appearing during assembly. *J Cell Biol* 165: 663-71.

Mayor T., Stierhof Y.D., Tanaka K., Fry A.M. and Nigg E.A. (2000). The centrosomal protein C-Nap1 is required for cell cycle-regulated centrosome cohesion. *J Cell Biol* 151: 837-46.

Meraldi P., Lukas J., Fry A.M., Bartek J. and Nigg E.A. (1999). Centrosome duplication in mammalian somatic cells requires E2F and Cdk2-cyclin A. *Nat Cell Biol* 1: 88-93.

Michaud E.J. and Yoder B.K. (2006). The primary cilium in cell signaling and cancer. *Cancer Res* 66: 6463-7.

Miyoshi K., Kasahara K., Miyazaki I. and Asanuma M. (2009). Lithium treatment elongates primary cilia in the mouse brain and in cultured cells. *Biochem Biophys Res Commun* 388: 757-62.

Miyoshi K., Kasahara K., Miyazaki I., Shimizu S., Taniguchi M., Matsuzaki S., Tohyama M. and Asanuma M. (2009). Pericentrin, a centrosomal protein related to microcephalic primordial dwarfism, is required for olfactory cilia assembly in mice. *FASEB J*

Mogensen M.M., Malik A., Piel M., Bouckson-Castaing V. and Bornens M. (2000). Microtubule minus-end anchorage at centrosomal and non-centrosomal sites: the role of ninein. *J Cell Sci* 113 (Pt 17): 3013-23.

Moritz M. and Agard D.A. (2001). Gamma-tubulin complexes and microtubule nucleation. *Curr Opin Struct Biol* 11: 174-81.

Moritz M., Braunfeld M.B., Sedat J.W., Alberts B. and Agard D.A. (1995). Microtubule nucleation by gamma-tubulin-containing rings in the centrosome. *Nature* 378: 638-40.

Moser J.J., Fritzler M.J. and Rattner J.B. (2009). Primary ciliogenesis defects are associated with human astrocytoma/glioblastoma cells. *BMC Cancer* 9: 448.

Nachury M.V., Loktev A.V., Zhang Q., Westlake C.J., Peranen J., Merdes A., Slusarski D.C., Scheller R.H., Bazan J.F., Sheffield V.C., et al. (2007). A core complex of BBS proteins cooperates with the GTPase Rab8 to promote ciliary membrane biogenesis. *Cell* 129: 1201-13.

Nakazawa Y., Hiraki M., Kamiya R. and Hirono M. (2007). SAS-6 is a cartwheel protein that establishes the 9-fold symmetry of the centriole. *Curr Biol* 17: 2169-74.

Nigg E.A. (2002). Centrosome aberrations: cause or consequence of cancer progression? *Nat Rev Cancer* 2: 815-25.

Nigg E.A. (2004). Centrosomes in Development and Disease. *Wiley-VCH Verlag GmbH & Co. KGaA*

Nigg E.A. (2007). Centrosome duplication: of rules and licenses. *Trends Cell Biol* 17: 215-21.

Nigg E.A. and Raff J.W. (2009). Centrioles, centrosomes, and cilia in health and disease. *Cell* 139: 663-78.

Nogales-Cadenas R., Abascal F., Diez-Perez J., Carazo J.M. and Pascual-Montano A. (2009). CentrosomeDB: a human centrosomal proteins database. *Nucleic Acids Res* 37: D175-80.

Nonaka S., Tanaka Y., Okada Y., Takeda S., Harada A., Kanai Y., Kido M. and Hirokawa N. (1998). Randomization of left-right asymmetry due to loss of nodal cilia generating leftward flow of extraembryonic fluid in mice lacking KIF3B motor protein. *Cell* 95: 829-37.

O'Connell K.F., Caron C., Kopish K.R., Hurd D.D., Kemphues K.J., Li Y. and White J.G. (2001). The C. elegans zyg-1 gene encodes a regulator of centrosome duplication with distinct maternal and paternal roles in the embryo. *Cell* 105: 547-58.

O'Toole E.T., McDonald K.L., Mantler J., McIntosh J.R., Hyman A.A. and Muller-Reichert T. (2003). Morphologically distinct microtubule ends in the mitotic centrosome of Caenorhabditis elegans. *J Cell Biol* 163: 451-6.

Ohta T., Essner R., Ryu J.H., Palazzo R.E., Uetake Y. and Kuriyama R. (2002). Characterization of Cep135, a novel coiled-coil centrosomal protein involved in microtubule organization in mammalian cells. *J Cell Biol* 156: 87-99.

Omran H., Sasmaz G., Haffner K., Volz A., Olbrich H., Melkaoui R., Otto E., Wienker T.F., Korinthenberg R., Brandis M., et al. (2002). Identification of a gene locus for Senior-Loken syndrome in the region of the nephronophthisis type 3 gene. *J Am Soc Nephrol* 13: 75-9.

Ortega S., Prieto I., Odajima J., Martin A., Dubus P., Sotillo R., Barbero J.L., Malumbres M. and Barbacid M. (2003). Cyclin-dependent kinase 2 is essential for meiosis but not for mitotic cell division in mice. *Nat Genet* 35: 25-31.

Ou Y., Ruan Y., Cheng M., Moser J.J., Rattner J.B. and van der Hoorn F.A. (2009). Adenylate cyclase regulates elongation of mammalian primary cilia. *Exp Cell Res* 315: 2802-17.

Palazzo R.E., Vogel J.M., Schnackenberg B.J., Hull D.R. and Wu X. (2000). Centrosome maturation. *Curr Top Dev Biol* 49: 449-70.

Pan J. and Snell W.J. (2005). Chlamydomonas shortens its flagella by activating axonemal disassembly, stimulating IFT particle trafficking, and blocking anterograde cargo loading. *Dev Cell* 9: 431-8.

Pazour G.J. and Bloodgood R.A. (2008). Targeting proteins to the ciliary membrane. *Curr Top Dev Biol* 85: 115-49.

Pazour G.J., Dickert B.L., Vucica Y., Seeley E.S., Rosenbaum J.L., Witman G.B. and Cole D.G. (2000). Chlamydomonas IFT88 and its mouse homologue, polycystic kidney disease gene tg737, are required for assembly of cilia and flagella. *J Cell Biol* 151: 709-18.

Pazour G.J. and Rosenbaum J.L. (2002). Intraflagellar transport and cilia-dependent diseases. *Trends Cell Biol* 12: 551-5.

Pearson C.G., Culver B.P. and Winey M. (2007). Centrioles want to move out and make cilia. *Dev Cell* 13: 319-21.

Pearson C.G., Osborn D.P., Giddings T.H., Jr., Beales P.L. and Winey M. (2009). Basal body stability and ciliogenesis requires the conserved component Poc1. *J Cell Biol* 187: 905-20.

Pedersen L.B., Geimer S., Sloboda R.D. and Rosenbaum J.L. (2003). The Microtubule plus end-tracking protein EB1 is localized to the flagellar tip and basal bodies in Chlamydomonas reinhardtii. *Curr Biol* 13: 1969-74.

Pedersen L.B. and Rosenbaum J.L. (2008). Intraflagellar transport (IFT) role in ciliary assembly, resorption and signalling. *Curr Top Dev Biol* 85: 23-61.

Pedersen L.B., Veland I.R., Schroder J.M. and Christensen S.T. (2008). Assembly of primary cilia. *Dev Dyn* 237: 1993-2006.

Pelletier L., O'Toole E., Schwager A., Hyman A.A. and Muller-Reichert T. (2006). Centriole assembly in Caenorhabditis elegans. *Nature* 444: 619-23.

Perez-Ferreiro C.M., Vernos I. and Correas I. (2004). Protein 4.1R regulates interphase microtubule organization at the centrosome. *J Cell Sci* 117: 6197-206.

Piel M., Meyer P., Khodjakov A., Rieder C.L. and Bornens M. (2000). The respective contributions of the mother and daughter centrioles to centrosome activity and behavior in vertebrate cells. *J Cell Biol* 149: 317-30.

Pihan G.A., Purohit A., Wallace J., Knecht H., Woda B., Quesenberry P. and Doxsey S.J. (1998). Centrosome defects and genetic instability in malignant tumors. *Cancer Res* 58: 3974-85.

Pihan G.A., Wallace J., Zhou Y. and Doxsey S.J. (2003). Centrosome abnormalities and chromosome instability occur together in pre-invasive carcinomas. *Cancer Res* 63: 1398-404.

Pugacheva E.N., Jablonski S.A., Hartman T.R., Henske E.P. and Golemis E.A. (2007). HEF1-dependent Aurora A activation induces disassembly of the primary cilium. *Cell* 129: 1351-63.

Quarmby L.M. (2004). Cellular deflagellation. *Int Rev Cytol* 233: 47-91.

Quintyne N.J., Reing J.E., Hoffelder D.R., Gollin S.M. and Saunders W.S. (2005). Spindle multipolarity is prevented by centrosomal clustering. *Science* 307: 127-9.

Rajagopalan V., Subramanian A., Wilkes D.E., Pennock D.G. and Asai D.J. (2009). Dynein-2 affects the regulation of ciliary length but is not required for ciliogenesis in Tetrahymena thermophila. *Mol Biol Cell* 20: 708-20.

Raynaud-Messina B., Mazzolini L., Moisand A., Cirinesi A.M. and Wright M. (2004). Elongation of centriolar microtubule triplets contributes to the formation of the mitotic spindle in gamma-tubulin-depleted cells. *J Cell Sci* 117: 5497-507.

Rodrigues-Martins A., Riparbelli M., Callaini G., Glover D.M. and Bettencourt-Dias M. (2007). Revisiting the role of the mother centriole in centriole biogenesis. *Science* 316: 1046-50.

Rogers G.C., Rusan N.M., Roberts D.M., Peifer M. and Rogers S.L. (2009). The SCF Slimb ubiquitin ligase regulates Plk4/Sak levels to block centriole reduplication. *J Cell Biol* 184: 225-39.

Rohatgi R., Milenkovic L. and Scott M.P. (2007). Patched1 regulates hedgehog signaling at the primary cilium. *Science* 317: 372-6.

Romio L., Fry A.M., Winyard P.J., Malcolm S., Woolf A.S. and Feather S.A. (2004). OFD1 is a centrosomal/basal body protein expressed during mesenchymal-epithelial transition in human nephrogenesis. *J Am Soc Nephrol* 15: 2556-68.

Rosenbaum J.L. and Witman G.B. (2002). Intraflagellar transport. *Nat Rev Mol Cell Biol* 3: 813-25.

Salathe M. (2007). Regulation of mammalian ciliary beating. *Annu Rev Physiol* 69: 401-22.

Salisbury J.L. (2008). Breaking the ties that bind centriole numbers. *Nat Cell Biol* 10: 255-7.

Satir P. and Christensen S.T. (2007). Overview of structure and function of mammalian cilia. *Annu Rev Physiol* 69: 377-400.

Saunders W. (2005). Centrosomal amplification and spindle multipolarity in cancer cells. *Semin Cancer Biol* 15: 25-32.

Sayer J.A., Otto E.A., O'Toole J.F., Nurnberg G., Kennedy M.A., Becker C., Hennies H.C., Helou J., Attanasio M., Fausett B.V., et al. (2006). The centrosomal protein nephrocystin-6 is mutated in Joubert syndrome and activates transcription factor ATF4. *Nat Genet* 38: 674-81.

Schmidt T.I., Kleylein-Sohn J., Westendorf J., Le Clech M., Lavoie S.B., Stierhof Y.D. and Nigg E.A. (2009). Control of Centriole Length by CPAP and CP110. *Curr Biol* 19: 1005-11.

Schneider L., Clement C.A., Teilmann S.C., Pazour G.J., Hoffmann E.K., Satir P. and Christensen S.T. (2005). PDGFRalphaalpha signaling is regulated through the primary cilium in fibroblasts. *Curr Biol* 15: 1861-6.

Schroder J.M., Schneider L., Christensen S.T. and Pedersen L.B. (2007). EB1 is required for primary cilia assembly in fibroblasts. *Curr Biol* 17: 1134-9.

Shah A.S., Ben-Shahar Y., Moninger T.O., Kline J.N. and Welsh M.J. (2009). Motile cilia of human airway epithelia are chemosensory. *Science* 325: 1131-4.

Sharma N., Berbari N.F. and Yoder B.K. (2008). Ciliary dysfunction in developmental abnormalities and diseases. *Curr Top Dev Biol* 85: 371-427.

Shekhar M.P., Lyakhovich A., Visscher D.W., Heng H. and Kondrat N. (2002). Rad6 overexpression induces multinucleation, centrosome amplification, abnormal mitosis, aneuploidy, and transformation. *Cancer Res* 62: 2115-24.

Sillibourne J.E., Tack F., Vloemans N., Boeckx A., Thambirajah S., Bonnet P., Ramaekers F.C., Bornens M. and Grand-Perret T. (2009). Autophosphorylation of PLK4 and Its Role in Centriole Duplication. *Mol Biol Cell*

Singla V. and Reiter J.F. (2006). The primary cilium as the cell's antenna: signaling at a sensory organelle. *Science* 313: 629-33.

Singla V., Romaguera-Ros M., Garcia-Verdugo J.M. and Reiter J.F. (2010). Ofd1, a Human Disease Gene, Regulates the Length and Distal Structure of Centrioles. *Dev Cell* 18: 410-424.

Soung N.K., Park J.E., Yu L.R., Lee K.H., Lee J.M., Bang J.K., Veenstra T.D., Rhee K. and Lee K.S. (2009). Plk1-dependent and -independent roles of an ODF2 splice variant, hCenexin1, at the centrosome of somatic cells. *Dev Cell* 16: 539-50.

Spektor A., Tsang W.Y., Khoo D. and Dynlacht B.D. (2007). Cep97 and CP110 Suppress a Cilia Assembly Program. *Cell* 130: 678-90.

Strnad P. and Gonczy P. (2008). Mechanisms of procentriole formation. *Trends Cell Biol* 18: 389-96.

Strnad P., Leidel S., Vinogradova T., Euteneuer U., Khodjakov A. and Gonczy P. (2007). Regulated HsSAS-6 levels ensure formation of a single procentriole per centriole during the centrosome duplication cycle. *Dev Cell* 13: 203-13.

Takeda S., Yonekawa Y., Tanaka Y., Okada Y., Nonaka S. and Hirokawa N. (1999). Left-right asymmetry and kinesin superfamily protein KIF3A: new insights in determination of laterality and mesoderm induction by kif3A-/- mice analysis. *J Cell Biol* 145: 825-36.

Tang C.J., Fu R.H., Wu K.S., Hsu W.B. and Tang T.K. (2009). CPAP is a cell-cycle regulated protein that controls centriole length. *Nat Cell Biol*

Thein K.H., Kleylein-Sohn J., Nigg E.A. and Gruneberg U. (2007). Astrin is required for the maintenance of sister chromatid cohesion and centrosome integrity. *J Cell Biol* 178: 345-54.

Travaglini L., Brancati F., Attie-Bitach T., Audollent S., Bertini E., Kaplan J., Perrault I., Iannicelli M., Mancuso B., Rigoli L., et al. (2009). Expanding CEP290 mutational spectrum in ciliopathies. *Am J Med Genet A* 149A: 2173-80.

Tsang W.Y., Bossard C., Khanna H., Peranen J., Swaroop A., Malhotra V. and Dynlacht B.D. (2008). CP110 suppresses primary cilia formation through its interaction with CEP290, a protein deficient in human ciliary disease. *Dev Cell* 15: 187-97.

Tsang W.Y., Spektor A., Luciano D.J., Indjeian V.B., Chen Z., Salisbury J.L., Sanchez I. and Dynlacht B.D. (2006). CP110 cooperates with two calcium-binding proteins to regulate cytokinesis and genome stability. *Mol Biol Cell* 17: 3423-34.

Tsang W.Y., Spektor A., Vijayakumar S., Bista B.R., Li J., Sanchez I., Duensing S. and Dynlacht B.D. (2009). Cep76, a centrosomal protein that specifically restrains centriole reduplication. *Dev Cell* 16: 649-60.

Tsou M.F. and Stearns T. (2006). Mechanism limiting centrosome duplication to once per cell cycle. *Nature* 442: 947-51.

Tsou M.F., Wang W.J., George K.A., Uryu K., Stearns T. and Jallepalli P.V. (2009). Polo kinase and separase regulate the mitotic licensing of centriole duplication in human cells. *Dev Cell* 17: 344-54.

Uetake Y., Loncarek J., Nordberg J.J., English C.N., La Terra S., Khodjakov A. and Sluder G. (2007). Cell cycle progression and de novo centriole assembly after centrosomal removal in untransformed human cells. *J Cell Biol* 176: 173-82.

Valente E.M., Silhavy J.L., Brancati F., Barrano G., Krishnaswami S.R., Castori M., Lancaster M.A., Boltshauser E., Boccone L., Al-Gazali L., et al. (2006). Mutations in CEP290, which encodes a centrosomal protein, cause pleiotropic forms of Joubert syndrome. *Nat Genet* 38: 623-5.

Van Beneden A. (1883). Recherches sur la maturation de l'oeuf, la Fé-condation et la division cellulaire. Bruxelles.

Veland I.R., Awan A., Pedersen L.B., Yoder B.K. and Christensen S.T. (2009). Primary cilia and signaling pathways in mammalian development, health and disease. *Nephron Physiol* 111: p39-53.

Vidwans S.J., Wong M.L. and O'Farrell P.H. (2003). Anomalous centriole configurations are detected in Drosophila wing disc cells upon Cdk1 inactivation. *J Cell Sci* 116: 137-43.

Vladar E.K. and Stearns T. (2007). Molecular characterization of centriole assembly in ciliated epithelial cells. *J Cell Biol* 178: 31-42.

Vorobjev I.A. and Chentsov Yu S. (1982). Centrioles in the cell cycle. I. Epithelial cells. *J Cell Biol* 93: 938-49.

Wang X., Tsai J.W., Imai J.H., Lian W.N., Vallee R.B. and Shi S.H. (2009). Asymmetric centrosome inheritance maintains neural progenitors in the neocortex. *Nature* 461: 947-55.

Wemmer K.A. and Marshall W.F. (2007). Flagellar length control in chlamydomonas--paradigm for organelle size regulation. *Int Rev Cytol* 260: 175-212.

Wilkinson C.J., Carl M. and Harris W.A. (2009). Cep70 and Cep131 contribute to ciliogenesis in zebrafish embryos. *BMC Cell Biol* 10: 17.

Wilson N.F., Iyer J.K., Buchheim J.A. and Meek W. (2008). Regulation of flagellar length in Chlamydomonas. *Semin Cell Dev Biol* 19: 494-501.

Wolff A., de Nechaud B., Chillet D., Mazarguil H., Desbruyeres E., Audebert S., Edde B., Gros F. and Denoulet P. (1992). Distribution of glutamylated alpha and beta-tubulin in mouse tissues using a specific monoclonal antibody, GT335. *Eur J Cell Biol* 59: 425-32.

Wordeman L. and Mitchison T.J. (1995). Identification and partial characterization of mitotic centromere-associated kinesin, a kinesin-related protein that associates with centromeres during mitosis. *J Cell Biol* 128: 95-104.

Yan X., Habedanck R. and Nigg E.A. (2006). A complex of two centrosomal proteins, CAP350 and FOP, cooperates with EB1 in microtubule anchoring. *Mol Biol Cell* 17: 634-44.

Yang J., Adamian M. and Li T. (2006). Rootletin interacts with C-Nap1 and may function as a physical linker between the pair of centrioles/basal bodies in cells. *Mol Biol Cell* 17: 1033-40.

Yang Z., Loncarek J., Khodjakov A. and Rieder C.L. (2008). Extra centrosomes and/or chromosomes prolong mitosis in human cells. *Nat Cell Biol* 10: 748-51.

Zhao L., Jin C., Chu Y., Varghese C., Hua S., Yan F., Miao Y., Liu J., Thompson W., Mann D., et al. (2009). Dimerization of CPAP orchestrates centrosome cohesion plasticity. *J Biol Chem*

Zheng Y., Wong M.L., Alberts B. and Mitchison T. (1995). Nucleation of microtubule assembly by a gamma-tubulin-containing ring complex. *Nature* 378: 578-83.

Zimmermann K.W. (1898). Beiträge zur Kenntnis einiger Drüsen und Epithelien. *Arch Mikrosk Anat Anz* 52: 552–706.

Zyss D. and Gergely F. (2009). Centrosome function in cancer: guilty or innocent? *Trends Cell Biol* 19: 334-46.

9. APPENDIX

Parts of this work are published in:

Thorsten I. Schmidt, Julia Kleylein-Sohn, Jens Westendorf, Mikael Le Clech, Sébastien B. Lavoie, York-Dieter Stierhof and Erich A. Nigg (2009) Control of centriole length by CPAP and CP110. *Curr Biol* 19: 1005-11.

10. CURRICULUM VITAE

Thorsten I. Schmidt

Born on October 14th, 1978 in Bonn, Germany

August 2006 – March 2010
PhD Student at the Max Planck Institute of Biochemistry, Martinsried, Germany
Department of Cell Biology, with Prof. Dr. Erich A. Nigg

May 2005 – March 2006
Diploma Thesis at the University of British Columbia, Vancouver, Canada
Centre for Molecular Medicine and Therapeutics, with Prof. Dr. Michael S. Kobor

October 2000 – March 2006
Biology Student and Diploma at the Eberhard-Karls University, Tübingen, Germany

August 2000
Member of the German National Team at the Olympic Games, Sydney, Australia

September 1999 – June 2000
Economics Student at the Leibnitz University, Hannover, Germany

July 1998 – August 1999
Public Service at the Agnes-Karll Hospital and the Olympiastützpunkt Niedersachsen, Hannover, Germany

August 1991 – June 1998
High School Diploma (Abitur) at the Kaiser-Wilhelm- und Ratsgymnasium, Hannover, Germany

List of Scientific Publications:

Nicole Levesque, Grace P. Leung, Alexandra Fok, **Thorsten I. Schmidt** and Michael S. Kobor (2010) Loss of H3 K79 trimethylation leads to suppression of RTT107-dependent DNA damage sensitivity through the translesion synthesis pathway. *J Biol Chem* [Epub ahead of print]

Thorsten I. Schmidt, Julia Kleylein-Sohn, Jens Westendorf, Mikael Le Clech, Sébastien B. Lavoie, York-Dieter Stierhof and Erich A. Nigg (2009) Control of centriole length by CPAP and CP110. *Curr Biol* 19: 1005-11.

11. ACKNOWLEDGEMENTS

First and foremost I would like to thank Erich Nigg for giving me the opportunity to graduate in his laboratory and for the invaluable advice and guidance during this time. I would also like to thank Zuzana Storchova and Thomas Cremer for their contribution to this work as members of my Thesis Advisory Committee. Moreover, I am indepted to Zuzana and her group members for kindly hosting me and allowing me to finish my thesis at the Max Planck Institute after Erich's move to the Biozentrum in Basel.

My grateful thanks also go to York Stierhof and his co-workers for the electron microscopy work and especially for their repeated effort of trying to find a needle in the haystack. I still admire Dagmar for her patience and persistence on my samples.

More than anyone else, I would like to thank Jens Westendorf. For being such a great person, for all the discussions, his never-ending technical advice, his contribution to my work by helping me with the FACS analysis and his fundamental effort regarding the generation of the U2OS T-REx myc-CPAP cell line, but mostly for the time we spent together neck on neck in the lab. A heartfelt `thank you all´ to those colleagues (Tom, Susanna, Klaus, Alison, Rainer, Anna, Roman and many more) who made the lab become a second home during the busy times. To Xiumin Yan, Mikael LeClech, Julia Kleylein-Sohn and Sébastien Lavoie I offer my thanks for getting me started in the lab, for sharing their time and expertise with me and for discussions on the project. I thank Claudia Szalma for her support in the lab, Elisabeth Bürgelt for her work during the production of the monoclonal CP110 antibody and Elena Nigg for several antibody purifications, her efforts during the production of the polyclonal antibodies and for being of help in plentiful other situations.

I am also thankful to Ina and Gernot for the great atmosphere in the office, for all the coffee breaks shared and for their friendship. I cordially wish them both success and the best of luck on their projects in Basel and for their future careers.

Thanks to Hedwig, Reinhold and Rita for encouraging (and sometimes criticising) me but first and foremost thank you for your ceaseless and exceptional support.

Lastly, I am indebted to my friends who always lent an understanding ear and with whom I shared so much enjoyable and unforgettable times during the past years while living in Munich.